ANTIMICROBIAL ACTIVITY OF ESSENTIAL OILS AND METALS AND THEIR INTERACTION WITH LAYERED SILICATES

DAVID PÉREZ IGLESIAS

A thesis submitted in partial fulfilment of the

requirements of the Manchester

Metropolitan University for the degree of

Master of Philosophy

School of Healthcare Science

Faculty of Science and Engineering

2018

Declaration

I declare that this work has not already been accepted for any degree and is not being currently submitted in candidature for any other than the degree of Master of Philosophy of the Manchester Metropolitan University

Acknowledgements

I would like to thank my Director of Studies Dr. Christopher Liauw for giving me the opportunity to undertake this project. His support and guidance through this project has been invaluable. I would also like to thank my supervisors Dr Kathryn Whitehead and Dr Graham Lees for their help and their strong expertise and knowledge they have brought to the research. Without this team of supervisors, I would not have succeeded in completing this research with all the circumstances surrounding this project.

The whole of the technical staff in the Manchester Metropolitan Microbiology and Chemistry departments deserve thanks for their help and guidance throughout my period of learning the techniques required to complete the research.

To Daniel, Diego, Jorge, Ortega and Ricard there is nothing I can thank you more but for your friendship. Not only this project, but this challenging experience would not have been possible without our conversations, jokes, dinners, lunches, drinks and a million of things more I just cannot list here. Thank you so much for being there whenever I needed it, having made everything so enjoyable and easy to deal with it.

É agora cando non podo esquecer a toda a miña familia e os meus amigos de volta a casa. A pesares de estardes lonxe, sempre; dalgún xeito estabades todos preto de min. Non houbo meirande empurrón durante todo este tempo que me axudase máis. Grazas a todos. Pero sobre tódalas cousas, grazas ós meus pais. Grazas por teren feito posible estar escribindo estas liñas nestes intres. Sen vos, nin sería o que son agora nin chegaría ata onde cheguei (e chegarei). Grazas de todo corazón.

Abstract

Essential Oils (EOs) and metal ions have been utilised and investigated for antimicrobial applications for centuries; antimicrobial resistance has led to renewed interest in such antimicrobials. This study assesses their use as broad-spectrum antimicrobial agents. The essential oils (EOs) investigated were; Rosewood oil (RO), Clove Leaf Oil (CLO), Orange Oil (OO), Myrtle Oil (MO) and Manuka Oil (MNO). The metal ions studied were; Silver (Ag), Palladium (Pd) and Platinum (Pt). The ultimate aim was to encapsulate the best performing antimicrobial agents in a layered silicate controlled release substrate for use in various polymer-based formulations.

The first stage of the study was targeted at assessment of the antimicrobial efficacy of these agents, both individually and in combination (to establish synergistic effects), against *Staphylococcus aureus* (gram-positive) and *Pseudomonas aeruginosa* (gram-negative). Antimicrobial efficacy was monitored using Zone of Inhibition, micro-dilution and checkerboard micro-broth dilution methods. Zone of Inhibition (ZoI) proved to be a reliable qualitative method for assessment of the antimicrobial activity of metal ions. Nutrient Agar (NA) was found to be the best growth media for higher metal concentrations (>100 mg/L) and Mueller-Hinton (MH) worked better at lower ion concentrations (<100 mg/L). However, ZoI tests (using wells, solid diffusion or vapour diffusion) were ineffective for assessment of the antimicrobial efficacy of EOs. On an individual basis, all the metal ions (Ag, Pd and Pt) gave a Minimum Inhibitory Concentration (MIC) of 25 mg/L, however, all metal ions, apart from Ag, gave Minimum Bactericidal Concentration (MBC) values higher than 25 mg/L. Of the individual EOs, MNO gave the highest level of antimicrobial performance (MIC of 2.5% (v/v)); no MBC values were recorded for the any of the EOs at the maximum concentration investigated (20%(v/v)). Blends of Ag (50 mg/L) + RO (20%(v/v)) and Ag (50 mg/L) + MNO (5%(v/v)) at a 1:2 ratio shared the highest level of antimicrobial performance, in terms of both MIC and MBC.

The next stage of the study involved investigation of incorporation of silver ions and the best performing EO (MNO), plus RO and CLO, due to their relatively simple compositions, into unmodified (sodium) montmorillonite and a range of organically modified montmorillonites (o-MMT). The sodium montmorillonite used was (Cloisite Na^+, Rockwood Additives) and the organically modified montmorillonites were (ranked in order of increasing gallery polarity); Cloisite 15A < Cloisite 20A < Cloisite 30B < Claytone APA < Tixogel VXZ (from Rockwood additives and BYK). Silver ions were incorporated in to Cloisite Na^+ only, via ion exchange. The adsorption of EOs was monitored using Thermal Gravimetric Analysis (TGA), X-ray diffraction (XRD) and Fourier Transform Infrared Spectroscopy (FTIR). The TGA data enabled determination of the amount of EO adsorption, after taking account of the amount of organic modifier in cases of o-MMT. The XRD data provided insight into the effect of EO adsorption on the stacking uniformity of the MMT platelets. Finally, FTIR data provided insight into oxidation of the EOs and supporting data to verify EO – organic modifier interactions that led to increases in MMT platelet stacking uniformity. O-MMTs with benzyl and hydrogenated tallow functionality (i.e., Claytone APA and Tixogel VZ) provided the best EO adsorption capacity with levels of g EO / 100g o-MMT being achieved. In several cases interaction between the EO components and the organic modifiers led to increased MMT platelet stacking uniformity this effect tended to be most pronounced with o-MMTs containing dehydrogenated tallow functional organic modifiers (i.e., Cloisites 15A and 20A). The CAPA loaded RO and MNO showed antimicrobial activity against *S. aureus*.

The adsorption (exchange) of silver ions into Cloisite Na^+ was monitored using Energy dispersive X ray spectroscopy (EDX), Atomic Absorption Spectroscopy (AAS) and XRD. The highest level of silver incorporated was 10.4 wt.%. EDX was the most reliable method for determining the amount of silver adsorbed as it was carried out on washed and unwashed samples, the former provided the most reliable estimate of the amount of silver ions actually incorporated into the MMT galleries, rather than simply being adsorbed on the external surfaces. The figure of 10.4 wt.% was obtained from a washed sample. XRD data showed that treatment of the Na-MMT platelets with Ag^+ aqueous solution, followed by drying led to a substantial disruption of stacking disorder. The Ag^+ intercalated MMT showed antimicrobial activity against *P. aeruginosa*.

INDEX

LIST OF TABLES

Chapter 2

Chapter 3

Table 3.5. Organic modifier levels and interlayer spacings in MMTs investigated – comparison with literature / manufacturer figures.

Table 3.6. Peak assignments for DRIFTS spectra of MMTs investigated (Figures 3 and 4)

Table 3.7. $\nu_{(CH\text{-}H)as}$ values for the o-MMTs investigated, listed in order of increasing organic modifier level (determined at MMU by TGA).

Table 3.8. Peak assignments for DRIFTS spectra of EOs investigated (Figures 3 and4)

Table 3.9. - CNa XRD Summarising peaks

Table 3.10. - CL15A XRD Summarising peaks

Table 3.11. – CL20A XRD Summarising peaks

Table 3.12. – CL30B XRD Summarising peaks

Table 3.13. – CAPA XRD Summarising peaks

Table 3.14. – TVZ XRD Summarising peaks

Table 3.15: Summary of interlayer spacings, EO adsorption levels and evidence of the templating effect.

Table 3.16: Values of $\nu_{(CH\text{-}H)as}$ and $\Delta\nu_{(CH\text{-}H)as}$ for the RO-MMT combinations (a negative value of $\Delta\nu_{(CH\text{-}H)as}$ indicates an increase in the level of ordering of surface modifier alkyl tails)

Table 3.17: Values of $\nu_{(CH\text{-}H)as}$ and $\Delta\nu_{(CH\text{-}H)as}$ for the CO-MMT combinations (a negative value of $\Delta\nu_{(CH\text{-}H)as}$ indicates an increase in the level of ordering of surface modifier alkyl tails)

Table 3.18: Values of $\nu_{(CH\text{-}H)as}$ and $\Delta\nu_{(CH\text{-}H)as}$ for the MO-MMT combinations (a negative value of $\Delta\nu_{(CH\text{-}H)as}$ indicates an increase in the level of ordering of surface modifier alkyl tails)

LIST OF FIGURES

Chapter 1

Chapter 2

Figure 2.4 – Antimicrobial activity (as measured by agar well ZoI) of ■ silver, ■ platinum and ■ palladium ions against *P. aeruginosa* at concentrations of; (a) 1000 mg/L, (b) 500 mg/L, (c) 100 mg/L, (d) 50 mg/L and (e) 10 mg/L, on the indicated media. Pd and Pt showed best antimicrobial efficacies at ion concentrations ≥ 100 mg/L, whilst Ag performed better at concentrations ≤ 100 mg/L.

Chapter 3

Figure 3.1 . Scheme of Sodium-MMT structure

Figure 3.2. Procedure used to encapsulate the EOs in MMT.

Figure 3.3. X-ray diffractogrammes of (a) CNa, (b) C15A, (c) C20A, (d) CAPA, (e) TVZ and (f) C30B.

Figure 3.4 (i). DRIFTS spectra (OH and CH stretching region) (5 wt.% dilution in KBr (see Section *3.2.4.3* for method)) of the MMTs investigated split into O-H and fingerprint regions; (a) CNa, (b) C20A, (c) C15A, (d) CAPA, (e) TVZ and (f) C30B.

Figure 3.4 (ii). DRIFTS spectra (fingerprint region) (5 wt.% dilution in KBr (see Section *3.2.4.3* for method)) of the MMTs investigated; (a) CNa, (b) C20A, (c) C15A, (d) CAPA, (e) TVZ and (f) C30B.

Figure 3.5 (i). Transmission FTIR spectra (OH and CH stretching region) of the essential oils split; (a) Manuka oil (MNO), (b) rosewood oil (RO) and (c) clove leaf oil (CLO).

Figure 3.5 (ii). Transmission FTIR spectra (fingerprint region) of the essential oils; (a) Manuka oil (MNO), (b) rosewood oil (RO) and (c) clove leaf oil (CLO).

Figure 3.6. Levels of EO adsorption in the MMTs investigated – Note MNO and CLO were generally the most compatible EOs. * denotes samples that were in the form of a greasy

mass indicating either limited compatibility with the EO or partial delamination of platelets due to strong compatibility with the EO.

Figure 3.7. XRD data for Cloisite Na^+, (a) CNa, (b)CNa-MNO, (c) CNa-RO and (d) CNa-CLO.

Figure 3.8. XRD data for Cloisite 15A; (a) C15A, (b)C15A-MNO, (c) C15A-RO and (d) C15A-CLO. * Denotes sample in form of greasy mass.

Figure 3.9. XRD data for Cloisite 20A (a) C20A, (b)C20A-MNO, (c) C20A-RO and (d) C20A-CLO. * Denotes sample in form of greasy mass.

Figure 3.10. XRD data for Cloisite 30B; (a) C30B, (b)C30B-MNO, (c) C30B-RO and (d) C30B-CLO. * Denotes sample in form of greasy mass.

Figure 3.11. XRD data for Claytone APA; (a) CAPA, (b) CAPA-MNO, (c) CAPA-RO and (d) CAPA-CLO. * Denotes sample in form of greasy mass.

Figure 3.12. XRD data for Tixogel VZ; (a) CAPA, (b) CAPA-MNO, (c) CAPA-RO and (d) CAPA-CLO. * Denotes sample in form of greasy mass.

Figure 3.13. DRIFTS spectra (2200 – 500 cm^{-1}) of RO-MMT combinations. The colour of the combination is indicated by the square in the right hand half of the spectrum. The amount of RO adsorbed is in g RO/100 g MMT (or o-MMT) is shown adjacent to each spectrum.

Figure 3.14. DRIFTS spectra (2200 – 500 cm^{-1}) of CLO-MMT combinations. The colour of the combination is indicated by the square in the right hand half of the spectrum. The amount of CLO adsorbed is in g CLO/100 g MMT (or o-MMT) is shown adjacent to each spectrum.

Figure 3.15. DRIFTS spectra (2200 – 500 cm^{-1}) of MNO-MMT combinations. The colour of the combination is indicated by the square in the right hand half of the spectrum. The

amount of MNO adsorbed is in g MNO/100 g MMT (or o-MMT) is shown adjacent to each spectrum.

Figure 3.16. Antimicrobial testing regime for EOs encapsulated in CLNa. (a) S Aureus and (b) P Aeruginosa. Numbers refer to the EOs as follows: 1. CLNa, 2. CLNa-RO, 3. CLNa-CLO, 4. CLNa-MNO.

Figure 3.17. Antimicrobial testing regime for EOs encapsulated in TVZ. (a) S Aureus and (b) P Aeruginosa. Numbers refer to the EOs as follows: 13. TVZ, 14. TVZ -RO, 15. TVZ -CLO, 16. TVZ -MNO.

Figure 3.18. Amount of silver effectively incorporated into the unmodified substrate (CLNa).

Figure 3.19. Amount of silver (%wt) effectively incorporated into the unmodified substrate (CLNa) before washing and after washing the samples.

Figure 3.20. XRD for Ag^{+} loaded CNa (a) Unmodified CNa, (b) 0.02 Ag, (c) 0.05 Ag, (d) 0.075 Ag, (d) 0.10 Ag

Figure 3.21. Antimicrobial activity assessment of Ag+ unmodified loaded MMTs against *S Aureus*. 21) CLNa, 22) CLNa + 0.025 M Ag+, 23) CLNa + 0.05 M Ag+, 24) CLNa + 0.075 M Ag+, 22) CLNa + 0.1 M Ag+

Figure 3.22. Antimicrobial activity assessment of Ag+ unmodified loaded MMTs against *P Aeruginosa* 21) CLNa, 22) CLNa + 0.025 M Ag+, 23) CLNa + 0.05 M Ag+, 24) CLNa + 0.075 M Ag+, 22) CLNa + 0.1 M Ag+

APPENDICES

Appendices

Chapter 1

Appendix 1 – Preparation of metal ions, controls solutions and compositions used for testing antimicrobial efficacy using Zone of Inhibitions (ZoI, wells)

Appendix 2 – Preparation of EOs in grapeseed oil used for testing antimicrobial efficacy (ZoI, wells)

Appendix 3 – Preparation of EOs in grapeseed oil used for testing antimicrobial efficacy (ZoI, solid diffusion and vapour diffusion)

Appendix 4 – Composition of the samples subject of study of MIC/MBC for Essential Oils

Appendix 5 – Composition of the samples subject of study of MIC/MBC for Metal Ions

Appendix 6 – Metal ion and Essential Oil concentrations present once mixed in the micro titre plate wells with the 150 μL of the cell suspension adjusted to $1x10^6$ CFU/mL in a double strength solution of TSB containing 0.15% (m/v) TBC and 1.5% (m/v) tween 20.

Appendix 7 – MIC data from MTP assays, showing the antimicrobial efficacy of the tested silver (Ag) at different concentrations (mg/L).

Appendix 8 – MIC data from MTP assays, showing the antimicrobial efficacy of the tested essential oils (RO, MNO) at different concentrations (%(v/v)).

Appendix 9 –MBC data from MTP assays, showing the antimicrobial efficacy of the tested silver (Ag) at different concentrations (mg/L).

Appendix 10 – MBC data from MTP assays, showing the antimicrobial efficacy of the tested essential oils (RO, MNO) at different concentrations (%(v/v)).

Appendix 11 - MIC data from MTP assays, showing the antimicrobial efficacy of the tested silver (Ag) at different concentrations (mg/L).

Appendix 12 – MIC data from MTP assays, showing the antimicrobial efficacy of the tested essential oils (RO, MNO) at different concentrations (%(v/v)).

Appendix 13 –MBC data from MTP assays, showing the antimicrobial efficacy of the tested silver (Ag) at different concentrations (mg/L).

Chapter 2

Appendix 1 – Preparation of EOs (rosewood oil, clove leaf oil and Manuka oil) to be incorporated into unmodified substrates (CLNa) and organic modified substrates (CL15A, CL20A, CL30B, Tix, Cly).

Appendix 2 – Results of incorporation of EOs (rosewood oil, clove leaf oil and Manuka oil) into unmodified substrates (CLNa) and organic modified substrates (CL15A, CL20A, CL30B, Tix, Cly) as for gr EOs/ 100 gr substrates. Values are an average taken from three replicates (standard deviations given in brackets).

Appendix 3 – Results of incorporation of EOs (rosewood oil, clove leaf oil and Manuka oil) into unmodified substrates (CLNa) and organic modified substrates (CL15A, CL20A, CL30B, Tix, Cly) in terms of basal space (d(A)) and diffraction angles (2θ).

Appendix 4 – Samples' colours (EO encapsulated into unmodified and modified MMTs)

Appendix 5 – Preparation of silver to be incorporated into unmodified substrate (CLNa).

Appendix 6 – Results of incorporation of silver into the unmodified substrate (CLNa) as for gr EOs/ 100 gr substrates. Values are an average taken from three replicates (standard deviations given in brackets).

Appendix 7 – Results of incorporation of silver into the unmodified substrate (CLNa) as for wt%. Values are an average taken from three replicates (standard deviations given in brackets).

List of abbreviations

AAS Atomic absorbance spectroscopy

Ag Silver

AgNO3 Silver Nitrate

AMR Antimicrobial resistance

ASTM American society for testing materials

C15A Cloisite 15A

C20A Cloisite 20A

C30B Cloisite 30B

CAPA Claytone APA

CFU Colony forming units

CLO Clove leaf oil

CLSI Clinical and Laboratory Standards Institute

DRIFTS Diffuse reflectance fourier transformed spectroscopy

EDX Energy dispersive X-ray spectroscopy

EO Essential oils

EU European union

FTIR Fourier transform infrared spectroscopy

HT Hydrogenated tallow

ISO International Organisation of Standardization

MBC Minimum Bactericidal Concentration

MH Mueller Hinton

MIC Minimum Inhibitory concentration

MMU Manchester Metropolitan University

MMT Montmorillonite

MNO Manuka oil

MTP Micro titre plate

MYO Myrtle oil

NA Nutrient agar

NCTC National collection of type cultures

OD Optical density

OO Orange oil

OM Organic modifier

Pd Palladium

Pt Platinum

REACH Regulation, evaluation, authorisation and restriction of chemicals

RO Rosewood oils

SDT Solid diffusion test

TBC 4-tert-butylcathecol

TGA Thermal gravimetric analysis

TSA Tryptic soy agar

TSB Tryptic soy broth

TVZ Tixogel VXZ

VDT Vapour diffusion test

XRD X-ray dispersion

WAXS Wide angle x-ray scattering

ZoI Zone of Inhibition

CHAPTER 1. INTRODUCTION

The primary objectives of the study were firstly to investigate the antimicrobial efficacy of selected essential oil and metallic antimicrobials and possible synergies in combinations of the latter. The second objective was to investigate the incorporation of the best performing essential oil and metallic antimicrobial agents into organically modified layered and unmodified layered silicates. It was anticipated that incorporation into layered silicates would lead to controlled release of the antimicrobials. Whilst the antimicrobial efficacy of the layered silicates was investigated, investigation of the controlled release characteristics and subsequent investigation of performance once incorporated into a polymer formulation were beyond the scope of this MPhil study.

1.1 Antimicrobial resistance

In his Nobel prize acceptance speech for the discovery of Penicillin, Alexander Fleming had already addressed the dangers of bacterial evolution that would ultimately result in resistance to Penicillin (KMPG-LLP, 2014). Almost seventy years later, bacteria have developed multiple antibiotic resistance, Fleming's warnings have become reality (KMG-LLP, 2014). Over the last twenty five years, no new class of antibiotics has been developed and bacteria are becoming increasingly resistant to several current antibiotics (World Bank Group, 2016).

As a result of this, Antimicrobial Resistance (AMR) has become a pressing health issue worldwide. AMR is defined as the natural process of bacteria – or some other infectious agents – that evolve resistance to existing antibiotics. This leads to a significant reduction of the lifespan of an antibiotic. The development of new antibiotics is required to combat these increasingly resistant infectious agents. An increase in the levels of AMR has been

witnessed over the past few decades. The overuse of antibiotics and a lack of new antibiotics becoming available are in part responsible for the internationally reported rise of AMR (Review on AMR, 2016).

The increasing prevalence of AMR across the world is a significant risk to society. AMR may result in loss of life and reduced quality of life, resulting in pre-antibiotic landscape and a significant increase in mortality rates (KMPG-LLP, 2014). A decrease in labour force (and an increasingly ageing society) could cause a sustained downturn in economic activity (Rand Europe, 2014). These are just a few examples of the problems arising from AMR and illustrate the importance/urgency of tacking the AMR threat (KMPG-LLP, 2014). The potential impact of AMR on society is likely to be vast and diverse and, assessing this impact is a complex task in itself (Rand Europe, 2014).

Treating products with biocides is among one of the many actions taken to combat AMR (PAN Germany, 2013). Several products are currently treated with biocides in order to preserve not only the products themselves, but also to produce specific functions. The role of biocides is to prevent bacteria, fungi, algae or viruses from growing. Biocide applications are diverse and used in product enhancements, as customers consider the products to be more hygienic and, in effect, offer preventive healthcare (Review on AMR, 2014).

Unfortunately, registration of biocide products used to treat surfaces has not yet been resolved or implemented by EU authorities (PAN Germany, 2014). No reliable market statistics for the amount of biocides used are available to date. Even when used for protective purposes, biocides themselves should not always be assumed harmless. The rationale behind adding them to products is to damage/kill or inhibit or permit growth of organisms that are harmful to humans. However, in many cases this toxicity to

microorganisms is likely to eventually give rise to unwanted effects on human health (PAN Germany, 2014). Therefore regulatory authorities must not only determine the efficacy of the biocidal agent against the target organism, but also assess the risks in relation to their use and their potential effects on the customers and the environment.

Despite the above, there are gaps in regulations related to biocide-related articles, however, steps are currently being taken at EU legislation level to refine and reinforce such regulations (PAN Germany, 2014). A new European regulation was resolved in September 2013 (PAN Germany, 2014) which summarised the legislation changes for all parties involved in the manufacturing of biocide-treated articles, thus identifying issues in regard to the implementation of the products and suggesting further actions and recommendations.

1.2 Microbiology

Extermination and/or deactivation of the bacteria is the core objective of this project. Bacteria are unicellular organisms with a cell diameter between 0.5 µm and 20 µm, the dimensional range classifies such species as microorganisms. Bacterial cells are also classified as prokaryotic, as their genetic information is not surrounded by a nuclear membrane (Tortosa et al, 2007).

Bacteria can be classified according to their reaction to specific dyes. Gram (1884) (Singleton et al., 2004) discovered that certain bacteria retain a purple dye washed with alcohol (Gram positive), whilst others do not and the dye agent is washed away (Gram negative). This difference between these bacteria types is related to the cell wall structure. Gram-negative bacteria have an inner cell wall made up of a thin peptidoglycan layer, which is a monolayer in most cases. There is a middle layer of periplasmic gel surrounding this thin peptidoglycan inner layer. The outer layer is a lipid bi-layer made up of a phospholipid layer on the inner

surface and lipopolysaccharide making up the other surface. Gram-positive bacteria have a non-flexible cell wall of 30-100 nm thickness that is mainly made up of peptidoglycan.

Growth of the wall occurs via formation of new layers from the inside. The outer layers will therefore be the oldest.

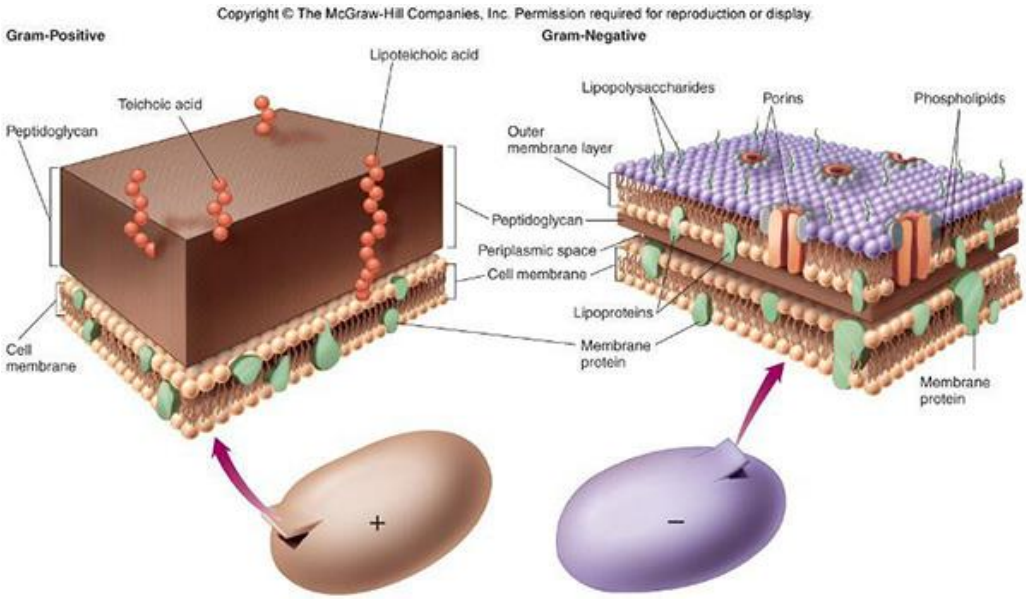

Figure 1.1. Gram Positive vs Gram Negative Bacteria (https://microbiologyinfo.com/differences-between-gram-positive-and-gram-negative-bacteria/)

Two bacteria (*Staphylococcus aureus* – Gram-positive - and *Pseudomonas aeruginosa* - Gram -negative) were selected as challenges for screening the antimicrobial activity of both metals and essential oils. These two bacteria are used in most of the standardized methods for assessing antimicrobial activity (ISO 16187, ASTM E 2149). These methods define the testing of at least one Gram-positive bacteria and one Gram-negative bacteria to assess the antimicrobial activity.

1.2.1 Staphylococcus aureus

S. aureus is a Gram-positive coccoid bacterium which is frequently found in the human respiratory tract and on the skin. It commonly colonizes human skin and mucosa without causing any problem. However, it can cause disease if entering the body by when an opportunity occurs (through broken skin or medical procedure). Should this bacteria enter the body, illnesses ranging from mild to life-threatening can develop. Such conditions include skin and wound infections, infected eczema, abscesses, infections of the heart valves, pneumonia and bacteraemia (Public Health England, 2014)

1.2.2 *Pseudomonas aeruginosa*

P. aeruginosa is a Gram-negative bacteria which is often found in soil and ground water. It is an opportunistic pathogen and rarely affects healthy individuals. It can cause a wide range of infections, especially in those with a weakened immune system. *P. aeruginosa* infections are also linked with contaminated water (Public Health England, 2014) with lung infections found in cysteic fibrosis patients.

1.3 Antimicrobial Agents

A wide range of substances and chemicals can be classed as antimicrobial agents. Some such as metals and essential oils, have been used since antiquity (Jones, 1996 and Lansdown, 2006) whilst others such as the synthetic antimicrobials benzalkonium chloride, chlorhexidine and triclosan, are more recent.

1.3.1. Metallic Antimicrobials

Metal based antimicrobials have been used for thousands of years. This is because of the so-called olygodynamic effect. This is a toxic effect shown by many metals to varying degrees, but can be particularly effective against bacteria. It is suggested that the metal ions denature enzymes of the target cells, for example, by binding to a reactive group (oxidation of cellular thiols, as one of many), thus resulting in their inactivation (Lemire et al. 2013). However, at the beginning of this century the use of metals as antimicrobial agents is undergoing a renaissance, partly due to antimicrobial resistance to several widely used antibiotics and antimicrobial (Hobman et al. 2014).

1.3.1.1 Silver

Silver is the most widely used antimicrobial agent in all major applications and as far as 2012 it accounted for about 87.6% of the market value of around $1.343 billion (MarketsandMarkets, 2012).

All silver-based antimicrobials act against bacteria through the action of silver ions (Ag^{+}). The effect of silver ions against microorganisms is well established and it is referred to as olygodynamic effect. Silver interacts with bacterial cells through three different mechanisms:

- Damage bacterial cell membrane (Sondi et al, 2004).
- Displacement of Ca^{2+} and Zn^{2+} ions (Sondi et al, 2004).
- Interaction with sulphur, oxygen or nitrogen (Dowling DP et al, 2001).

Silver ions show unique qualities when used as antimicrobial agents:

- They are active against a broad range of Gram-positive and Gram-negative bacteria in different media (Schierholz et al, 1998).
- They are effective in very low concentrations (50 ppb Ag+) (Gilchrist et al, 1991).
- They have a low risk for bacteria developing resistance (Damm et al, 2006).

Silver and nano-particulate silver fall under Registration, Evaluation, Authorisation and restriction of Chemicals REACH (EU 1097/2006) (FoE United States, 2009), unless a specific application is covered by another regulation.

The core varieties of commercially available silver based antimicrobial include; silver ion exchange materials (including silver zeolites), silver salts, metallic silver and organo-silver compounds (Sherman, Dec 2011, Windler L. et al. 2013). Some examples of alternative types of silver that may be used as antimicrobials include:

- Silver ion exchange materials including silver zirconium phosphates, silver zeolites and silver glasses
- Silver salts including silver chloride (AgCl), nano-particulate silver chloride and silver chloride titanium dioxide hybrids and mixtures.
- Metallic silver can be in the form of filaments and electrolytically coated fibres, silver nano-particles and mixtures containing metallic silver.
- Organo-silver compounds.

Silver coatings are increasingly used in range of products such as fibres, washing machines, dyes/paints and varnishes, polymers, medical applications, silks, ceramics and various consumer applications such as disinfectants, cosmetics and cleaning agents.

1.3.1.2 Palladium and Platinum derivatives

Palladium and platinum derivatives were also evaluated in this study together with silver. Both palladium and platinum have already been investigated as antimicrobial agents both as a part of coordination complexes with either natural or synthetic bioactive organic ligands and on their individual form. Samota (2009) showed an increase in the antimicrobial activity of the metal complexes relative to the ligands in isolation. Promising results were obtained indicating that ligands play a secondary role, the metal ion is therefore the truly active component. More recently the antimicrobial activity of Pd and Pt ions (with no bioactive ligand) has been assessed against Gram-positive and Gram-negative bacteria. Adams et al (2014) examined the antimicrobial capacity of palladium nanoparticles, thus providing not only an indication of their usefulness as target antimicrobial compounds, but also their potency as potential environmental pollutants. Staszek at al (2014) reported the preparation of palladium and platinum nanoparticles (NPs) by sputtering directly into glycerol and examined their further antimicrobial activity against Gram-negative and Gram-positive bacteria. Palladium NPs proved to be more biological active than their platinum NPs counterparts in this study against the tested organisms.

1.3.2 Essential Oils

Essential Oils (EO) are vegetation (plant) synthesized volatile organic compounds that have been used for a variety of applications for many thousands years. Applications have included; fragrances, flavouring additives and even preservatives for crops (Hammer et al., 1999). In recent years, EOs have attracted scientific interest due to their likelihood of being used as biologically active compounds with antimicrobial and antiviral activities (Lang et al., 2011).

EO can be extracted from plant material via a number of methods such as supercritical CO_2 extraction, hydro and steam distillation and solvent extraction (El-Mougy et al., 2009). EO are a complex mixture of organic chemicals, although a significant proportion of the components are based on repeating isoprene units known as terpenes.

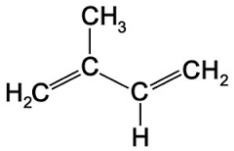

Figure 1.2. Isoprene structure

Terpenes found in the main structure of most EOs are made up of two isoprene units (monoterpenes) or three isoprene units (sesquiterpenes). The structure can be linear or cyclic.

Mono and sesqui terpenes often feature functional group containing such as oxygen, nitrogen and sulphur, the latter though is rather uncommon. Linalool is the most widely encountered of these substituted terpenes (Figure 1.3).

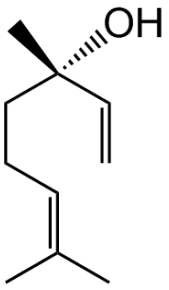

Figure 1.3. Structure of Linalool

As previously mentioned EOs are receiving renewed attention as biologically active compounds that can kill / damage microorganisms. Due to their significant antimicrobial activity against Gram-positive and Gram-negative microorganisms (Lang et al., 2011), EOs

were not only used in ancient Egypt for embalming, but have also been used and explored ever since for their antimicrobial effects (Baser et al, 2010). Whilst plants and plant-derived compounds have been used therapeutically since ancient times, during these times there was no knowledge of microorganisms. As time has progressed EOs have been further investigated, the individual components have been isolated / characterised and their antimicrobial effects have been reported (Hammer et al., 1999, Lang et al., 2011 and El-Mougy et al., 2009). These effects range from inhibition of microbial growth to, in some cases, killing a wide variety of Gram-positive and Gram-negative bacteria, fungi and parasites.

Despite encouraging results indicating bioactivity of EOs, clinical trials of new EO based medicines have not been attempted. Claims related to the therapeutic application of EOs are still speculative and lacking in evidence, peer reviewed investigation into such claims are also lacking (Baser et al, 2010). This is unfortunate because being multi-component systems; EOs may be effective against drug resistant microorganisms and hence help to combat AMR.

1.3.2.1 Rosewood Oil

Rosewood oil is isolated from *Aniba rosaeodoran* and its content is primary linalool (80-97%) with small amounts of terpineol, nerol and geraniol (Davis et al., 1999). Linalool has been shown to have antimicrobial properties and is therefore likely to be largely responsible for the antimicrobial activity of RO. Literature reports have shown rosewood oil to have anxiolytic, sedative and anticonvulsant properties, as well as the antimicrobial properties mentioned previously (Hammer at al., 1999)

1.3.2.2 Clove Leaf Oil

Clove leaf oil is extracted from the aromatic flower buds of *Syzygium aromaticum*, which are native to Indonesia. Its primary component is eugenol (72-90%), which is responsible for the aroma (Razafimamonjison et al., 2014). In its oil form it is mainly used in dentistry as anodyne (painkiller).

1.3.2.3 Orange Oil

Orange Oil is produced by cells within the rind of an orange fruit. It is composed mainly by d-limonene (more than 90%) and is often used in place of pure d-limonene (Baser et al., 2010).

1.3.2.4 Manuka Oil

Manuka Oil is extracted from the shrub *Leptospermum scoparium,* which originated in New Zealand. The oil extracted from this plant has been commercially available to aroma therapists for more than a decade. Attention has been paid to the potential antiseptic and antibacterial properties of Manuka oil. Sesquiterpenes are one of the major components of manuka oil (up to 70% depending on the regional variety). Recent investigations (Maddock-Jennings et al., 2005) have led to the conclusion that the triketones (up to 30% depending on the regional variety) contribute significantly to its antimicrobial activity. It is widely used as antiseptic on skin. Literature reports manuka oil is also used as an insecticidal agent (Porter and William, 1999).

1.3.2.5 Myrtle Oil

Myrtle oil is isolated from *Myrtus communis*, it is a commonly encountered plant in the Mediterranean area, and is mainly used as animal and human food and, in folk medicine, for

treating some disorders. Pirboulati (2014) studied the antimicrobial activity of myrtle leaves against *Erysipelothrix rhusiopathiae* (Gram-positive), not only demonstrating this activity, but also showing the major components of the oil were α-pinene (22.3%-55.2%), 1,8-cineole (8.7%-43.8%) and linalool (6.4%-14.5%).

1.4. Interaction between combined antimicrobials

Over the last few years, the absence of new antibiotics has led to an extensive use of existing drugs, thus increasing the level of resistance to them. This threat is being countered via the use of combinations of antibiotic drugs as it is argued that resistance to the combination will not yet have developed and it will be more difficult for the organism to develop such resistance (Cotterel et al., 2007).

When two antimicrobial agents (i.e. antibiotic drugs, nano-antibiotics and essential oils) are combined one of the following four outcomes can occur (Kalan et al., 2011).

- Synergy is when the effect of the combination of two drugs is greater than the summed effect of the individual drugs
- Additivity is when the combined effect is equal to the sum of the effect of the individual drugs.
- Antagonism is when the combined effect is less than the sum of the effect of the individual drugs
- Autonomy is when the effect of the combination is that equal to the most active antibiotic in the combination

1.5. Controlled release systems for antimicrobials

The use of antibacterial and antifungal substances to stop bacteria and fungi from growing is well established. However, a common problem is that most antimicrobials are not chemically compatible with the host polymer, be it a thermoplastic or surface coating system. Furthermore, the antimicrobial active molecules are often of lower molar mass and hence volatile and/or easily extractable or removed from the polymer surface to be protected. This incompatibility and volatility/extractability leads to the antimicrobial being released from the polymer formulation far too rapidly. The latter effect leads to initial over-dosage, rapid depletion and short-lived antimicrobial activity. Researchers therefore have been actively seeking methods via which the antimicrobials can be released in a sustained manner.

A number of controlled release systems for antimicrobials have been studied. Early work investigated use of gel silicas for encapsulation of isothiazolinones and terpenes (Coulthwaite et al., 2005), studies then progressed to exploration of layered silicates, both synthetic and natural, for acting as reservoirs for Triclosan and essential oils (Kinninmonth et al., 2014 and Liauw et al., 2011). The more recent work has examined synthetic zeolites as carriers for silver (Dong et al., 2014). The current investigation further investigates organically modified and unmodified natural layered silicates as carriers for essential oils and metal ions, respectively.

Both metallic ions and essential oils (EO) antimicrobials will benefit enormously from encapsulation within layered silicates; EOs are particularly volatile and incompatible with many polymers, leading to surface blooming and rapid loss by evaporation. Addition of metal salts directly to a polymer formulation could lead to excessively rapid release.

Some published studies on controlled release systems for EOs in polymeric materials have focused on organic carriers. The major limitation of organic carriers is that they cannot withstand the harsh thermal, pressure and shear conditions used for the production or manufacturing of polymers. Under such conditions, the organic carriers are often damaged, leading to rapid loss of the EOs form the formulation (Kinninmonth et al., 2013). The absorption/adsorption of EOs into inorganic porous materials followed by incorporation into the polymer system could prevent these materials from being damaged under polymer processing-conditions and provide eventual sustained release of the EOs.

Organically modified and unmodified (sodium) montmorillonite (o-MMT and Na-MMT, respectively) were the subject of this MPhil study. MMT has a high specific surface area (Dong et al., 2014) typically because of its layered structure, organic modification also allows tailoring of the polarity of the galleries between platelets. It can therefore be argued that MMT/o-MMT are ideal adsorbants for organic materials such as EOs and metal ions, respectively. The latter can be incorporated via exchange reactions with the metal ions originally present in the MMT galleries.

1.5.1. Smectite clays including montmorillonite

The inorganic carriers that were the subject of this study are generally known as Smectite clay minerals. Montmorillonite is a common example of a smectite. Such minerals are naturally occurring hydrous aluminium phyllosilicates that often incorporate variable amounts of iron, magnesium, alkali metals, alkali earths and some other cations (Pavlidou et al., 2007)

Depending on the arrangement of tetrahedral silicate sheets or octahedral alumina sheets, clay minerals are classified as 1:1 or 2:1. A 1:1 clay mineral consists of an octahedral alumina

sheet and a tetrahedral silicate sheet, whilst a 2:1 clay mineral consists of a tetrahedral silicate sheet in between two octahedral alumina sheets. Smectites fall within the latter category (Odom, 1984).

Silica sheets are made up of a silicon atom being surrounded by four oxygen atoms, thus forming a tetrahedron. The apex of the tetrahedron is pointing towards the octahedral alumina (or mixed aluminium/magnesium oxide) sheet that forms the central layer.

Alumina (or mixed Al/Mg oxide) sheets share the oxygen atoms located at the top of the tetrahedron. Hydroxyl ions sit between the oxygen atoms at the apex of the tetrahedral to partially balance the charge on the structure, giving a theoretical composition of $(OH)_4Si_8Al_4O_{20}nH_20$. The platelets however, have an overall negative charge due to the mix of Al and Mg oxide. The amount of negative charge is dependent on the ratio of Al to Mg. The negative charge is balanced by metal cations that sit on the surface of the platelets and therefore reside within the gallery spaces between the platelets (Figure 1.4)

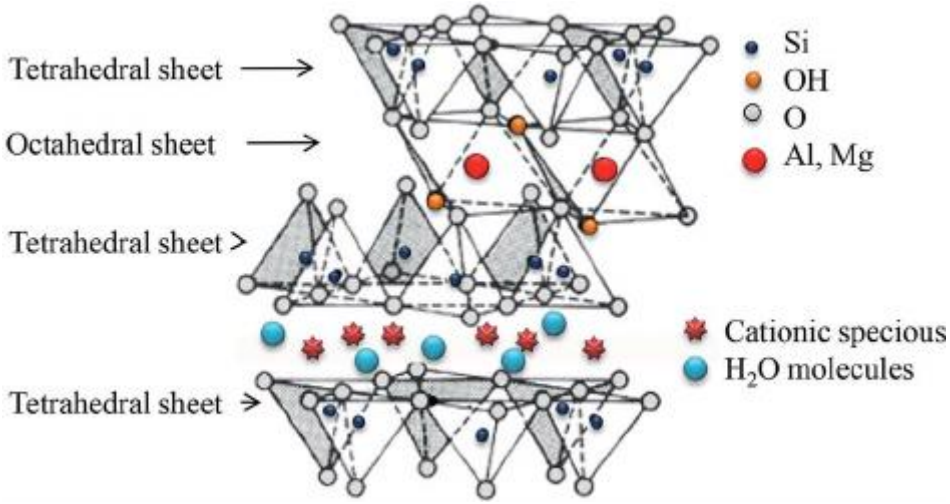

Figure 1.4. Typical Smectite structure

(https://www.researchgate.net/figure/274095227_Smectite-structure-of-a-2-1-clay-mineral-showing-two-tetrahedral-sheets-sandwiched)

The cations in the gallery can be exchanged with other cations, both metallic and organic. Small molecules can also be adsorbed within the galleries. The platelets have a thickness of 0.95-0.96nm (Odom, 1984). The distance between the layers and the galleries is dependent on the size of the ions. Metal ions in the gallery are surrounded by a hydration sphere of water molecules, this results in a hydrophilic environment. Substitution of the metal cations with an organic cation such as octadecyl ammonium will lead to an increase in the spacing between the platelets and cause the gallery environment to become hydrophobic. The latter will lead to adsorption of organic molecules such as essential oils.

1.6 Thesis methodology

The project consisted of two interlinked parts;

a) Aim 1: Antimicrobial testing efficacy regime (Chapter 2).

The first stage of this project was to identify the best EO/metal combination in terms of the antimicrobial activity against the proposed microbial challenges (*S. aureus* and *P. aeruginosa*). A set of metal ions (Silver, Palladium and Platinum) and EOs (Rosewood Oil, Orange Oil, Myrtle Oil, Clove Leaf Oil and Manuka Oil) were initially assessed individually against the bacteria. The next step was to investigate the effect of blending selected EO and metallic antimicrobials to observe any synergy or antagonism.

b) Aim 2: Encapsulation of the most potent antimicrobial agents on MMT/o-MMT, characterisation of the latter and rudimentary antimicrobial assessment (Chapter 3).

The first part of chapter 3 covers the incorporation (adsorption) of the selected antimicrobial agents into either MMT or o-MMT. A range of o-MMTs with varying gallery polarity was evaluated for EO compatibility and adsorption capacity using thermal

gravimetric analysis (TGA), wide angle X-ray scattering (WAXS) and diffuse reflectance infrared Fourier transform spectroscopy (DRIFTS).

Metal ions were incorporated into MMT via ion exchange. The level of metal adsorption was monitored using atomic absorption spectroscopy (AAS) of the treating solutions and energy dispersive analysis (EDX) of the treated MMT, both unwashed and washed.

Rudimentary assessment of the antimicrobial efficacy of the metal and EO loaded MMT/o-MMT was also performed.

CHAPTER 2. ANTIMICROBIAL EFFICACY TESTING REGIME

Summary

Essential Oils (EOs) and metal ions have been used and studied for their antimicrobial performance against pathogens for centuries. This study assessed their use as broad spectrum antimicrobial agents for commercial purposes on paints, coatings or elastomeric formulations with intended antibacterial activity. The EOs; Rosewood Oil (RO), Clove Leaf Oil (CLO) Orange Oil (OO), Myrtle Oil (MO), and Manuka Oil (MNO) and metals; silver (Ag), palladium (Pd) and platinum (Pt), were examined as individual oils and metal ions and then as blends. The microbial challenges were *Staphylococcus aureus* (Gram-Positive) and *Pseudomonas aeruginosa* (Gram-Negative); antimicrobial efficacy against these organisms was assessed using Zone of inhibition (ZoI), micro dilution and checkerboard micro broth dilution method. ZoI proved to be a reliable qualitative method for assessment of the antimicrobial metallic ions. Nutrient Agar (NA) was found to be the most effective media for higher metal ion concentration (>100 mg/L) and Mueller-Hinton (MH) agar was more effective at lower metal ion concentrations (<100 mg/L). However, ZoI tests (using wells, solid diffusion or vapour diffusion) proved to be ineffective for assessment of the antimicrobial efficacy of EOs. For individual metal ions, all three metals tested (Ag, Pd and Pt) gave a Minimum Inhibitory Concentration (MIC) of 25 mg/L, silver was the only ion that gave a Minimum Bactericidal Concentration (MBC) of 25 mg/L, all the other metals examined gave higher MBC values. For individual essential oils, MNO gave the highest level of antimicrobial performance at an MIC of 2.5%(v/v), none of the EO were potent enough to give MBC values at the highest concentrations investigated. Blends of Ag (50 mg/L) + RO

(20%(v/v)) and Ag (50 mg/L) + MNO (5%(v/v)) in a 1:2 ratio shared the highest level of antimicrobial performance, as measured MIC and MBC.

2.1. Introduction

The antimicrobial activities of metallic antimicrobial agents (Ag, Pd and Pt in their ionic form) and a range of essential oils (rosewood oil (RO), clove leaf oil (CO), orange oil (OO), myrtle oil (MO) and Manuka oil (MNO)) was evaluated against selected targeted microorganisms (*S. aureus* and *P. aeruginosa*). This screening was carried out using Zones of Inhibition (ZoI), as well as a solid diffusion test and vapour diffusion test. Minimum inhibitory concentration (MIC) and minimal bactericidal concentration (MBC) were also determined using dilution methods. The most effective individual metallic ions and essential oils were then assessed in combination using micro-titre plate assays in order to observe synergistic combinations.

The scope of this project is to demonstrate the effectiveness of EOs individually (and blended with metallic ions) as antimicrobial agents. The selection of EO for this project is based on the breadth of their activity (i.e. effective against both bacteria and fungi) and then tested against the selected target microorganisms (*S. aureus* and *P. aeruginosa*).

2.1.1 Screening and evaluating methods

Antimicrobial resistance (AMR) has led to true interest in researching and developing new antimicrobial agents originated from several different sources (Balouiri et al., 2016). As a result of this growing interest, it is of a great importance to define and further develop a number of methods that will allow screening and evaluating the antimicrobial activity of the agents and their usefulness against those microbes posing antimicrobial resistance. Over the

last decades, several methods have been developed, being the most common ones diffusion and dilution methods.

2.1.1.1 Agar dish-method method

Being developed in 1940 (Heatly, 1944), agar diffusion methods are now routinely established in a large number of clinical microbiology laboratories around the world. The Clinical and Laboratory Standards Institute (CLSI) publish standards for such tests. This test provides a measure of the susceptibility of the bacteria to antibiotic activity and it is carried out using zone of inhibition assays (ZoI). The ZoI is the area on an agar plate where growth of an organism is prevented by an antibiotic/antibacterial agent, the greater the antimicrobial activity, the greater the diameter of the inhibited zone observed around the sample.

However, it is worth pointing out that ZoI assays do not provide information regarding bactericidal effects of the antimicrobial agent tested. ZoI does not distinguish between bactericidal and bacteriostatic affects. The amount of antimicrobial agent diffused into the agar is impossible to determine, therefore MIC cannot be determined from ZoI data. On the other hand, diffusion test are low cost, simple and have relatively rapid throughput, the data obtained is also relatively easy to understand. The aforementioned advantages led to diffusion test methods becoming reference methods for antimicrobial screening of plant extracts, essential oils and other biocides (Das et al., 2010).

2.1.1.2. Dilution method

Dilution methods are the most appropriate for determination of minimum inhibitory concentration (MIC) values, since the concentration of the tested antimicrobial agent in the

agar (agar dilution) or broth medium (broth dilution) can be estimated. Minimum inhibitory concentrations are defined as the lowest concentration of an antibiotic/antimicrobial agent that will inhibit the visible growth of a microorganism after overnight incubation. MIC is often coupled with minimum bactericidal concentration (MBC) as for providing full information in regards to the efficacy of a given antimicrobial agent against a microbe and is defined as the lowest concentration of an antibiotic/antimicrobial agent required to kill a particular bacteria. Usually MBC is determined by agar diffusion test methods (Balouiri et al., 2016).

Dilution method standards are also defined by CLSI and provide with advised guidelines for a uniform procedure for telling which is to act as a reference for most clinical microbiology laboratories.

2.2 Methods

2.2.1. Growth of Bacteria in Different Media

2.2.1.1 Maintenance of microorganisms

The microorganisms *S. aureus* (NCTC 6571) and *P. aeruginosa* (NCTC 12903) were used for this investigation. Stock cultures were stored in a freezer at -80 °C. When the microorganisms were required, cultures were thawed and inoculated onto nutrient agar media and incubated at 37 °C for 24 h. Following use, stock cultures were re-frozen. Inoculated agar plates were kept refrigerated over the investigation at 4 °C, and were replaced every four weeks in order to maintain the cells physiologically.

2.2.1.2 Sub-culturing microorganisms

A fresh sub-culture of both microorganisms was prepared every two weeks by streaking onto a fresh agar plate Trypticase soy agar (TSA) and incubating the plate at 37 °C for 24 h.

2.2.1.3 Preparation of overnight broth

Trypticase soy broth (TSB, Oxoid CM0067, UK) was made as per manufacturer's instructions (3 g TSB in 100 mL of distilled water), autoclaved at 121 °C for 15 minutes, then cooled at room temperature. A sterile loop was used to remove one colony from the sub-cultured agar plates, this was then inoculated into a sterile Trypticase soy broth (TSB) and then incubated at 37 °C for 24 h.

2.2.1.4 Preparation of agar

For the initial investigation, six different media were prepared for culturing: Trypticase soy agar (TSA, Oxoid CM0331, UK), Nutrient Agar (NA, Oxoid CM0003, UK), ISO Agar (Oxoid CM0471, UK), Mueller-Hinton Agar (MH, Oxoid CM0337, UK), Thyoglicollate Agar (Oxoid CM0331, UK), Letheen Agar (LabM, Lab 185, Lancashire, UK). The latter were made up in accordance with the manufacturer's instructions then autoclaved at 121 °C for 15 minutes and cooled to 55 °C, then poured into triple vent Petri dishes (SLS Select, UK).

2.2.1.5 Estimation of bacterial numbers

Ten-fold dilutions were prepared to generate a dilution series from 10^{-1} to 10^{-8}. One hundred microlitres from each dilution was added to the surface of a dried agar plate (repeated twice). The bacterial suspension was dried onto the surface and incubated at 37 °C for 24 h.

The dilutions were performed in order to estimate the colony forming units per millilitre (CFU/mL). The average number of colonies observed from streaking out 100 µL onto the agar surface was multiplied by 10 in order to obtain the CFU in 1 mL. This value was further divided by the dilution factor to determine CFU/mL of the original broth culture.

2.2.2 Antimicrobials

Metal ions and essential oils were used as antimicrobials agents for this investigation.

2.2.2.1 Metals

Silver (Fluka 39361), palladium (Fluka 78437) and platinum (Fluka 47037) solutions were obtained from Sigma Aldrich (UK). The metals were reacted with acids (see Section 1.3.1.1) to produce water soluble salts of the required metal concentration.

2.2.2.2 Essential Oils

Rosewood oil (6709), clove leaf oil (6683), orange oil (6554), myrtle oil (7695), and manuka oil (7695) (all from Essential oils direct (UK)), were diluted to the required concentration using grapeseed oil.

2.2.3 Zone of Inhibition

Zone of Inhibition (ZoI) assays are widely used in microbiology to test for the susceptibility of bacteria to an antimicrobial agent.

Three ZoI methods were used to assess antimicrobial efficacy against the selected microorganisms: Wells (metals and essential oils), solid diffusion test/discs (essential oils) and vapour diffusion test (essential oils).

2.2.3.1 ZoI from wells in the agar

(i) Metal ions: Trypticase soy broth (100 mL) was inoculated with *S. aureus* or *P. aeruginosa*. They were incubated overnight in an orbital incubator at 37 °C for 24 h at 130 rpm. The cultures were removed from the incubator and the cells washed by centrifuging at 3600 rpm for 10 minutes. The supernatant was then removed and cells were re-suspended in 25 mL of sterile distilled water. The cells suspension was adjusted to an optical density (OD) of 1.0 at 540 nm using a spectrophotometer (Jenway model 6305 Bibby Scientific Ltd, Essex, UK). Sterile Petri dishes were filled with 25 mL of the media. In this investigation TSA, NA, Thioglycollate, Leethen, ISO and Mueller-Hinton media were tested. One hundred microlitres of the bacteria were spread out across the surface, then three wells per dish were punched into the agar surface using a sterilised cork borer (70 % vol ethanol and flamed). A cell suspension adjusted to 1.0 OD was used for the estimation of CFU/mL as described in 1.1.5 – Estimation of bacterial numbers.

Three metal commercial solutions (silver, platinum or palladium, 1000 mg/L in 5% HNO_3 (for Ag) and 1000 mg/L in 2% HCl (for Pt and Pd) were diluted to the following concentrations (1000 mg/L, 500 mg/L, 100 mg/L, 50 mg/L and 10 mg/L) and then assessed for antimicrobial activity by ZoI. Each of the solutions (100 μL) was added to a previously punched well in the agar. Samples were incubated at 37 °C for 24 h. A summary of the preparation of formulations described in the above section is presented (Appendix 1, Chapter 1), as well as a summary of the results obtained (Appendix 2, Chapter 2)

(ii) Essential oils: In order to carry out the ZoI assay for *S. aureus* and *P. aeruginosa,* samples were prepared as described in Section 2.2.1.4. The media tested were NA and TSA (due to results obtained with metal ions, the media tested was narrowed down to those showing the best antimicrobial efficacy in terms of the ZoI recorded).

Five essential oils (rosewood, clove leaf, orange, myrtle and manuka) were tested at the following dilutions in grape seed oil: 5% (v/v), 2.5% (v/v), 1% (v/v) and 0.5% (v/v). One hundred microlitres of each oil at each dilution were added to wells in agar plates. The samples were incubated at 37 °C for 24 h. A summary of the preparation of formulations described in the above section is presented (Appendix 3, Chapter 1)

2.2.3.2 Diffusion tests for antimicrobial efficacy of essential oils

(i) Solild diffusion test (SDT): The bacteria were prepared as described in Section 2.2.1.4. Following bacterial inoculation of the agar, three 10 mm diameter sterile blank absorbent cellulose discs (Whatman Grade A filter paper, UK) were placed on the agar surface of each media and 100 µL of the corresponding essential oil tested (2.5%, 1% and 0.5% (v/v) in grapeseed oil) was pipetted onto the disc. Samples were then incubated at 37°C for 24 h.

(ii) Vapour diffusion test (VDT): The bacteria were prepared as described in Section 2.2.1.4. Following bacterial inoculation of the agar, three 10 mm sterile blank discs were attached onto the inside lid of the Petri dish using Vaseline, such that the disc surface faced the agar surface of each media. One hundred microliters of the corresponding essential oil tested (2.5%, 1% and 0.5% (v/v) in grapeseed oil) was added to the disc. Samples were then incubated at 37 °C for 24 h. A summary of the preparation of formulations described in both the above section is presented (Appendix 4, Chapter 1).

2.3 Determination of Minimum Inhibitory Concentration (MIC) and Minimum Bactericidal Concentration (MBC)

Both methods were used to assess the antimicrobial efficacy of the selected agents (metal ions and essential oils) against the bacteria, *S. aureus* and *P. aeruginosa.* Further tests involving blending the best performing agent of each type (at the selected concentration) were also carried out in order to assess the potential synergy of the mixtures.

2.3.1 Preparation

A single colony of either *S. aureus* or *P. aeruginosa* was inoculated into 100 mL of TSB. The inoculated cultures were incubated overnight at 37 °C for 24 h in an orbital incubator at 130 rpm, and growth was observed the following day. The cells suspension was adjusted to $1x10^6$ CFU/mL. The CFU were counted on agar and estimated to be $1x10^9$ CFU/mL, so a further dilution using distilled water was made to obtain $1x10^7$ CFU/mL. The final dilution was made using a double strength TSB with Triphenyl Blue Chloride TBC (Sigma Aldrich, UK) and Tween 20 (Sigma Aldrich, UK) to obtain the desired $1x10^6$ CFU/mL.

2.3.2 Metal ions - MIC

2.3.2.1 Determination of minimum inhibitory concentration

Using a 96 flat-bottomed micro titre plate (MTP) (Figure 1) wells A1 to A5 were filled, using an auto pipette, with 75 µL of the target cell suspension (*S. aureus* or *P. aeruginosa*) at $1x10^6$ CFU/mL in an overnight culture of double strength TSB containing 0.15 % (m/v) TBC and 1.5 % (m/v) Tween 20. Seventy five microlitres of metal ions (silver, palladium and platinum) at the desired concentrations were added to appropriate wells (well A1 containing the highest concentration and A5 containing the lowest concentration, metal ions concentrations were

1000 mg/L, 500 mg/L, 100 mg/L, 50 mg/L and 10 mg/L). The metal ions and cell suspension were thoroughly mixed using an auto-pipette. This process was repeated using the other columns to obtain two more replicates. The MTP was covered, using lids supplied by the manufacturer, and placed in an incubator at 37°C for 24 h. After 24 h the plates were inspected for growth, which was indicated by a blue colour produced by the TBC metabolic dye. The well corresponding to the minimum inhibitory concentration (MIC) was taken to be the first well showing no sign of blue colouration. A summary of the formulations described in the above section is presented (Appendix 5).

2.3.2.2 Determination of minimum bactericidal concentration

Minimum bactericidal concentration (MBC) was performed by taking a 10 µL aliquot of contents from each well that displayed no sign of visible growth, and 10 µL of contents from the first well that showed growth. To check for bacterial growth, each 10 µL aliquot was then placed onto the agar plates that were previously divided into eight radial sectors. The plates were incubated at 37 °C for 24 hours. The first concentration which produced no growth from the 10 µL aliquot was taken to be the MBC

		1	2	3	4	5	6	7	8	9	10	11	12
A													
B													
C													
D													
E													
F													
G													
H													

Figure 2.1. Ninety six well micro titre plate used to illustrate how the MIC, MBC and synergy methods were carried out.

2.3.3 Essential oils

2.3.3.1 MIC determination for essential oils

For the MIC determination of individual essential oils, the procedure described in Section 2.3.2.1 was followed. For this test however, 75 µL of essential oils (rosewood oil (RO), clove leaf oil (CLO), orange oil (OO), myrtle oil (MYO) and manuka oil (MNO)) at the desired concentrations were added to appropriate wells (well A1 containing the highest concentration and A5 containing the lowest concentration, EO concentrations were 20%, 10%, 5%, 1% (v/v) in grapeseed oil). A summary of the formulations described in the above section is presented (Appendix 4, Chapter 1).

2.3.3.2 MBC determination for essential oils

For the MBC determination of individual essential oils, the procedure described in Section 2.3.2.2 was followed.

2.4 Investigation of Possible Antimicrobial Synergy Between Metals and Essential Oils

Synergy tests were carried out by blending the metal that demonstrated both the best bacteriostatic and bactericidal effect (Ag) with the two EOs showing the best antimicrobial efficacy (RO and MNO).

After screening both metal ions and essential oils individually using the MIC/MBC tests, it was decided that silver (Ag, 100 mg/L and 50 mg/L), rosewood oil (RO, 20% (v/v)) and manuka oil (MNO, 5% (v/v)) will be further tested for synergistic activity. Following this, four synergistic combinations were investigated: Ag(100 mg/L) + RO (20% (v/v)), Ag(100 mg/L) + MNO (5% (v/v)), Ag(50 mg/L) + RO (20% (v/v)), Ag(50 mg/L) + MNO (5% (v/v)). A summary of the final concentrations tested for each sample is presented (Appendix 7, Chapter 1).

2.4.1 Investigation of synergy using the micro-titre plate method

Using a 96 well flat-bottomed micro-titre plate, 100 µL of the first compound (Ag at the specified concentration) and 50 µL of the second compound (RO or MNO at the specified concentration) were pipetted into the well A3 to give a 2:1 dilution. Seventy five microlitres of both compounds were then pipetted into the well A4 to give a 1:1 dilution and 50 µL of the first compound (Ag) and 100 µL of the second compound (RO or MNO) were pipetted into A5 to give a 1:2 dilution. One hundred and fifty microlitres of the cell suspension adjusted to 10^6 CFU/mL (see Section 2.3.1.) in a double strength solution of TSB containing

0.15 % (m/v) TBC and 1.5 % (m/v) tween 20. The cell suspension was added to each well in columns A3, A4, A5 (row A) working downwards until reaching row D. The samples were thoroughly mixed using a multi-channel pipette. One hundred and fifty microlitres of the mixture of the inoculation and compounds was removed from wells in row A and transferred down to row B, and mixed thoroughly. The operation was repeated across all the wells in a downward direction, until reaching row D, where 150 µL were disposed of after being removed from wells. The MTPs were covered, using lids supplied by the manufacturer, and placed in an incubator at 37 °C for 24 hours. There were inspected next day for growth. Growth was indicated by a blue colour produced by the TBC metabolic dye. The well corresponding to the minimum inhibitory concentration (MIC) was taken to be the first well showing no sign of blue colouration.

2.5 Results

2.5.1 Estimation Bacterial Numbers (CFU/mL)

Prior to starting the inoculation of the bacteria on each media, the cell suspension was adjusted to 1.0 OD. An overnight suspension was diluted in a ten-fold series (10^{-1} to 10^{-8}) and spread over the different media. Following cell counts the bacterial population growing on each media was the following (CFU/mL) (Figure 2.2) on a 10^{-6} dilution of the bacteria.

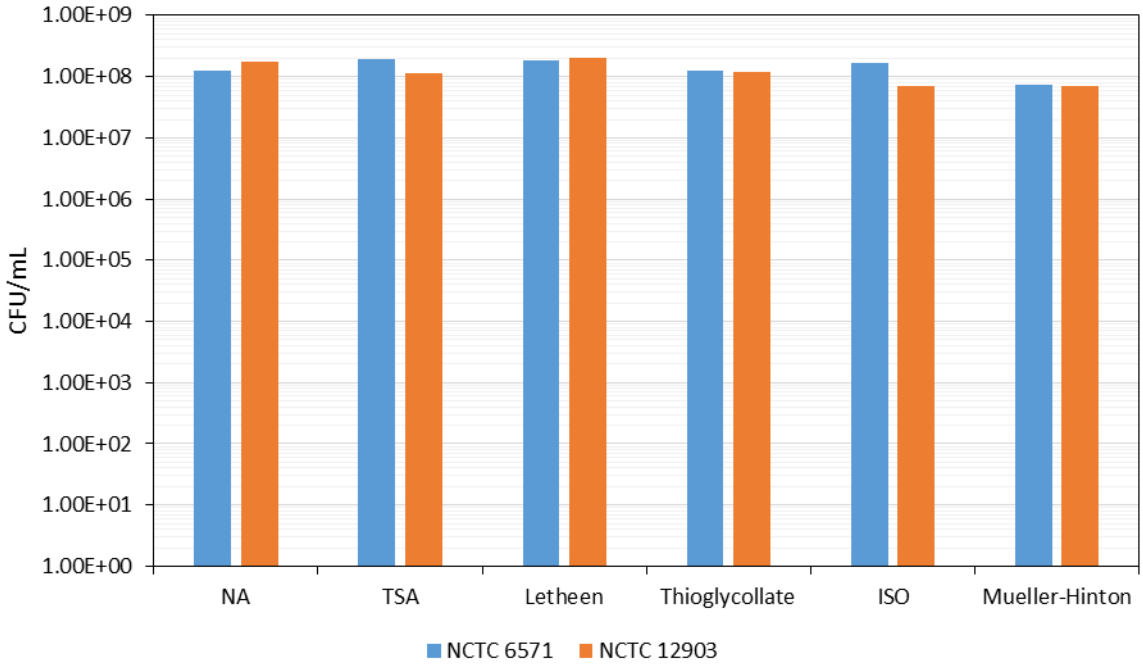

Figure 2.2 – Bacterial population on the media tested (NA = nutrient agar, TSA = tryptone soya agar, Letheen = Letheen agar, Thioglycollate, ISO = ISO agar and MH = Mueller-Hinton agar) after overnight incubation at 37 °C (*S. aureus* and *P. aeruginosa*). Results showed all the bacterial population ranges over $1x10^8$ CFU/mL, after being adjusted to 1.0 OD at 540 nm.

2.5.2 Zone of Inhibition

2.5.2.1 Wells in the agar

(i) Metals: Each of the three metallic ions (silver (Ag), palladium (Pd) and platinum (Pt)) and their controls (hydrochloric acid (HCl) and Nitric Acid (HNO_3)) were tested for antimicrobial efficiency against *S. aureus* and *P. aeruginosa* (Figure 2.3 and Figure 2.4). The results for each microorganism and concentration can be summerised by the following key points;

S. aureus at 1000 mg/L and 500 mg/L for 1000 mg/L, for all the media screened at this concentration, both palladium and platinum ions showed the best antimicrobial efficacy. At

a concentration of 100 mg/L, a shift in the antimicrobial activity of the metal ions was observed; Letheen and Thiogycollate agars were the only media tested on which both platinum and palladium ions showed the best antimicrobial efficacy. However, on the TSA, ISO and MH agars, the silver ions presented the best antimicrobial efficacy, whilst on NA only the palladium ions showed antimicrobial efficacy. At concentrations of 50 mg/L**,** only silver ions presented antimicrobial efficacy on the TSA and Letheen agar. For the rest of the media, no ZoI results were observed. At 10 mg/L again differences were observed depending on the type of growth media used. Only silver ions presented antimicrobial efficacy on the MH agar. For the rest of the media, no results were observed in terms of ZoI produced.

The ZoI using wells demonstrated slightly different results against *P. aeruginosa,* at 1000 mg/L**,** as previously reported for *S. aureus*, both palladium and platinum ions showed the best antimicrobial efficacy. However in contrast to *S. aureus*, at 500 mg/L, platinum and palladium ions showed the best antimicrobial efficacy on Letheen, ISO, Thioglycollate and MH agar. However, on TSA, and NA, silver ions presented the best antimicrobial efficacy. At 100 mg/L, both palladium and platinum ions showed the best antimicrobial efficacy whereas at 50 mg/L, silver metal ions presented antimicrobial efficacy on NA, TSA and MH agar. Palladium and platinum showed higher antimicrobial efficacy on letheen agar. No antimicrobial activity was observed on Thioglycollate and ISO agar. Finally at 10 mg/L, as previously reported for *S. aureus*, at this concentration only the silver ions presented antimicrobial efficacy on MH agar. For the rest of the media, no results were observed in terms of ZoI measured.

Overall, it was observed that for both *S. aureus* and *P. aeruginosa,* that the best antimicrobial efficacies at higher concentrations (> 100 mg/L) were achieved by palladium and platinum ions, whilst better antimicrobial efficacy was obtained at lower concentrations (≤ 100 mg/L) are achieved by silver ions. It has been also demonstrated MH to give the most sensitive results at low concentrations (10mg/L).

2.1 – Zone of Inhibition data for *S aureus*, showing the antimicrobial efficacy of Ag, Pd, and Pt ions at different concentrations in mm. Values reported are an average taken from three replicates (standard deviations given in brackets).

1000 mg/L						
	NA	TSA	Letheen	Thioglycollate	ISO	MH
Ag	20.83 (0.41)	18 (0.63)	28.33 (1.37)	16.83 (0.41)	15.83 (0.48)	17.83 (0.75)
Pt	38.67 (1.63)	28.83 (0.75)	44.17 (1.17)	32.5 (0.84)	42.5 (2.17)	37 (1.09)
Pd	38.67 (1.10)	29.67 (0.47)	48.83 (0.90)	32.83 (0.37)	42.67 (1.86)	36.83 (0.69)
500 mg/L						
	NA	TSA	Letheen	Thioglycollate	ISO	MH
Ag	18.5 (0.84)	15.33 (0.52)	20.83 (0.41)	13.16 (0.41)	16.17 (1.17)	16.17 (0.75)
Pt	27.5 (1.52)	22.5 (0.55)	39 (0.89)	21 (4)	29.17 (2.63)	29.5 (1.22)
Pd	27.67 (1.37)	24.33 (1.70)	39 (0.89)	23.5 (0.5)	34.17 (1.57)	28.67 (0.74)
100 mg/L						
	NA	TSA	Letheen	Thioglycollate	ISO	MH
Ag	-	13 (0.63)	12.17 (0.41)	-	15.16 (0.75)	12.67 (0.52)
Pt	-	-	19 (0.63)	12.5 (0.55)	-	-
Pd	12.5 (0.5)	-	18.5 (0.76)	13.33 (0.47)	-	-
50 mg/L						
	NA	TSA	Letheen	Thioglycollate	ISO	MH
Ag	-	12.83 (0.41)	12.33 (0.52)	-	-	-
Pt	-	-	-	-	-	-
Pd	-	-	-	-	-	-
10 mg/L						
	NA	TSA	Letheen	Thioglycollate	ISO	MH
Ag	-	-	-	-	-	-
Pt	-	-	-	-	-	-
Pd	-	-	-	-	-	-

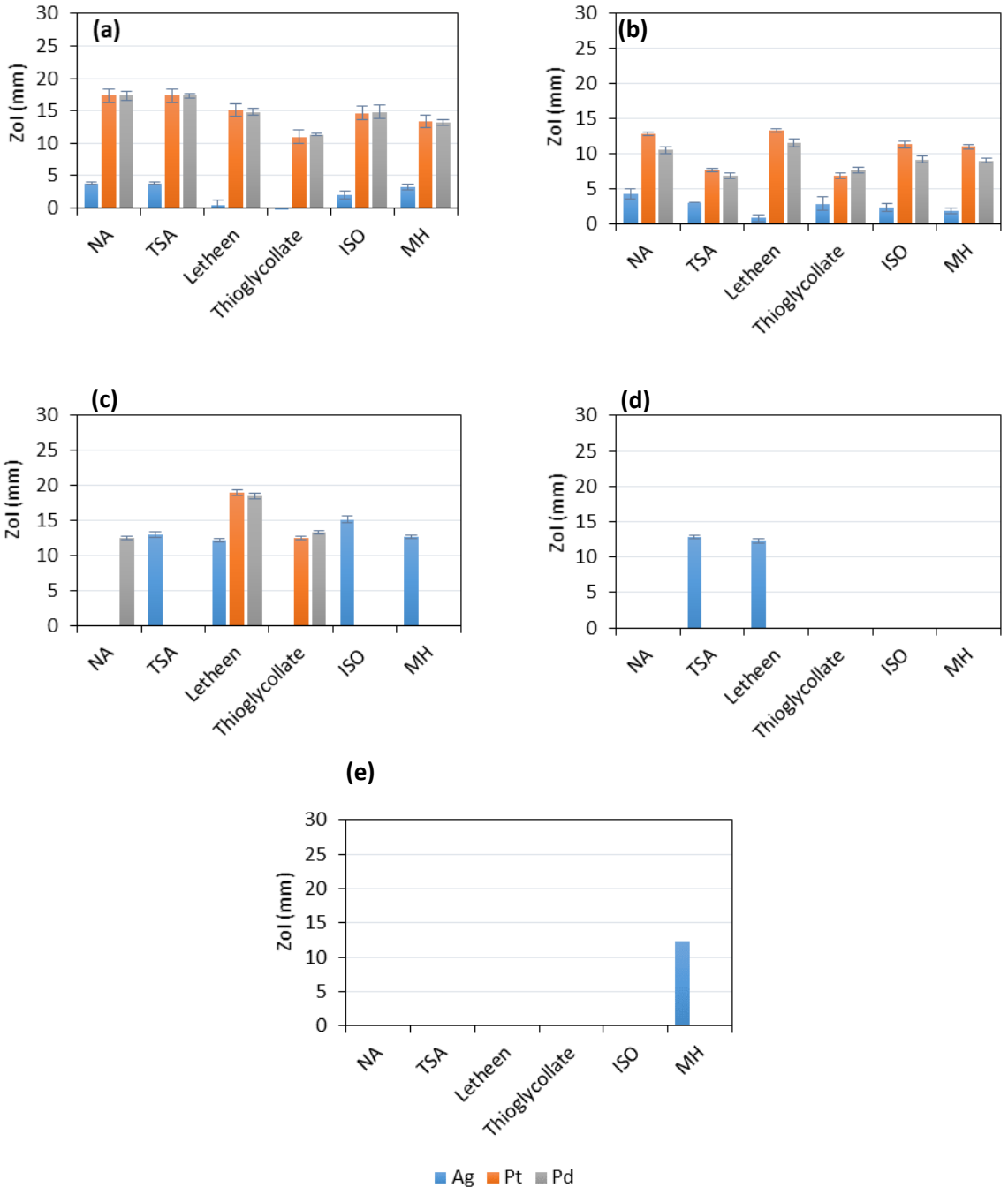

Figure 2.3 – Antimicrobial activity (as measured by agar well ZoI) of silver, platinum and palladium ions against *S. aureus* at concentrations of; (a) 1000 mg/L, (b) 500 mg/L, (c) 100 mg/L, (d) 50 mg/L and (e) 10 mg/L, on the indicated media. Pd and Pt achieve the best antimicrobial efficacies at ion concentrations ≥ 50 mg/L, whilst better efficacies at ≤ 50 mg/L are achieved by Ag.

Table 2.2 – Zone of Inhibition data for *P aeruginosa*, showing the antimicrobial efficacy of Ag, Pd, and Pt ions at different concentrations in mm. Values reported are an average taken from three replicates (standard deviations given in brackets).

1000 mg/L						
	NA	TSA	Letheen	Thioglycollate	ISO	MH
Ag	23.67 (1.96)	18.17 (0.41)	23.33 (1.21)	16.67 (0.82)	15.5 (0.55)	18.17 (0.75)
Pt	42.17 (1.47)	35.33 (12.11)	43.83 (1.17)	30.17 (0.98)	31 (0.89)	33.17 (1.72)
Pd	40.83 (1.34)	30 (0)	43.17 (1.34)	29.33 (0.74)	13.83 (1.41)	31 (1)
500 mg/L						
	NA	TSA	Letheen	Thioglycollate	ISO	MH
Ag	22 (1.27)	17 (0)	17.33 (0.82)	15.83 (1.72)	13.82 (0.98)	17.17 (0.75)
Pt	32.83 (0.41)	23.67 (0.52)	34.17 (0.41)	22.83 (0.75)	24 (0.59)	26 (0.63)
Pd	30.5 (0.96)	22.83 (0.69)	32.33 (0.94)	23.67 (0.74)	21.83 (0.74)	24 (0.58)
100 mg/L						
	NA	TSA	Letheen	Thioglycollate	ISO	MH
Ag	17 (0)	14.83 (0.41)	12 (0)	-	-	-
Pt	21.17 (0.98)	23 (0.63)	19.83 (0.41)	12.33 (0.51)	12.67 (0.52)	15.83 (0.75)
Pd	16.33 (0.74)	13.5 (0.5)	16.33 (0.74)	12.83 (0.68)	12.33 (0.47)	12.5 (0.5)
50 mg/L						
	NA	TSA	Letheen	Thioglycollate	ISO	MH
Ag	16.67 (0.81)	14.5 (0.55)	-	-	1.48 (0.04)	-
Pt	16 (0.89)	13 (0)	14.83 (0.41)	-	-	-
Pd	-	-	12.14 (0.37)	-	-	-
10 mg/L						
	NA	TSA	Letheen	Thioglycollate	ISO	MH
Ag	-	-	-	-	-	12.33 (0.52)
Pt	-	-	-	-	-	-
Pd	-	-	-	-	-	-

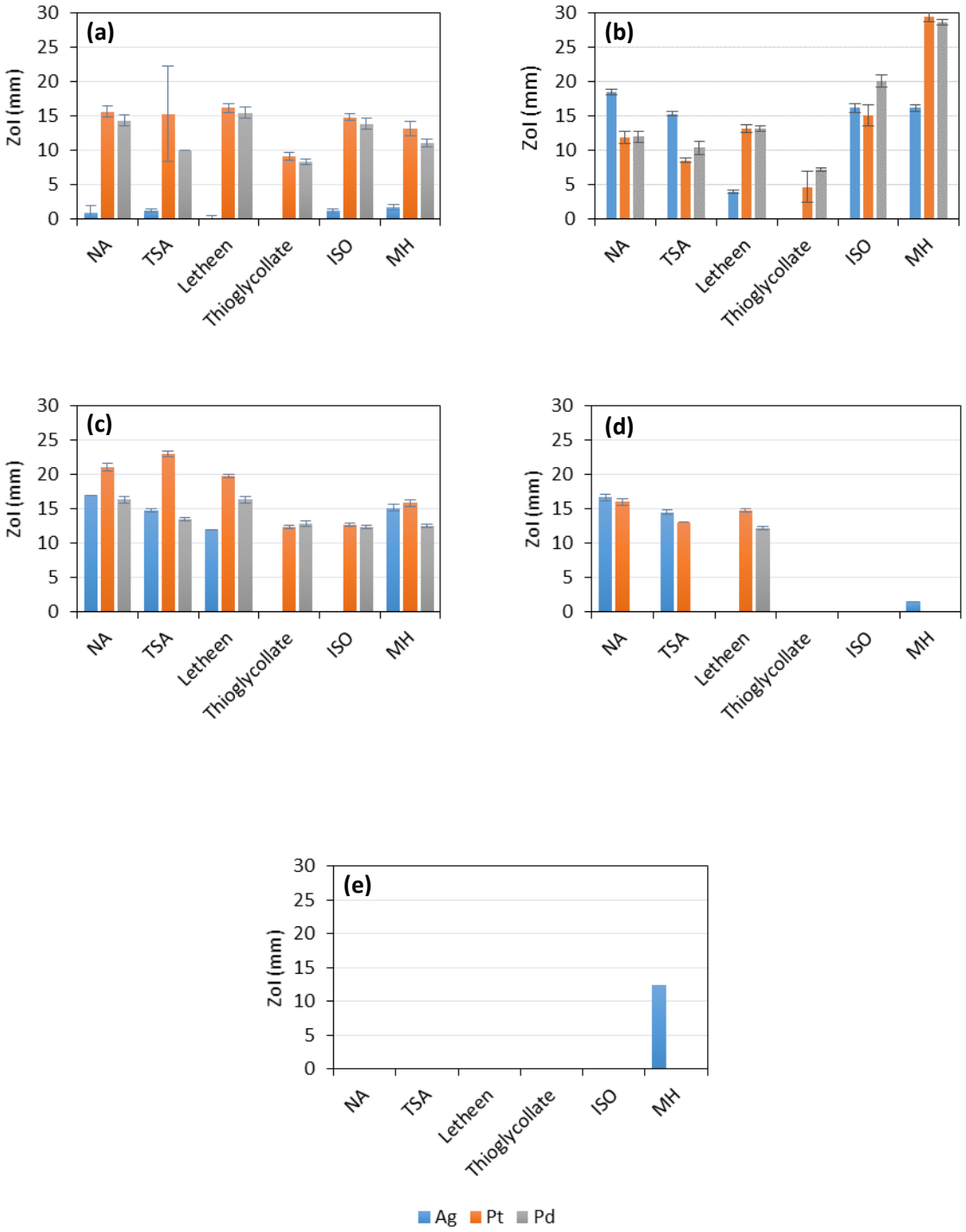

Figure 2.4 – Antimicrobial activity (as measured by agar well ZoI) of silver, platinum and palladium ions against *P. aeruginosa* at concentrations of; (a) 1000 mg/L, (b) 500 mg/L, (c) 100 mg/L, (d) 50 mg/L and (e) 10 mg/L, on the indicated media. Pd and Pt showed best antimicrobial efficacies at ion concentrations ≥ 100 mg/L, whilst Ag performed better at concentrations ≤ 100 mg/L

(ii) Essential oils: Although metal ions demonstrated ZoI against bacteria when essential oils were tested at concentrations of 5% (v/v), 2.5% (v/v), 1% (v/v) and 0.5% (v/v) they did not form zones of inhibition using the agar well assay method.

2.5.2.2 Diffusion tests for antimicrobial efficacy of essential oils

(i) Solid diffusion test (SDT): Because the well method had not produced ZoI for the essential oil, the solid diffusion test (SDT) method was used. Again when using the solid disc method, essential oils did not form zones of inhibition (ZoI) at concentrations of 2.5% (v/v), 1% (v/v) and 0.5% (v/v).

(ii) Vapour diffusion test (VDT): Since neither of the previous assays had worked the vapour diffusion test (VDT) method was used to determine if the EO volatiles would be active against the bacteria. However, essential oils did not form zones of inhibition (ZoI) using the vapour diffusion disk assay method.

2.5.3 MIC/MBC Determination

2.5.3.1 Metal ions – MBC/MIC

Each of the three metal ions (silver (Ag), palladium (Pd), platinum (Pt)) were tested on TSB media for antimicrobial efficacy against *S. aureus* and *P. aeruginosa* (Table 2.1).

All three metals tested (Ag, Pd, Pt) inhibited the visible growth of an overnight culture of the targeted microorganisms at 25 mg/L, at the lowest concentration investigated. However, the MBC for Ag was 25 mg/L, whilst for the other metal ions tested, the concentration required for killing the bacteria was greater than 25 mg/L.

Table 2.3 – MIC and MBC data from MTP assays, showing the antimicrobial efficacy of Ag, Pd, and Pt ions at different concentrations (mg/L). Values reported are an average taken from three replicates (standard deviations given in brackets).

Metal Ion	*Staphylococcus aureus*		*Pseudomonas aeruginosa*	
	MIC (mg/L)	MBC (mg/L)	MIC (mg/L)	MBC (mg/L)
Ag	25 (0)	25 (0)	25 (0)	25 (0)
Pd	25 (0)	>25 (0)	25 (0)	>25 (0)
Pt	25 (0)	>25 (0)	25 (0)	>25 (0)

For the subsequent synergy experiments, only Ag was selected as it was effective at usefully low concentration not only in tests on different growth media and the MIC test, but also most importantly, in the MBC tests. Economic factors were also taken into account on selecting Ag for further tests, as it was the cheapest metal of those screened.

2.5.3.2 Essential oils – MBC/MIC

Each of the five essential oils (rosewood oil (RO), clove leaf oil (CO), orange oil (OO), myrtle oil (MYO) and manuka oil (MNO)) were tested for antimicrobial efficacy against *S. aureus* and *P. aeruginosa* (Table 2.2).

The best essential oil in terms of antimicrobial efficacy was manuka oil, showing an MIC of 2.5 % (v/v) in all the three replicates performed. None of the essential oils were bactericidal at the concentrations investigated (no MBC could be recoded at concentrations less than 10

% (v/v)). The MIC / MBC determinations for the EOs did not always give clear results; for example, rosewood oil gave an indication of antimicrobial activity by a noticeable reduction in colouration of the metabolic dye. They also appeared to be a concentration dependent; high concentrations did not give such definitive results. Rosewood oil was therefore included alongside manuka oil in subsequent investigations. Clove leaf oil also showed a weak indication of antimicrobial activity but was not considered sufficiently active for further evaluation.

Table 2.4 – MIC and MBC data from MTP assays, showing the antimicrobial efficacy of the tested essential oils (RO, CO, OO, MYO, MNO) at different concentrations. Values area an average taken from three replicate).

EO Type	*Staphylococcus aureus*		*Pseudomonas aeruginosa*	
	MIC (% (v/v))	MBC (% (v/v))	MIC (% (v/v))	MBC (% (v/v))
RO	>10 (0)	>10 (0)	>10 (0)	>10 (0)
CO	>10 (0)	>10 (0)	>10 (0)	>10 (0)
OO	>10 (0)	>10 (0)	>10 (0)	>10 (0)
MYO	>10 (0)	>10 (0)	>10 (0)	>10 (0)
MNO	2.5 (0)	>10 (0)	2.5 (0)	>10 (0)

2.5.3.3 FIC values for MIC synergy tests

The FIC was used to determine the synergistic antimicrobial efficacy of the metals and essential oils in combination in a solution

Table 2.5 – FIC values for MIC synergy tests.). Values reported are an average taken from three replicates (standard deviations given in brackets)

	Ag100 + R20	Ag50 + R20	*Ag100 + Mn5*	*Ag50 + Mn5*
2:1	*1.19 (0.22)*	*0.99 (0)*	*1.66 (0)*	*0.99 (0)*
1:1	*1.25 (0.21)*	*1(0)*	*1.5 (0)*	*1 (0)*
1:2	*0.88 (0.19)*	*1 (0)*	*1.33 (0)*	*1 (0)*

2.6 Discussion

The metal ions and essential oils were screened as potential antimicrobial agents against *S. aureus* and *P. aeruginosa*, first individually the best antimicrobials from ZoI screening were then combined and investigated for possible synergy.

2.6.1 Zone of Inhibition

2.6.1.1 Metals

Mueller Hinton (MH) agar is recommended by Clinical and Laboratory Standards Institute (CLSI) (Balouiri et al., 2016) as standard media for antimicrobial susceptibility testing methods. In this study, the metallic ions showing potential antimicrobial activity (silver, palladium and platinum) were tested on six different media including MH (NA, TSA, ISO,

Thioglycollate and Letheen) so to assess the best growth media for a Gram-positive organism (*S. aureus*) and a Gram-negative organism (*P. aeruginosa*).

Overall, the results showed that both palladium and platinum showed the strongest antimicrobial efficacy at higher metal ion concentrations (> 100 mg/L) if tested on NA or TSA growth media. On the other hand, silver ions were most effective at lower concentrations (≤ 100 mg/L) if tested on MH growth media.

The assessment of metals as antimicrobial agents using ZoI as method covered not only the concentration of the metals at which they displayed better antimicrobial efficacy, but also the media at which a given antimicrobial efficacy testing regime is to be performed to obtain clearer and better results.

If the antimicrobial efficacy against organisms is to be compared, clear and more distinguishable results were obtained and recorded for *P. aeruginosa*. In terms of best antimicrobial susceptibility, for those concentrations greater than 100 mg/L, best growth media were NA, TSA and Letheen for both organisms tested. However, for concentration lower than 100 mg/L, MH growth media showed the best susceptibility.

Five different concentrations (1000 mg/L, 500 mg/L, 100 mg/L, 50 mg/L and 10 mg/L) were tested for each metallic ion (Ag, Pd and Pt). The results showed that both palladium and platinum displayed the strongest antimicrobial activity at higher metal ion concentrations (>100 mg/L). Preliminary studies investigating the antimicrobial activity of Pd and Pt have already been published (Samota et al., 2009, Adams et al., 2014 and Stazsek et al., 2014). However, Pd and Pt were not tested as an individual metallic ions, but as complexes linked to bioactive ligands (Samota et al., 2009). Initial results reported that the use of the chelated metals not only decreased Pd and Pt concentrations at which Pd and Pt complexes showed

antimicrobial activity, but also increased the diameter of the area observed round the sample (ZoI).

Silver on the other hand, showed the most effective antimicrobial at lower concentrations (<100 mg/L). Most of the characterization of silver as antimicrobial agent has been made using dilution methods tests (MIC/MBC).

Those media showing the best results were used for assessing the ZoI of essential oils, which eventually led to a set of best performing antimicrobial agents (metallic ions and essential oils). There were further evaluated for MIC/MBC, as well as for potential synergistic activity (using also dilution methods tests).

2.6.1.2 Essential Oils

ZoI testing in all forms tried (well and solid (disk) and vapour diffusion) was ineffective for assessment of the antimicrobial activity of essential oils in this study. Previous studies (Goñi et al., 2009). showed promising antimicrobial activity results in the vapour phase in the combination of essential oils (cinnamon and clove), however, the mixtures were diluted in diethyl ether and strains cultured over MH agar. In this study, essential oils were highly diluted in grapeseed oil and cultured on NA and TSA agar. Since a comparison was to be made between the two sets of results, the same methods were to be followed (although EOs might respond differently in media compared to metals).

2.6.2 MIC/MBC

MICs/MBCs have been already reported in the literature as methods to determine whether essential oils (Hammer et al., 1999) and metal ions (Schiertholz et al., 1998 and Holla et al., 2012) show antimicrobial activity. The former yielded results that support the notion that

plant essential oils and extracts can have an actual role as pharmaceutical and preservative ingredients, and the latter confirms the revival of metal ions as antimicrobial agents. Comprehensive methods have been described for the testing several essential oils following a similar method (microdiluted nutrient broth) against a number of microorganisms, as well as a number of studies assessing antimicrobial efficacy of Ag^+ metal ions (Schiertholz et al., 1998).

Tween 20 (Gómez López et al., 2005) and grapeseed oil (Caravaglia et al., 2016) have been reported with antimicrobial activity and further controls should have been conducted to assign properly whose antimicrobial activity is actually responsible for on this study.

2.6.2.1 Metal Ions

Overall, for both microbes (*S. aureus* and *P. aeruginosa*) similar MIC results were reported. All three metal ions tested (Ag, Pd and Pt) gave MIC values of 25 mg/L. However, Ag alone gave an MBC of 25 mg/L, whereas for Pd and Pt, the MBCs reported were greater than 25 mg/L. Given this observation, Ag^+ demonstrated the best antibacterial efficacy.

The MIC and MBC performance of Ag^+ in various media and against numerous organisms has been widely reported in the literature (Schiertholz et al., 1998, Jung at al., 2008 and Sondi et al., 2004). Both the media and the organism obviously affect the MIC/MBC values obtained. Schierholz (1998) compiled the antimicrobial efficacy data of Ag^+ following inoculation on different MH broth media and MIC values of 1-10 mg/L and MBC values of 10 mg/L were obtained against *S. aureus.* The results obtained in our study (25 mg/L for MIC and >25 mg/L for MBC), suggest that silver was roughly half as effective as claimed by Schiertholtz (1998), this may be due to use of the TSB growth medium rather than MH, as used by Schiertholtz. However, Holla (2012) tested an Ag^+ based antimicrobial agent

(NOVARON™). MIC and MBC performances were evaluated against *Streptococcus mutans* inoculated in MH broth dilution. The MIC was reported between 20 and 40 mg/L and MBC around 40 mg/L for this system, although reported against different bacterium.

Palladium and Platinum metallic ions have been recently subject of study in terms of antimicrobial performance (Vaidya et al., 2017). Adams et al., (2014) and Staszek et al., (2014) studied these ions in a chelated form as mentioned previously. Findings in the comparison between hydrated of the ligands themselves and the effect of the ligands on the antimicrobial activity of the metal ions.

2.6.2.2 Essential oils

The best essential oil in terms of antimicrobial efficacy was manuka oil, showing an MIC of 2.5 % (v/v). RO and to a lesser extent CO, showed limited antimicrobial activity; partial elimination of the blue metabolic dye was observed in some cases. The other essential oils investigated, OO, and MyO showed no antimicrobial activity. No MBCs were recorded for any of the essential oils within the concentration range investigated (up to 10 % (v/v)). Hammer et al., (1999) reported the antimicrobial activity of a number of essential oils (orange, rosewood and clove) against numerous microorganisms (including *S. aureus* and *P. aeruginosa*) on which OO showed the best antimicrobial performance against the target bacteria. In similar studies assessing antimicrobial activity of EOs, (Goñi et al., 2009) concluded that the antimicrobial activity of EOs against bacteria could be related to the cell wall composition of the targeted microbes.

Based on antimicrobial performance of the EOs in this study, it was decided to further investigate Manuka oil (MNO) and rosewood oil (RO) in synergy experiments.

2.6.3.3 Synergy Tests

The combination of drugs is an emerging option for antibacterial resistance therapy and is currently being investigated (Cottarel, 2009). The antimicrobial activity of metallic ions and essential oils has been reported in previous works (Schiertolz et al, 1998 and Hammer et al, 1999). Following combinative drug strategies, Ahmad and Viljoen (2014) studied the *in vitro* antimicrobial activity of *Cymbopogon* essential oil and its interaction with silver ions. In this particular study, the results suggested that *Cymbopogon* and silver metallic ion provided potential novel combinations that acted synergistically.

In regards to the current study, FIC was used to determine the synergistic antimicrobial efficacy of the metals with essential oils in combination in a solution. FIC determined that indifferent activities ($0.5 < FIC > 4.0$) were demonstrated, neither synergistic nor antagonistic interactions.

2.7 Conclusions

Nutrient Agar (NA) at higher metal concentrations (>50 mg/L) and Mueller-Hinton (MH) at lower concentrations (<50 mg/L) proved to be the best bacterial growth media to determine the antimicrobial efficacy of metallic ions (only for Ag+).

All the three metals tested (silver, palladium and platinum) gave an MIC of 25 mg/L. Further MBC results confirmed Ag as the best performing antimicrobial of the set. The MBC of Ag^{+} was the same as the MIC, i.e. 25 mg/L.

The best essential oil in terms of antimicrobial efficacy was MNO, showing an MIC of 2.5% (v/v). FIC eventually showed indifferent activities for those combinations between metals and essential oils claiming the best antimicrobial performance individually

CHAPTER 3. ENCAPSULATION OF ANTIMICROBIAL AGENTS IN LAYERED SILICATES

Summary

This last section assessed the suitability of unmodified and modified layered silicate (Montmorillonite (MMT)) substrates as adsorption media for essential oils (EOs) and silver ions (Ag^+) in order to develop a reservoir for controlled release of EOs and Ag into a variety of polymer based systems, ranging from surface coatings to thermoset and thermoplastic formulations.

The EOs (Rosewood oil (RO), Clove oil (CLO), and Manuka oil (MNO)) were incorporated from solution in toluene into unmodified sodium MMT (CNa) and organically modified montmorillonites (o-MMT) of increasing polarity (Cloisite 15A < Cloisite 20A < Claytone APA < Tixogel VXZ < Cloisite 30B < Cloisite Na+). Silver (as ions) was incorporated into the unmodified (MMT) (CNa) via an ion exchange reaction. In order to assess the adsorption levels achieved for each layered structure tested, a number of instrumental techniques were used.

The assessment of EO adsorption capacity of the MMTs was carried out using Thermal Gravimetric Analysis (TGA), X-ray diffraction (XRD) and Fourier Transform Infrared Spectroscopy (FTIR) in diffusive reflectance mode (DRIFTS). The TGA study provided the mass of EOs incorporated (expressed per 100g of MMT), as well as the amount of organic modifier present in the o-MMTs. The XRD study gave insight in to the arrangement of the layered structures arising from EOs adsorption. Finally, FTIR not only confirmed the

presence of EOs in the MMTs, but also provided some insight into the nature of the interaction between the EOs and the MMTs.

The assessment of silver ion adsorption was carried out using energy dispersive X-ray analysis (EDX), X-ray diffraction (XRD) and atomic absorbance spectroscopy (AAS). XRD was carried out in order to see if intercalation by silver occurred, leading to an increase in interlayer spacing. EDX was used to assess the level of silver in unwashed and washed samples of silver loaded Na-MMT. The AAS study aimed to estimate the amount of Ag^{+} present in the structure by the determination of the Ag^{+} ions that were not incorporated into the MMT.

The TGA, XRD and DRIFTS data for the EO loaded MMT indicated that EO incorporation from solution in toluene was successful. For all the three EOs (RO, CLO and MNO) the highest levels of adsorption were attained with layered silicates modified with benzyl-di-methyl-hydrogenated tallow ammonium chloride (i.e. Tixogel VZ and Claytone APA). Adsorption levels were 24g/100g and 25g/100g for Tixogel VZ and Claytone APA, respectively. Results for ion silver incorporation showed that the pre-adsorption method was effective for Na-MMT and that the more concentrated the silver nitrate solution, the higher the level of incorporation.

3.1 Introduction

The pre-requisite for a controlled release effect is prolific adsorption of the EOs and Ag ions into the layered silicates. With the latter in mind, interactions between the three most antimicrobial EOs (rosewood oil, clove leaf oil and manuka oil), silver ions, and the layered silicate structures were evaluated. Unmodified sodium montmorillonite (Cloisite Na+ (CNA)) and organically modified layered silicate structures (Cloisite 15A (C15A). Cloisite 20A (C20A),

Cloisite 30B (C30B), Tixogel VZ (TVZ) and Claytone APA (CAPA)) provide a wide range of gallery polarities. The incorporation of these antimicrobials has been assessed using a number of characterisation techniques including thermal gravimetric analysis (TGA), X-ray diffraction (XRD), Fourier transform infrared spectroscopy (FTIR), energy dispersive X ray spectroscopy (EDX) and atomic absorption spectroscopy (AAS).

Incorporation of the antimicrobial agents into layered silicates was anticipated to afford them a degree of protection during incorporation into polymer melts, and then control the subsequent release of both EOs and silver during use, thus prolonging the antimicrobial activity.

3.1.1. Montmorillonites and use as reservoir

Montmorillonites are part of the smectite family of minerals (section 1.5.1) and they feature large surface areas due to the galleries between the layers forming the structure, thus making them suitable adsorbant agents.

In montmorillonite (MMT), for every five Al^{3+} ions in the octahedral sheet there is one Mg^{2+} ion, giving the general composition $[(Al_4\text{-}xMg_x)Si_8O_20(OH_4)]$ where x is ⅔. Due to the magnesium ions having a lower charge (+2) than the aluminium (+3), there is now a charge imbalance in the material. To address this, cations usually Na^+, are adsorbed onto the external and internal surfaces of the material to make the overall charge neutral and giving the general formula $Na_x[(Al_2\text{-}xMg_x)Si_4O_{10}(OH_2)]$.

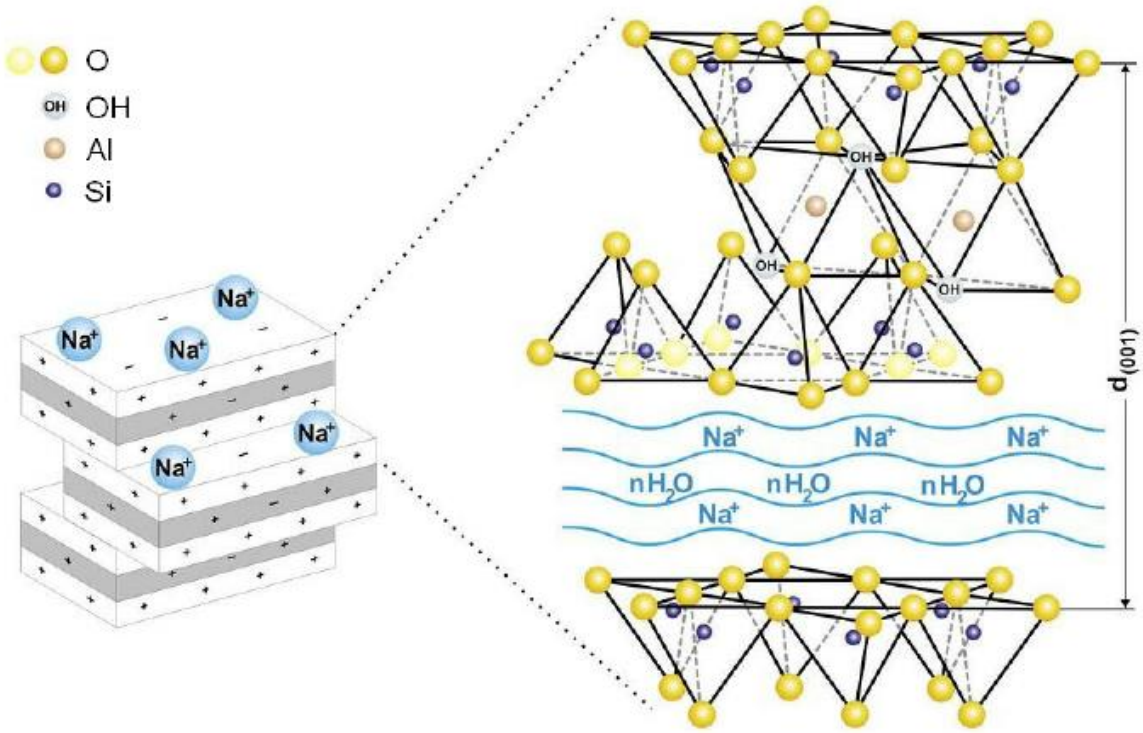

Figure 3.1 . Sodium-MMT structure (www.bentonite.net)

Like many other smectites, MMT swells in water. Compared with other clays, MMT undergoes a considerable expansion due to the water penetrating the interlayer spaces. The amount of MMT expansion is related to the type of exchangeable cation in the sample. The presence of sodium (as the predominant exchangeable cation) can result in the clay swelling several times its original volume. The latter is often followed by dissociation of the platelets, giving rise to gel like behaviour of unmodified MMT dispersions in water.

Hartwell (1965) described a number of important applications for MMTs including, a key component of drilling mud (for the oil industry), soil conditioning (to help retain water in drought-prone soils) or as a desiccant (to remove moisture from air and gases).

As previously stated, the high specific surface area of MMTs, leads to their use as adsorbants for many industrial applications. This adsorption phenomena have been widely reported and documented in the literature (Hartwell, 1965)

Adsorption interactions with MMTs have been reported as early as the 1940s, when the hydration mechanism of MMT bearing a range of cations was first described (Hendricks et al, 1940). The next advance was when Cowan and White (1958) confirmed the occurrence of an exchange reaction between Na-MMTs and various linear quaternary ammonium salts.

Following those studies, research has progressed to applications including water treatment, land remediation and controlled release systems for functional molecules. The adsorption of antibiotics into MMTs is an example of water treatment / land remediation application. Due to prolific use, antibiotics are excreted from people and farm animals and are therefore present in the environment. This in itself has arguably contributed to the increase in bacterial resistance to certain antibiotics. The leakage of antibiotics into soils does not result in sufficiently high enough concentrations to inhibit proliferation of bacteria, but these small doses can certainly cause bacteria to become resistant to antibiotic contaminants (Call et al.,2013)

Not only are antibiotics reported to show a tendency to bind with particles in soil (Kramer, 2005), but also the antimicrobial activity of soil-bound antibiotics is also well known and documented (Kelleners et al., 2005). In regards to the incorporation / adsorption of antibiotics into MMTs, several investigations have been conducted since the late 70s. Porubcan (1978) reported the incorporation of clindamycin and tetracycline into a layered silicate via a cation exchange mechanism and the incorporation of digoxin by a reversible adsorption mechanism at different level of acidic pH. Further investigations studied the

incorporation of tetracycline into a layered silicate from aqueous solutions (Li et al., 2010). More recent work has examined the mechanisms that drive the adsorption of tetracycline onto MMTs, it was found that metal complexes increase access to the smectite layers (Aristilde et al., 2016).

Once antibiotics are adsorbed on to (in to) the MMT galleries desorption will be slow, leading to a controlled (sustained) release effect. Researchers have been therefore seeking methods via which the antimicrobials can be released in a sustained manner.

The materials science and microbiology research groups at MMU have explored a number of controlled release systems for antimicrobials. Early work investigated use of gel silicas for encapsulation of isothiazolinones and terpenes (Coulthwaite et al., 2005), studies then progressed to exploration of layered silicates, both synthetic and natural, as reservoirs for Triclosan and essential oils (Kinninmonth et al., 2014 and Liauw et al., 2011). The more recent work has examined synthetic zeolites as carriers for silver (Dong et al., 2014 and Belkair et al., 2015).

The current investigation reported in this MPhil thesis, further investigates organically modified and unmodified natural layered silicate carriers for essential oils and metal ions, respectively. The second part of the study investigated exchange of sodium ions in the MMT with silver ions. The use of unmodified layered silicates to adsorb Ag ions has been studied over the last years and it is well documented by Magaña et al., (2008) and Malackova et al., (2011) to name a few. Malackova (2011) has served as the starting point for the set of experiments described in this thesis in regard to the use of $AgNO_3$ at different concentrations in order to assess the best conditions for the Ag^+ adsorption into the Na-MMT investigated.

3.2 Experimental

3.2.1 Materials

3.2.1.1 Layered silicate substrates

BYK (formerly Rockwood Additives Ltd, Moorfield Rd Widnes, Lancashire, WA8 3AA, UK) provided Tixogel VZ and Claytone APA organically modified montmorillonites (o-MMTs). The unmodified sodium montmorillonite (Na-MMT) (Cloisite Na) and o-MMTs; Cloisite 15A, Cloisite 20A, Cloisite 30B, were supplied by Rockwood Additives (Moorfield Rd Widnes, Lancashire, WA8 3AA, UK). These are summarised and given reference codes (that will be used from hereafter) in Table 3.1.

Table 3.1 – Substrates used on this study.

Substrate	Coding	Organic Modifier
Closite Na (unmodified Na MMT)	CNa	Cloisite Na is a natural un modified sodium montmorillonite
Closite 15A (o-MMT)	CL15A	Quaternary dimethyl-di-(hydrogenated tallow) ammonium chloride salt.
Closite 20A (o-MMT)	CL20A	Quaternary dimethyl-di-(hydrogenated tallow) ammonium chloride salt.
Closite 30B (o-MMT)	CL30B	Quaternary Di(hydroxyethyl)-methyl-hydrogenated tallow ammonium chloride salt.
Tixogel VZ (o-MMT)	TVZ	Quaternary benzyl-di methyl hydrogenated tallow ammonium chloride salt.
Claytone APA (o-MMT)	CAPA	Quaternary benzyl-di methyl hydrogenated tallow ammonium chloride salt

Table 3.2 – Details of organic modification including modifier structure, modifier level and (001) reflection angle (2θ) and (001) spacing.

Name	Substrate Structure	2θ	d (nm)	% OM
CLNa	Closite Na (unmodified smectite)	7.13	12.38	
CL15A	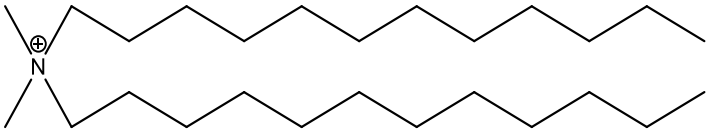	2.95	29.88	39.77
CL20A	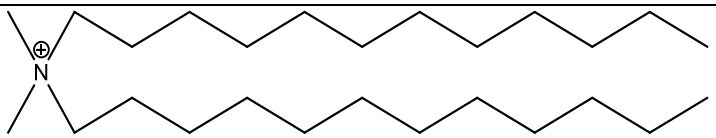	3.43	26.40	35.10
CL30B	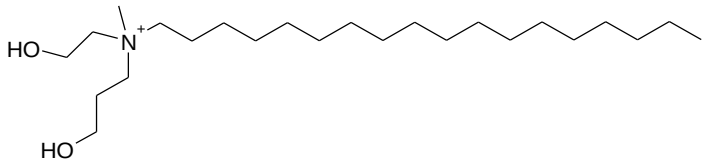	4.68	18.86	28.13
Tixogel	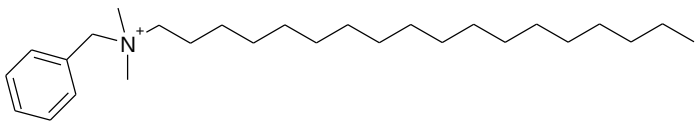	4.81	19	27.13
Claytone	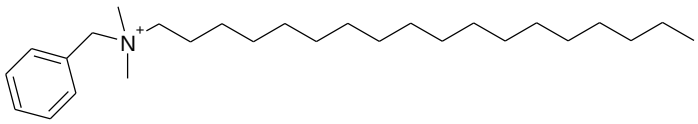	4.57	19.6	33.94

The values corresponding to both (001) reflection angle (2θ) and $d_{(001)}$ are from the literature (Pegoretti at al., 2008), whilst the levels of OM (Organic modifiers) are experimentally determined by TGA (see section 3.2.4.1)

3.2.1.2 Essential Oils

The following essential oils (EOs), rosewood oil (6709), clove leaf oil (6683) and manuka oil (7695) were obtained from Essential Oils direct, UK (the numbers in parenthesis refer to the Essential Oils Direct product numbers), and used as received.

Essential oils are a complex mixture of chemical components the majority of which are based on repeating isoprene units called terpenes. The major components in the EOs investigated are given in Table 3.3.

Table 3.3 – Structures of Key Components of Essential Oils used

Essential Oils	Major component	% (Up to)	Structure
Rosewood Oil	Linalool	80-97	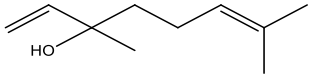
Clove Leaf Oil	Eugenol	72-90	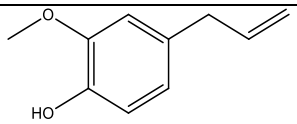
Manuka Oil	Caryophyllene (sesquiterpene)	16	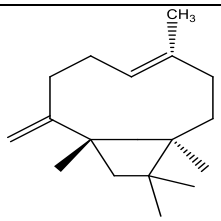
	Geraniol (monoterpene)	17	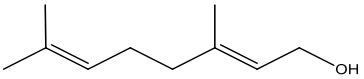
	Pinene (monoterpene)	17	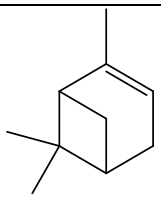
	Linalool (monoterpene)	17	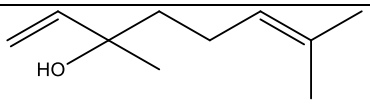
	Humelene (sesquiterpene)	16	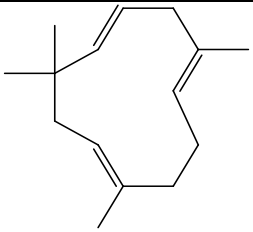
	Lepstosermone (Triketone)	6	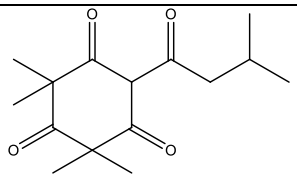

3.2.1.3. Silver Nitrate

Silver Nitrate was obtained from ReAgent (UK, (SINI-1542-43)), and used as received.

3.2.2 Encapsulation of essential oils in layered silicates

Following previous work at MMU, it was considered most practical for the EO loading of the MMTs to be carried out by pre-adsorption from solution in toluene.

Being an aromatic solvent, toluene is compatible with the gallery environments of the selected o-MMTs and is a good solvent for the essential oils investigated. The toluene therefore carries the EO into the expanded MMT galleries. On evaporation of the toluene, most of the EO becomes encapsulated within the MMT/o-MMT galleries, as the components of the EOs concerned are compatible with the o-MMT gallery environment.

A solution of the given EO was prepared (0.5 g EO in 12 mL of toluene). One gram of the substrate (MMT) was then added to a beaker and the resulting mixture was manually stirred for 2 minutes. The contents of the beaker were then poured into a foil tray. The solvent and unbound EOs components were allowed to evaporate overnight in the draft of a fume cupboard, no heat was applied. A schematic of the procedure is given in Figure 3.2. The resulting EO loaded MMT was ground using a Waring laboratory grinder until a fine powder was obtained.

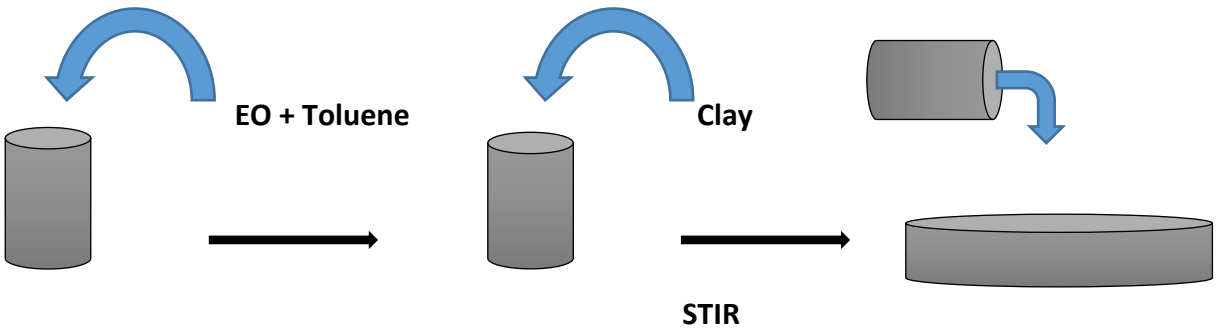

Figure 3.2. Procedure used to encapsulate the EOs in MMT.

3.2.3 Encapsulation of silver in layered silicates

The incorporation of silver into the unmodified MMT (CLNa) was performed according to a procedure described in Prauss (2008), in which Ag^+ adsorption on Na^+ rich Wyoming montmorillonite (MMT) was studied.

3.2.4 Characterisation of Essential Oils and Silver Loaded Layered Silicates

The adsorption process of EOs was characterised using thermal gravimetric analysis (TGA), X-ray diffraction (XRD) and FTIR-DRIFTS.

3.2.4.1 Thermal Gravimetric Analysis (TGA)

TGA is a method of thermal analysis that measures the change in mass of a sample as a function of increasing temperature, or a change in mass as a function of time at constant temperature. The gaseous atmosphere around the sample can be controlled (i.e. air, oxygen or inert gasses).

TGA was used to examine these loaded substrates in order to determine the level of EO adsorption within the MMTs after the pre-adsorption treatment (Section 3.2.2). A high level of adsorption can be an indicator of effective controlled release of EO. In the case of the o-MMTs, the amount of organic modifier was determined and taken into account when calculating the level of EO adsorption into the o-MMTs. The organic modifier levels determined were compared with those reported in the literature.

The amount of EOs adsorbed into either the unmodified MMT (CNa) or the o-MMTs was thus determined using non-isothermal TGA over a temperature range of 20°C to 900°C in an air atmosphere. A Perkin-Elmer TGA 4000 was used for this investigation. The untreated and EO treated samples (10-20 mg) were initially heated from room temperature to 110°C at a

rate of 20°Cmin^{-1} and held there for 5 minutes, to ensure removal of loosely bound surface water. Then the temperature was raised to 900°C, at a rate of 10°C/min^{-1}, and held there for 5 minutes, to ensure complete removal of structural water. The lattice water contained in the MMT was determined using the unmodified substrate (CNa) and therefore accounted for in the calculation to determine the EO levels in the treated samples. The levels of EOs incorporation into the galleries substrate are calculated as follows:

a) Lattice water (free water) contained in the MMT

$$\text{Residue fraction (Na-MMT)}\ (R^{900}_{fNa-MMT}) = \frac{W^{110}_{NaMMT}}{W^{900}_{NaMMT}}$$

b) EOs adsorbed into Na-MMT

$$\text{Mass of EO in MMT}\ (W_{EO}) = W^{110}_{NaMMTEO} - \left[\frac{W^{900}_{NaMMTEO}}{R^{900}_{f}}\right]$$

c) Organic modifier (OM) mass (o-MMT) and index (mass OM / mass o-MMT)

$$\text{Mass of organic modifier}\ (W_{OM}) = W^{20}_{o-MMT} - \left[\frac{W^{900}_{o-MMT}}{R^{900}_{fNa-MMT}}\right]$$

$$\text{Mass of MMT in o-MMT}\ (W_{MMT}) = \frac{W^{900}_{o-MMT}}{R^{900}_{fNa-MMT}}$$

$$\text{Ratio of organic modifier mass to MMT mass}\ (R_{OM}) = \frac{W_{OM}}{W_{MMT}}$$

d) EOs adsorbed into o-MMT

$$\text{Mass of OM and EO in EO loaded o-MMT}\ (W_{EO+OM}) = W^{20}_{EO\ o-MMT} - \left[\frac{W^{900}_{EO\ o-MMT}}{R^{900}_{fNa-MMT}}\right]$$

$$\text{Mass OM in EO loaded o-MMT}\ (W_{OM}) = \left[\frac{W^{900}_{EO\ o-MMT}}{R^{900}_{fNa-MMT}}\right] R_{OM}$$

$$\text{Mass of EO in EO loaded o-MMT } (W_{EO}) = W_{EO+OM} - W_{OM}$$

$$\text{EO loading in o-MMT (mass of EO/100g organoclay)} = \frac{W_{EO}}{W_{o-MMT}} 100$$

gr EOs = (gr EOs + OM) – gr OM

3.2.4.2 X-ray Diffraction (XRD)

X ray powder diffraction is an analytical technique mainly used for phase identification of a crystalline material and provides information on unit cell dimension and other structure-related parameters. The material to be analysed is usually finely ground and homogenized to ensure a random orientation of crystal structures.

The purpose of using XRD on these EO loaded o-MMTs and MMT is to establish whether the EO entered the galleries and changed the average interlayer spacing and / or the level of stacking uniformity. The former can be observed by a shift of the (001) reflection to lower angles and the latter by a reduction in peak width and increase in intensity, accompanied by the appearance of higher order reflections, i.e., (002), (003) etc. These reflections can be confirmed by examining the respective d-spacings as $d_{(002)} = 1/2\ d_{(001)}$, $d_{(003)} = 1/3\ d_{(001)}$ etc.

The XRD was carried out using a PANalytical X'pert X-ray diffractometer (XRD) employing Cu K_α radiation (40kV and 40mA) and a PIXcell detector, the run parameters are shown in Table 3.4.

Table 3.4 - Analysis parameters for XRD.

Configuration (spinner)	*Scan properties*	
Scan axis (Gonio)	*Start angle*	**0**
	End angle	**30**
Generator (tension 40 mV, current 40 mV)	*Step size*	**0.026**
	Time per step	**50**

Samples were taken from the substrates loaded with EOs using pre-adsorption method and analysed.

3.2.4.3 Diffuse reflectance Fourier infrared transform spectroscopy (DRIFTS) and transmission FTIR

The bending and stretching resonant frequencies of covalent bonds coincide with the infrared region of the electromagnetic spectrum. Therefore, irradiation of a sample with infrared radiation over this frequency range will result in energy absorption when the irradiating frequency is equal to the stretching / bending resonant frequencies of a covalent bond. A particular compound will therefore have a unique spectrum of resonant frequencies. Furthermore, the chemical environment of a bond will affect its ability to vibrate and its resonant frequency. Therefore, an infrared absorption spectrum can provide valuable insight into molecular structure. In Fourier transform infrared spectroscopy the sample is irradiated with pulses (scans) of polychromatic infrared radiation and the spectrum is generated using Fourier transform algorithms. The greater the number of scans the higher the signal to noise ratio as the random nature of noise enables its removal from the data. The high signal to noise ratio of FTIR enables sampling techniques such as diffuse reflectance Fourier Transform infrared spectroscopy (DRIFTS).

DRIFTS is widely used to analyse powder samples such as fillers; the powder sample is usually diluted with an infrared transparent diluent such as finally ground potassium bromide (KBr). Due to the random orientation of powder particles in the KBr some of the infrared angles of incidence against the particle surface are low or glancing, this leads to a long path length through a surface coating on a particle and hence gives a degree of surface sensitivity (Liauw and Ashton, 2003).

For this study, a Thermo – Nicolet Nexus FTIR spectrometer fitted with a Spectra-Tech DRIFTS cell was used. The spectrometer and sample compartment were purged of water and CO_2 free air, using a Balaston purge gas generator. The samples were diluted to 5 wt.% with finely ground KBr and spectra were made up of 164 scans with resolution set to a 4 cm^{-1}. The background spectrum was obtained using the same finely ground KBr, and the same number of scans and resolution. The micro-sampling cup was used in this investigation.

The FTIR spectra of the EOs were taken in transmission using the standard transmission sample holder with the EO smeared between NaCl plates. Transmission spectra were also made up of 164 scans with resolution set to 4 cm^{-1}.

3.2.4.4 Atomic Absorption Spectroscopy (AAS) (for silver loaded MMT)

Atomic absorption spectroscopy (AAS) enables the quantitative determination of chemical elements using the absorption of optical radiation (light) by free atoms in the gaseous state. In analytical chemistry it is widely used for determining the concentration of a particular element in the sample to be analysed.

AAS was used to determine the amount of unbound Ag in the supernatant liquor above the silver nitrate treated MMT. In order to determine the latter, a calibration curve must be

constructed using solutions containing known amounts of silver. As the initially added amount of silver was known and the amount of silver in the supernatant liquor is also known (via AAS), the amount of silver both within the MMT galleries and on the outer surfaces of the aggregates can therefore be determined.

A calibration curve was prepared using a Ag standards 25 ppm, 50 ppm, 75 ppm, 100 ppm (Fisher Scientific UK, Loughborough, Leicestershire). Aliquots (four replicates of each) of supernatant liquors from MMT treatments, using initial concentrations of 0.02 mol/L, 0.05 mol/L, 0.075 mol/L and 0.1 mol/L were taken and analysed using AAS. In some cases, the aliquots were diluted by a known factor to bring the concentration into the range of the calibration curve. The amount of silver present in the supernatant liquor was calculated, using the calibration equation, and then the amount of silver within the MMT galleries and on the outer surfaces of the aggregates then determined by difference, and results then expressed in Ag/100 CLNa.

A Varian Spectra AA 220 FS Atomic Absorption Spectrophotometer was used for AAS analysis.

3.2.4.5 Energy Dispersive X-ray Spectroscopy (EDX) (for silver loaded MMT)

EDX is an analytical technique used for the elemental analysis. The elements are determined from the unique energy of X-rays emitted from a given element when struck by electrons, usually within the chamber of an electron microscope. Due to quantised energy levels within atoms, each element produces a unique range of X-rays of known energy.

The purpose of using EDX on the silver loaded MMT is to determine the amount of silver that is adsorbed within the MMT galleries and on the outer surfaces of the MMT

aggregates. It is expected that the silver on the outside of the particles will be removed by water washing.

Therefore, samples obtained immediately after isolation by centrifugation and drying (with no washing) and samples that were washed with distilled water and then further centrifuged with 25 mL of distilled water at 3500 rpm, were examined. The latter should provide an estimate of the amount of silver actually within the MMT galleries. EDX was performed, using an EDAX, Trident^{TM} system with 40 mm^2 silicon drift detector, fitted to a Zeiss Supra VP SEM. Electron beam energy was 8keV and results were expressed as wt% using a ZAF correction.

3.3 Results

The results section is divided into three parts; the first part covers characterisation of the layered silicates by TGA and XRD and analysis of the essential oils using FTIR. The second part explores the interaction between the essential oils and the layered silicates (both Na-MMT and o-MMT). The antimicrobial activity of the EO loaded MMTs was also assessed via a rudimentary screening method. The third part explores the interaction between silver ions in Na-MMT using AAS, EDX, XRD and rudimentary antimicrobial assessment. It is anticipated that both the MMT/EO and MMT/Ag interactions will lead to encapsulation of these antimicrobial species.

3.3.1 Characterisation of layered silicates

3.3.1.1 TGA analysis of layered silicates

The organic modifier levels in the layered silicates (determined by TGA (Section 3.2.4.1) are compared with the manufacturers figure (where available) in Table 3.5. Differences in measurements partially attributed to wetness of samples (mainly (CNa).

Table 3.5. Organic modifier levels and interlayer spacings in MMTs investigated – comparison with literature (Scaffaro et al., 2013) / manufacturer (BYK) figures.

MMT	Organic modifier level (MMU TGA) (wt.%)	Manufacturer / literature figure for organic modifier level (wt.%)	Interlayer spacing (MMU XRD) (nm)	Interlayer spacing (manufacturer / literature figure) (nm)
CNa	0	0	0.57	0.23
C20A	34.97	35.10	1.62	1.64
C15A	39.76	39.77	2.29	1.89
TVZ	26.69	27.13	0.94	-
CAPA	33.17	33.94	0.94	-
C30B	25.65	28.13	0.93	0.87

3.3.1.2 XRD analysis of layered silicates

XRD diffractogrammes (counts versus 2θ graphs) are shown in Figure 3.3. The interlayer spacings obtained from the (001) reflections are shown in Table 3.5 together with literature / manufacturers figures for interlayer spacing. It is evident from Figure 3.3 that treatment with the organic modifier increases the interlayer spacing. Treatment with an organic modifier also improves stacking uniformity as evidenced by the increased sharpness of the reflection peaks relative to the unmodified (CNa). The extent of improvement in stacking uniformity is however moderate as the reflections are of relatively low intensity and there are no obvious higher order reflections. As stacking uniformity and number of platelets per tactoid increases, reflection intensity increases and higher order reflections (002), (003) etc. begin to appear (Liauw at al., 2007). In the case of the X-ray diffractogrammes of the layered silicates analysed here, a number of conclusions can be made. None of the o-MMTs were intercalated with vertically orientated hydrogenated tallow (HT) alkyl tails, for this to have occurred the interlayer spacing should have been about 2.6 nm. By virtue of its high modifier level, C15A showed the highest interlayer spacing (2.3 nm), possibly confirming the slanted arrangement proposed by Pukánszky et al., (2006). With its reduced amount of modifier, the interlayer spacing in C20B (1.6 nm) may be consistent with a mixture of a tri-layer and the slanted arrangement proposed by Pukánszky (2006). TVZ, CAPA and C30B had interlayer spacings consistent with a horizontal bi-layer of HT alkyl tails. The Na-MMT had a slightly higher interlayer spacing than expected this may be due to increased ambient water adsorption.

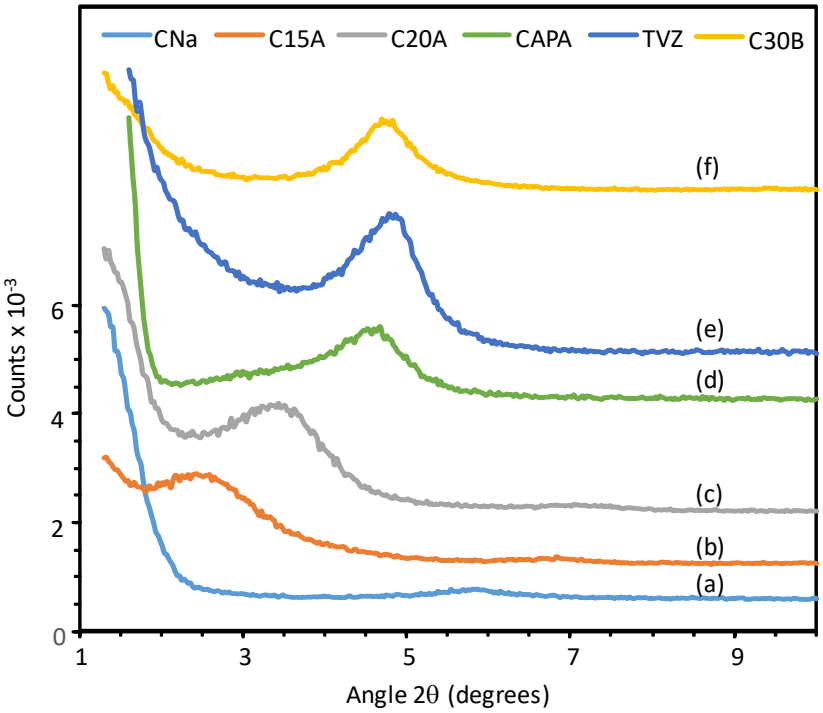

Figure 3.3. X-ray diffractogrammes of (a) CNa, (b) C15A, (c) C20A, (d) CAPA, (e) TVZ and (f) C30B.

3.3.1.3 FTIR analysis of layered silicates

FTIR spectra of the MMTs investigated are presented in Figures 3.4(i) and (ii). The major peaks in the spectra are assigned in Table 3.6.

Table 3.6. Peak assignments for DRIFTS spectra of MMTs investigated (Figures 4(i) and 4(ii))

Peak Position (cm^{-1})	Assigments
3600 cm^{-1}	Si-OH groups within the mineral structure
3500 cm^{-1}	Hydrogen bonded O-H stretching (a broad band)
3100 – 3000 cm^{-1}	Aromatic and alkenic H-C=C-H stretch vibrations
3000 – 2800 cm^{-1}	C-H stretching bonds from aliphatic CH_2 bonds
1700 cm^{-1}	Carbonyl stretching band
1500 – 1300 cm^{-1}	C-H bending of the aliphatic CH_2 groups and / or C-O-H bending

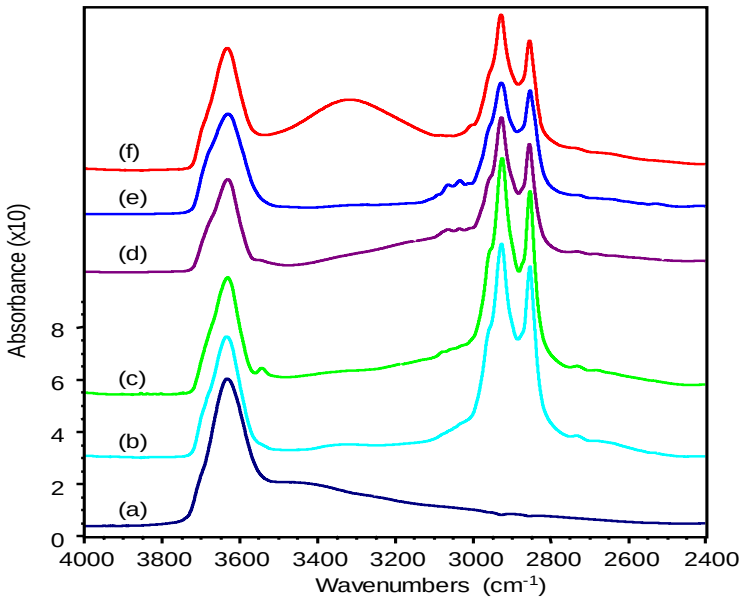

Figure 3.4(i). DRIFTS spectra (OH and CH stretching region) (5 wt.% dilution in KBr (see Section *3.2.4.3* for method)) of the MMTs investigated split into O-H and fingerprint regions; (a) CNa, (b) C20A, (c) C15A, (d) CAPA, (e) TVZ and (f) C30B.

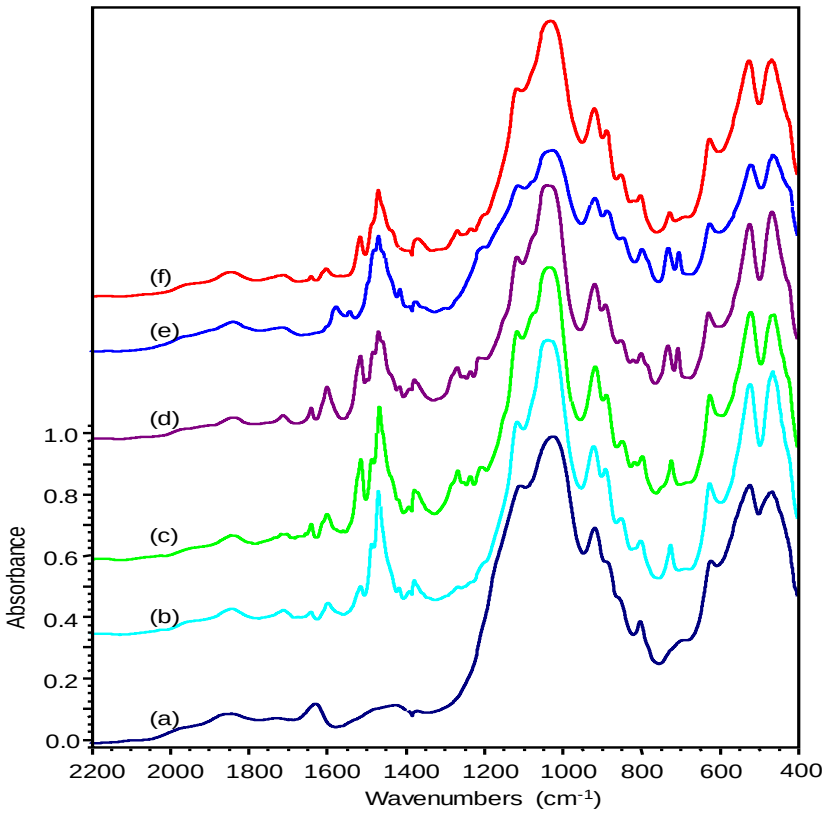

Figure 3.4(ii). DRIFTS spectra (fingerprint region) (5 wt.% dilution in KBr (see Section *3.2.4.3* for method)) of the MMTs investigated; (a) CNa, (b) C20A, (c) C15A, (d) CAPA, (e) TVZ and (f) C30B.

The relative levels of organic modifier can be correlated to the size of the C-H stretching bands relative to the Si-O bands. Key features of the o-MMTs are readily identifiable from the spectra; the hydrogen bonded OH stretch of the hydroxylethyl groups in C30B (making it the most polar in terms of hydrogen bonding interaction of the o-MMTs examined); the aromatic C-H stretching bands of the benzyl functional intercalants in TVZ and CAPA are also visible. The methylene asymmetric C-H stretching frequencies ($\nu_{(CH\text{-}H)as}$) originating solely from the hydrogenated tallow (HT) alkyl tails of all the o-MMTs (apart from C30B that has four extra methylene groups from the two hydroxyethyl substituents) are shown in Table 3.7 and vary from 2923 cm^{-1} (C20A and C15A) to 2926 cm^{-1} (C30B). In self-assembled alkyl

tails that are in a highly ordered (crystalline) array the $\nu_{(CH-H)as}$ is in the range 2918 to 2915 cm^{-1}.

Table 3.7. $\nu_{(CH-H)as}$ values for the o-MMTs investigated, listed in order of increasing organic modifier level (determined at MMU by TGA).

o-MMT	$\nu_{(CH-H)as}$ of hydrogenated tallow alkyl chain(s) (cm^{-1})
C30B	2925.6
TVZ	2923.9
CAPA	2924.5
C20A	2923.0
C15A	2923.2

Therefore the organic modifier HT chains in the o-MMTs examined are not particularly well ordered, an observation that is consistent with the relatively poor platelet stacking uniformity observed from the XRD data. However, C20A and C15A feature HT chains that are the most ordered due to the level of organic modifier and that there are two HT chains per molecule. C30B has that highest $\nu_{(CH-H)as}$, possibly due to the combination of contributions from the four methylene groups in the two hydroxyethyl substituents in its organic modifier and its single HT chain. The organic modifier in TVZ and CAPA also has a single HT chain per molecule. However, the $\nu_{(CH-H)as}$ values are not ranked as expected on the basis of organic modifier level; the lower organic modifier level in TVZ may have led to a significant portion of the HT tails being in contact with the gallery surface leading to lower than expected $\nu_{(CH-H)as}$. In CAPA the higher level of organic modifier may have led to an increased proportion of the HT chains that were not in contact with the platelet surface, the single HT chain per molecule prevents close packing leading to a higher $\nu_{(CH-H)as}$ than for C20A that has a similar modifier level to CAPA.

3.3.1.4 FTIR analysis of essential oils

The essential oils (EOs) were run in transmission as a liquid film supported on a NaCl disk. Spectra of the OH and CH stretching regions for the EOs are shown in Figure 3.5(i) and the carbonyl and fingerprint regions shown in Figure 3.5(ii). The most commonly encountered peaks are shown in Table 3.8. RO and CLO are the only two EOs that showed a strong hydrogen bonded OH stretching vibration centred at 3500 – 3400 cm^{-1} this can be assigned to the major components, linalool (80-97 %) and eugenol (72-90 %) in RO and CLO, respectively.

Table 3.8. Peak assignments for DRIFTS spectra of EOs investigated (Figures 5(i) and 5(ii))

Peak Position (cm^{-1})	Assigments
3500 cm^{-1}	Hydrogen bonded O-H stretching
3100 – 3000 cm^{-1}	Aromatic and alkenic H-C=C-H stretch vibrations
3000 – 2800 cm^{-1}	C-H stretching bonds from aliphatic CH_2 bonds
1700 cm^{-1}	Carbonyl stretching band
1500 – 1300 cm^{-1}	C-H bending of the aliphatic CH_2 groups and / or C-O-H bending

MNO showed a much weaker OH stretching vibration due to this oil having mainly hydrocarbon based components. Hydrogen bonding interactions of the EO OH groups with the layered silicate surface and/or the organic modifier will result in broadening of stretching frequency distribution and possibly attenuation of the vibrations.

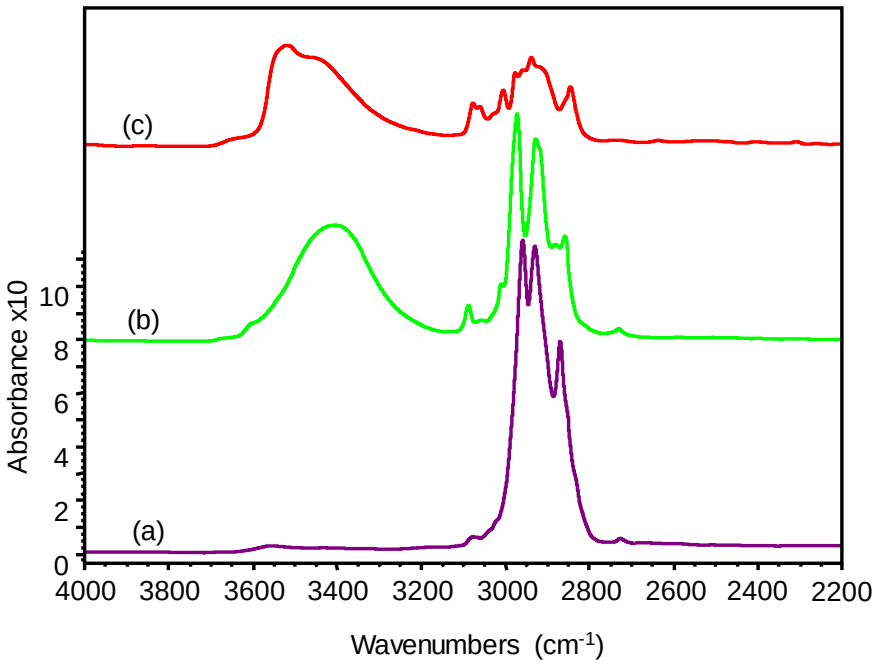

Figure 3.5(i). Transmission FTIR spectra (OH and CH stretching region) of the essential oils split; (a) Manuka oil (MNO), (b) rosewood oil (RO) and (c) clove leaf oil (CLO).

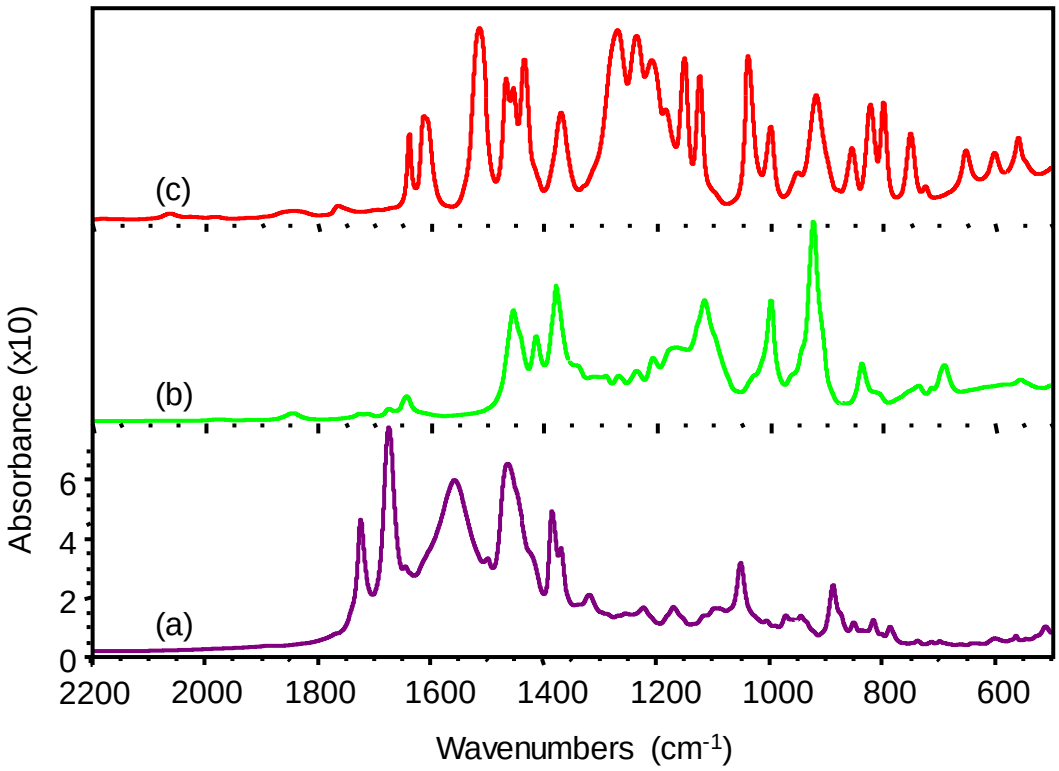

Figure 3.5(ii). Transmission FTIR spectra (fingerprint region) of the essential oils; (a) Manuka oil (MNO), (b) rosewood oil (RO) and (c) clove leaf oil (CLO).

All of the three EOs showed aromatic and alkenic C-H stretch vibrations. RO showed a weak absorption at 3086 cm^{-1} and a somewhat stronger absorption at 3006 cm^{-1}. CLO showed two relatively weak absorptions at 3076 and 3060 cm^{-1} (aromatic C-H, phenyl ring) and one more intense absorption at 3003 cm^{-1} (terminal vinyl group) and MNO one weak peak at 3100 cm^{-1}. Interaction with the MMT surface and/or the organic modifier may lead to a change in the frequency of the aromatic / alkenic C-H stretching vibrations. Furthermore reaction of the alkenic groups in particular with the unmodified layered silicate surface was also apparent from the DRIFTS spectra. The corresponding aromatic and alkenic C-H deformation bands appear around 1600 cm^{-1}.

All of the three EOs analysed exhibited aliphatic C-H stretching vibrations; RO at 2970, 2926, 2880 and 2857 cm^{-1}; CLO at 2975, 2957 and 2943 cm^{-1} and MNO at 2958,2930 and 2870 cm^{-1}

[1]. The aliphatic C-H stretching absorptions, present in all the EOs were likely to be obscured by the C-H absorptions of the organic modifiers in the case of the organically modified layered silicates. However, interaction of the EOs with the unmodified silicates may result in shifting of the aliphatic C-H stretch absorptions, depending on the mode of adsorption.

MNO exhibited particularly strong carbonyl stretching bands (1724 and 1674 cm^{-1}) that can be assigned to the Lepstosermone component (ca. 6% Maddock-Jennings et al., 2005). Both CLO and MNO exhibited substantially weaker carbonyl stretching bands, due to the major constituents not featuring carbonyl groups, however, the minor constituents of these oils do feature carbonyl species. It is also worth mentioning that a number of peaks between 1500 and 1300 cm^{-1}, which are mainly attributed to either C-H bending of the aliphatic CH_2 groups and/or C-O-H bending, are unlikely to be hidden by those originated for either the unmodified or unmodified layered silicate structures. Hence, these bands would still be present on a layered silicate structure further loaded with EOs. Finally, the large number of peaks above 1100 cm^{-1} were not significant as far as these adsorption studies are concerned, as they were masked by IR absorptions associated with the substrate.

3.3.2 Encapsulation of essential oils in layered silicates

3.3.2.1 TGA analysis of essential oil loaded layered silicates

For thermal gravimetric analysis (TGA), seventy-two samples were analysed according to the method described in Section 3.2.4.1. The amount of EO incorporated into each of the o-MMTs is expressed in g EO/100 g MMT. The raw data and example calculations are in Appendix 2 (Chapter 2). The most strongly adsorbing MMT for each EO can be summarised as follows, and is shown in Figure 3.6.

- *Rosewood oil*

The highest amount of RO per 100 g of substrate was reported for Tixogel VZ with 11.6 g RO/100 g of Tixogel.

- *Clove leaf oil*

The highest amount of CLO per 100 g of substrate was reported for Claytone APA with 23.42 g CLO/100 g of Claytone APA.

- *Manuka oil*

The highest amount of MNO per 100 g of substrate was reported for Claytone APA with 24.71 g MnO/100 g of Claytone APA.

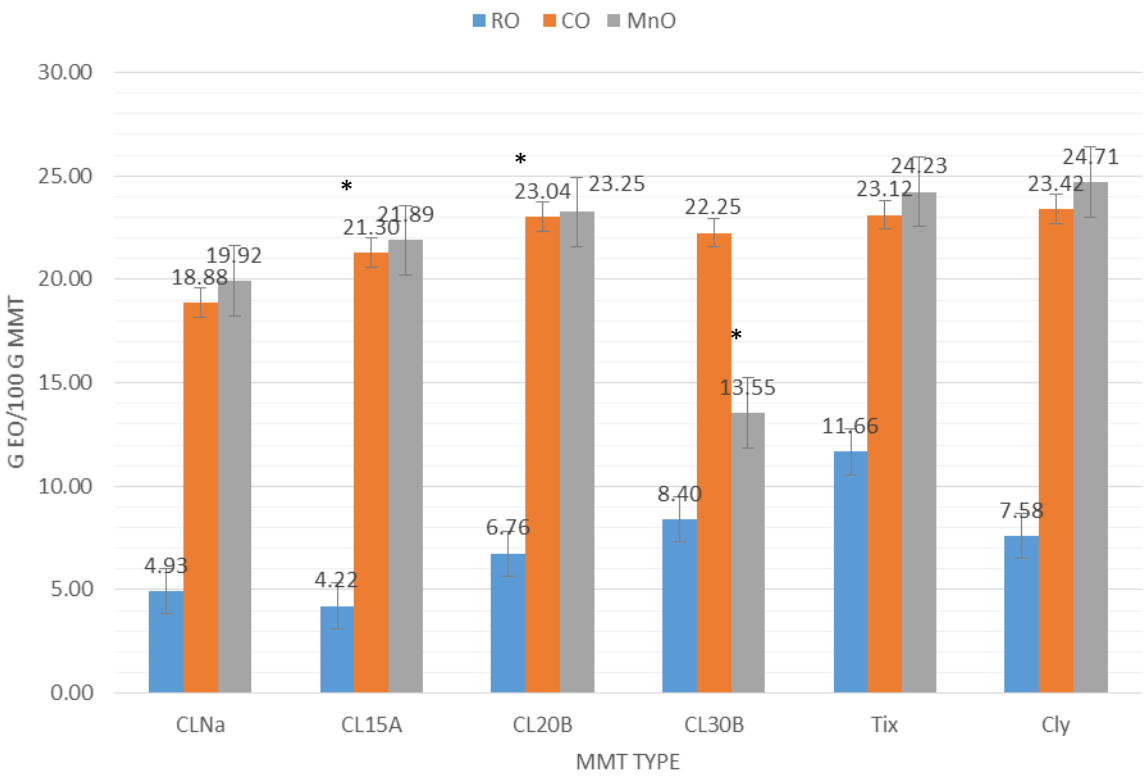

Figure 3.6. Levels of EO adsorption in the MMTs investigated – Note MNO and CLO were generally the most compatible EOs. * denotes samples that were in the form of a greasy

mass indicating either limited compatibility with the EO or partial delamination of platelets due to strong compatibility with the EO.

3.3.2.2 XRD analysis of essential oil loaded layered silicates

For all the EOs (rosewood oil, clove leaf oil and manuka oil) tested on the unmodified substrates (CLNa) and the organic modified substrates (C15A, C20A, C30B, Tixogel VXZ and Claytone APA), the internal rearrangement caused by the incorporation of the EOs into the substrates was studied.

It should be noted that C15A-CLO, C20A-CLO and C30B-MNO were in the form of a greasy mass rather than free flowing powder. The former state indicated that the MMT could not absorb all the EO without substantial delamination (to give the greasy mass). Alternatively, there may have been limited compatibility between the EO and the gallery resulting in limited absorption of the EO and the particles effectively being suspended in the EO – also giving greasy mass. In general these samples gave very weak or absent reflection peaks in the 2θ=0 to 10° range, indicating stronger likelihood of the first of these two scenarios. This led to the need to also examine the (110) reflections of the MMTs at ca. 2θ=20°. As the (110) reflection is from planes within the platelets themselves, their appearance is less dependent on platelet stacking uniformity, though coincident (110) planes in a uniformly stacked tactoid will give more intense (110) reflections.

For the EO loaded MMTs that gave clearly resolvable peaks in the 2θ=0 to 10° range, an increase in the interlayer distance relative to the respective unloaded MMT was generally reported. Due to Bragg's law, gallery expansion causes the (100) reflection peak to shift to lower angles on the counts vs angle 2θ plot. The presence of higher order reflections

(indicating uniform platelet stacking) was confirmed by examining the numerical relationship between the d values of the first second and third peaks ($d_{(002)}$ = ½$d_{(001)}$ and $d_{(003)}$ = ⅓$d_{(001)}$). Each substrate will now be considered in more detail.

Cloisite Na^+ (CNa): (the unmodified layered structure) only showed some degree of gallery expansion for the samples treated with clove leaf oil and, to a lesser extent, Rosewood oil. A possible explanation of CLO treated samples showing gallery expansion is due to the small molecular size of the major component of clove leaf oil, eugenol, which fits on the gallery space between platelets. It should be noted that CNa usually has an (001) 2θ value of 7°, giving a $d_{(001)}$ of 1.24nm (Kato, 2008). Treatment with all the EO have therefore led to an increase in interlayer spacing thus explaining the relatively high adsorption levels and the colours of the samples (see section 3.3.1.4)

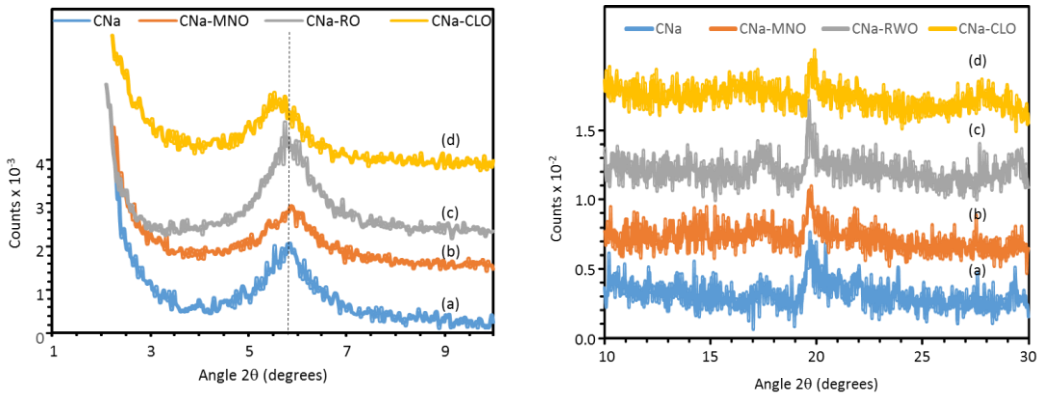

Figure 3.7. XRD data for Cloisite Na^+, (a) CNa, (b)CNa-MNO, (c) CNa-RO and (d) CNa-CLO.

Table 3.9. - CNa XRD Summarising peaks

	1ST PEAK		2ND PEAK		3RD PEAK		TEMPLATING EFFECT
	2θ	d(nm)	2θ	d(nm)	2θ	d(nm)	
CNa	5.85	1.51	-	-	-	-	No
CNa-MO	5.87	1.50	-	-	-	-	No
CNa-RO	5.74	1.54	-	-	-	-	No
CNa-CO	5.53	1.60	-	-	-	-	No

Cloisite 15A (C15A): All three EOs led to a significant increase in the interlayer spacing; in the case of CLO the level of compatibility was sufficient to almost completely eliminate any registry between the MMT platelets, leading to formation of a greasy mass. Attention, however, is drawn to a very weak but sharp reflection peak at ca. 2.3°, indicating the presence of a small fraction of uniformly spaced platelets within the sample. RO, however, showed rather weaker interaction that resulted in a significant increase in stacking uniformity as evidenced by the increase in reflection intensity, narrowing of peak width and the emergence of higher order reflections, as confirmed in Figure 3.7. MNO interaction also resulted in several peaks but the (001) reflection is weaker than expected, but the d values for the second and third peaks nevertheless indicated higher order reflections (Table 3.9). As RO is mainly composed of linalool, the nature and uniformity of interaction with the organic modifier causes the HT alkyl tails to become uniformly orientated and thus facilitates their self-assembly into quasi –crystalline arrays. The same effect was observed on adsorption of Triclosan into C15A (Liauw et al 2014). In the latter study, simple molecular simulation confirmed the thermodynamic feasibility of the interactions. Facilitation of the

quasi-crystalline arrays of HT alkyl tails leads to an increase in platelet stacking uniformity and can be described as a templating effect.

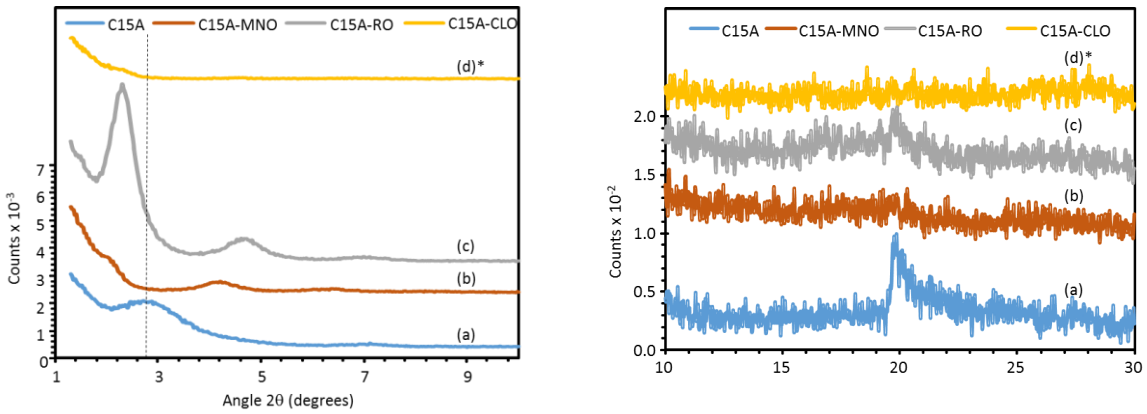

Figure 3.8. XRD data for Cloisite 15A; (a) C15A, (b)C15A-MNO, (c) C15A-RO and (d) C15A-CLO. * Denotes sample in form of greasy mass.

Table 3.10. Data for the first three reflection peaks from C15A based combinations

	1ST Peak		2ND Peak		3RD Peak		Higher order reflections	Templating effect
	2θ(°)	d (nm)	2θ(°)	d (nm)	2θ(°)	D (nm)		
C15A	2.72	3.24	-	-	-	-	No	NA
C15A-MNO	2.17	4.07	4.19	2.10	6.45	1.36	Yes	Weak
C15A-RO	2.30	3.89	4.61	1.91	7.00	1.26	Yes	Strong
C15A-CLO	-	-	-	-	-	-	-	V Weak

Cloisite 20A (C20A): C20A is version of C15A, but the former has a lower organic modifier level. Because of this similarity, interaction of C20A and CLO also gave a greasy mass, but this time the small peak at ca. 2.3° is barely discernible (Figure 3.9), indicating even greater of elimination of registry between MMT platelets. As with C15A, interaction with RO led to the HT alkyl tail templating effect (Table 3.11) and an increase in stacking uniformity.

Interestingly MNO led to a much more noticeable templating effect on interaction with C20A, this may be due to increased space between adsorbed organic modifier molecules and may have facilitated templating by the wider variety of molecules present in MNO.

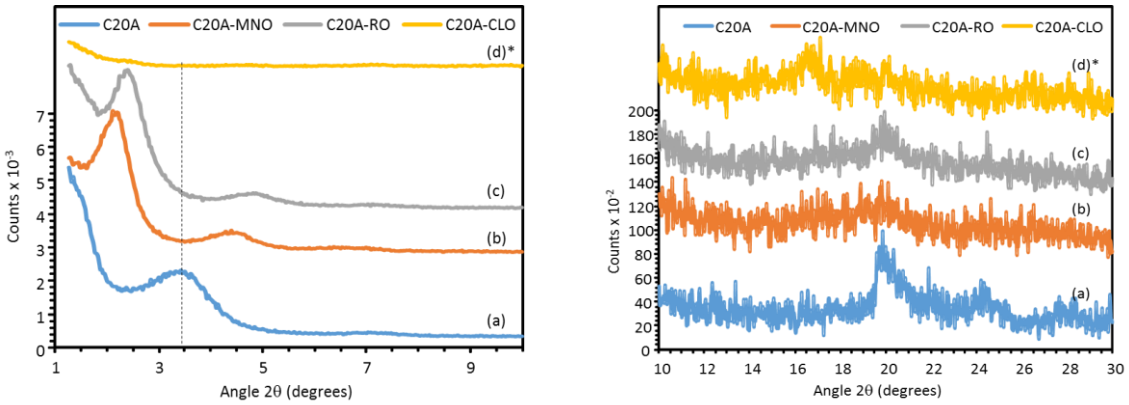

Figure 3.9. XRD data for Cloisite 20A (a) C20A, (b)C20A-MNO, (c) C20A-RO and (d) C20A-CLO. * Denotes sample in form of greasy mass.

Table 3.11. Data for the first three reflection peaks from C20A based combinations

MMT combination	1ST Peak		2ND Peak		3RD Peak		Higher order reflections	Templating effect
	2θ (°)	d(nm)	2θ (°)	d(nm)	2θ (°)	d(nm)		
C20A	3.43	2.57	-	-	-	-	No	NA
C20A-MNO	2.11	4.17	4.40	2.01	6.37	1.38	Yes	Strong
C20A-RO	2.41	3.63	4.82	1.83	7.13	1.28	Yes	Strong
C20A-CLO	2.40	-	-	-	-	-	-	V. weak

Cloisite 30B (C30B): Interaction of C30B with MNO led to formation of a greasy mass with the vast majority of any existing registry between MMT platelets being lost. Only RO and CLO led to a templating effect, though this was not as significant as observed with C20A and C15A (Figure 3.10). The diversity in molecular shapes of the components of MNO made templating difficult (Table 3.12), as several of the components may interact with the

intercalant molecules and/or the platelet surface. The latter, together with the relatively small amount of intercalant in C30B, led to random gallery expansion and highly disordered stacking of platelets. RO and CLO consist of just one major component and are more polar than MNO, these aspects resulted in stronger and more uniform interaction with the organic modifier of C30B. The latter resulted in a slight, but noticeable, HT alkyl tail templating effect (Figure 3.9, Table 3.11). From the low intensity of the (001) and (002) reflections, stacking disorder was evident in a large proportion of the sample. As the intercalant molecules, and hence HT alkyl tails, were widely spread in C30B, templating of the tails was difficult, unless EO components filled the gaps between them, thus forcing them into a slanted or vertical orientation.

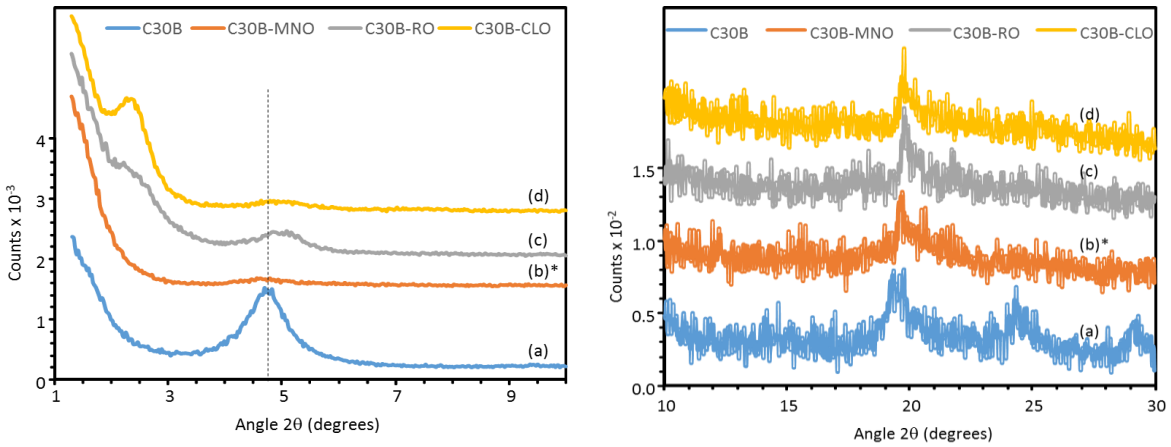

Figure 3.10. XRD data for Cloisite 30B; (a) C30B, (b)C30B-MNO, (c) C30B-RO and (d) C30B-CLO. * Denotes sample in form of greasy mass.

Table 3.12. Data for the first three reflection peaks from C30B based combinations

MMT combination	1st Peak		2nd Peak		3rd Peak		Higher order reflections	Templating effect
	2θ (°)	d(nm)	2θ (°)	d(nm)	2θ (°)	d(nm)		
C30B	4.69	1.88	-	-	-	-	No	NA
C30B-MNO	-	-	4.55	1.94	-	-	No	No
C30B-RO	2.06	3.63	4.82	1.83	-	-	Yes	weak
C30B-CLO	2.35	3.76	4.55	1.94	-	-	Yes	weak

Claytone APA (CAPA): In this case, none of these samples were in the form of a greasy mass. CLO-CAPA showed three reflection peaks of low intensity (Figure 3.11), indicating a limited proportion of ordered stacking, CLO is therefore arguably too compatible with the gallery environment of CAPA. On the other hand, in the MNO and RO containing samples, the level of stacking uniformity has increased significantly relative to the CAPA itself, the templating effect is therefore strong in both cases (Table 3.13). The relative compatibility of CLO, MNO and RO with the gallery environment of CAPA is consistent with the aromatic (benzyl) functionality of the organic modifier.

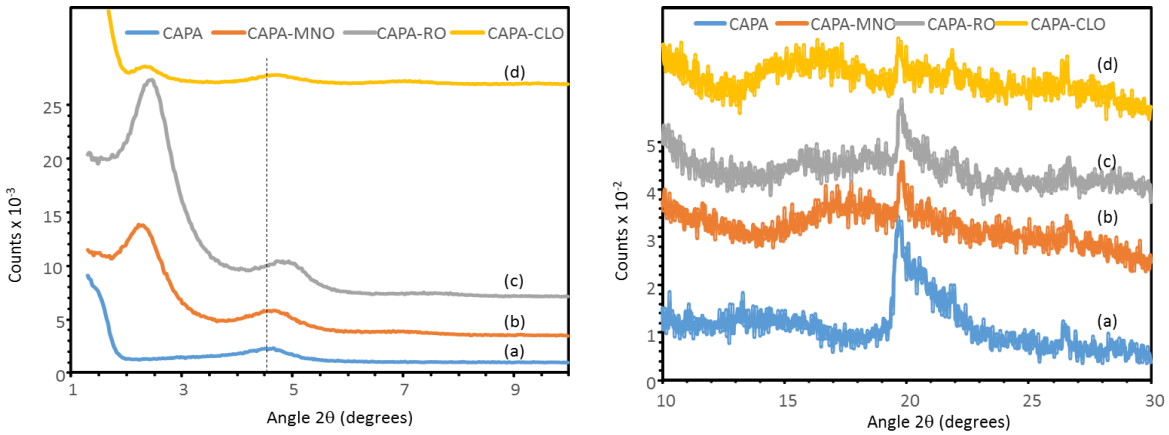

Figure 3.11. XRD data for Claytone APA; (a) CAPA, (b) CAPA-MNO, (c) CAPA-RO and (d) CAPA-CLO.

Table 3.13. Data for the first three reflection peaks from CAPA based combinations

MMT combination	1st Peak		2nd Peak		3rd Peak		Higher order reflections	Templating effect
	2θ (°)	d(nm)	2θ (°)	d(nm)	2θ (°)	d(nm)		
CAPA	4.67	1.89	-	-	-	-	No	NA
CAPA-MNO	2.31	3.82	4.22	2.04	-	-	Yes	Strong
CAPA-RO	2.47	3.59	4.82	1.83	-	-	Yes	V. Strong
CAPA-CLO	2.33	3.79	4.67	1.89	-	-	Yes	weak

Tixagel VZ (TVZ): As with CAPA, none of these samples were in the form of a greasy mass, this is not unexpected as both TVZ and CAPA share the same benzyl functional organic modifier, the level of modifier though is slightly higher in CAPA (34 wt.% in the latter, as opposed to 27% wt in TVZ).

From the counts scale of the XRD diffractogramme stack (Figure 3.12), it is evident that the TVZ based combinations showed much less order that the equivalent CAPA based combinations. This observation is probably due to the HT alkyl tails being too far apart to interact with each other. Only the CLO-TVZ and MNO-TVZ combination gave any hint of a templating effect (Table 3.14)

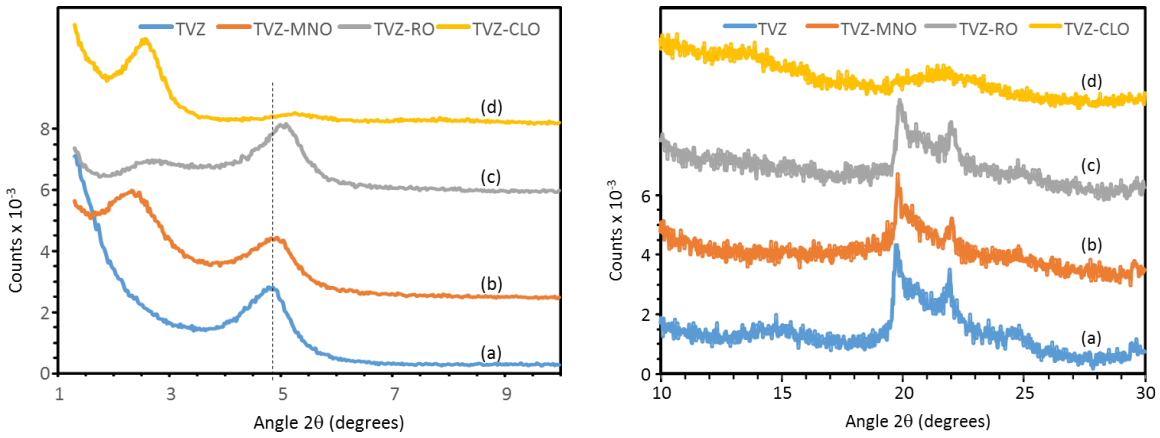

Figure 3.12. XRD data for Tixogel VZ; (a) CAPA, (b) CAPA-MNO, (c) CAPA-RO and (d) CAPA-CLO.

Table 3.14. – TVZ XRD (a) CAPA, (b) CAPA-MNO, (c) CAPA-RO and (d) CAPA-CLO.

MMT combination	1st Peak		2nd Peak		3rd Peak		Higher order reflections	Templating effect
	2θ (°)	d(nm)	2θ (°)	2θ (°)	d(nm)	2θ (°)		
TVZ	4.67	1.89	-	-	-	-	No	NA
TVZ-MNO	2.33	3.78	4.82	1.82	-	-	Yes?	weak
TVZ-RO	2.70	3.27	5.04	1.74	-	-	Yes?	v. weak
TVZ-CLO	2.33	3.79	5.25	1.68	-	-	Yes?	weak

Summary – XRD of EO loaded MMTs: The interlayer distance values are summarised in Table 3.15, alongside the corresponding EO adsorption levels and the extent of any templating effect. It is evident that $d_{(001)}$ reaches a limiting value due to the length of the HT chains of the organic modifiers. The level of EO adsorbed also reaches a limiting value that may be related to the overall volume of the gallery space. The templating effect does not necessarily go hand in hand with high levels of EO adsorption; RO gave a templating effect in all cases but the level of adsorption remained low, due to specific interactions with the

organic modifiers. Cases of high EO adsorption were in some cases accompanied by the templating effect. There appeared in some cases to be a fine line between high adsorption and templating and high adsorption and formation of a greasy mass, i.e. substantial loss of registry between MMT platelets. Had the level of EO added initially been lower a stronger templating effect may well have been observed as the gallery would not have been overloaded with EO. Based on the data reviewed thus far, the most suitable o-MMTs for EO reservoir applications appear thus far to be CAPA and TVZ as their adsorption capacities are high and they show a templating effect.

3.3.2.3 DRIFTS of essential oil loaded MMTs

FTIR-DRIFTS was used to confirm the incorporation of the essential oils (EO) in the unmodified and the modified layered silicates. In addition to the latter, it may also be possible to investigate the nature of the interaction between the major components of the essential oils and the organic modifiers present in the modified layered silicates. The strength of the latter interaction is likely to affect the rate of EO release. Previous work (Kininmonth et al, 2014) has also shown that acidic sites in unmodified layered silicates can lead to chemical modification of EO components, DRIFTS also provided insight into reactions of this nature. On examining the data obtained it became evident that it was the 2200 to 500 cm^{-1} region that showed the most obvious spectral changes, stacked spectra of these regions will therefore be shown in the report. The C-H stretching region shows in some cases some attenuation and shifting of alkenic and aromatic C-H stretching absorptions. The frequency of the methylene asymmetric C-H stretching vibrations ($\nu_{(CH\text{-}H)as}$) can provide insight into the state of order of the alkyl tails of the surface modifier molecule

Table 3.15. Summary of interlayer spacings, EO adsorption levels and evidence of the templating effect. * Denotes sample in form of greasy mass.

o-MMT / EO combination	Interlayer spacing (nm)	EO level (g/100g)	Templating effect
CNa	0.34	-	NA
CNa-MNO	0.57	19.9	NA
CNa-RO	0.64	4.93	NA
CNa-CLO	0.65	18.9	NA
C15A	2.05	-	NA
C15A-MNO	3.27	21.9	Weak
C15A-RO	2.90	4.22	Strong
C15A-CLO*	-	21.3	V. Weak
C20A	1.70	-	NA
C20A-MNO	3.14	23.3	Strong
C20A-RO	2.76	6.76	Strong
C20A-CLO*	-	23.0	V. Weak
C30B	0.95	-	NA
C30B-MNO*	-	13.6	None
C30B-RO	2.58	8.40	Weak
C30B-CLO	2.77	22.4	Weak
TVX	0.96	-	NA
TVZ-MNO	2.87	24.24	Weak
TVZ-RO	2.60	11.66	V. Weak
TVZ-CLO	2.50	23.13	Weak
CAPA	1.02	-	NA
CAPA-MNO	2.95	24.71	Strong
CAPA-RO	2.67	7.58	V. Strong
CAPA-CLO	2.85	23.42	Weak

Previous work (Liauw et al, 2014) has shown that co-intercalation can lead to templated self-assembly of the surface modifier alkyl tails; the latter is accompanied by an increase in interlayer spacing and a significant increase in stacking uniformity. It is well established that an increase in ordering of alkyl tails (such that they are in an all trans conformation and in a crystalline / quasi-crystalline self-assembled structure) leads to a reduction in $\nu_{(CH\text{-}H)as}$ towards 2915 cm^{-1} (typical of highly crystalline wax crystals) and away from liquid – state values of ca. 2930 cm^{-1}. Values of $\nu_{(CH\text{-}H)as}$ will therefore be tabulated and can serve as an indicator to further verify the templating effect that can occur as a result of co-intercalation.

Rather than a particular o-MMT providing unique spectral features on interaction with most of the EOs, it was instead found that a given EO generally gave common features across all the MMTs, therefore a stack of spectra will be presented for each EO. It was noticed that there was also a variation in sample colour, a snapshot of each sample taken from a flat-bed scan (obtained using a Samsung MultiXpress X4300LX printer/copier/scanner and saved in PDF format) of the sample bag is shown as a small square of colour on each spectrum. The amount of EO adsorbed is also given alongside each spectrum. The spectra are presented in order of decreasing intercalant (organic modifier) level, from C15A (39.8 wt% organic modifier) at the top to CNa (unmodified MMT) at the bottom. Each oil will now be considered in turn.

Rosewood Oil (RO) – MMT spectra: RO is the simplest of the EOs and consists mainly of linalool (ca. 80 to 97 % (Davis et al., 1999)). The EO-MMT stack is shown in Figure 3.13. RO did not adsorb strongly on any of MMTs investigated, this may explain the relatively light colour of the RO-MMT mixtures / co-intercalates. The $\nu_{(CH\text{-}H)as}$ and $\Delta\nu_{(CH\text{-}H)as}$ (the latter is the difference between $\nu_{(CH\text{-}H)as}$ of the o-MMT-EO blend and the $\nu_{(CH\text{-}H)as}$ of the o-MMT as

received) values are given in Table 3.16. The most significant feature of the RO-MMT series of spectra are carbonyl bands at 1709, 1636 and 1575 cm^{-1}. These carbonyl species may have been formed as a result of oxidation of the linalool at the OH group and also possibly at the double bonds. The C-H bending vibrations of RO at 1452, 1411 and 1376 cm^{-1} were perturbed as a result of the structural changes arising from significant oxidation / rearrangement of linalool.

The $\nu_{(CH-H)as}$ and $\Delta\nu_{(CH-H)as}$ values for the RO-C15A combination certainly indicated an increase surface modifier alkyl tail ordering that is observed in the XRD data. The two hydrogenated tallow alkyl chains of the organic modifier in C15A and C20A facilitate ordering, this is particularly true for C15A due to the higher modifier level. Surface modifiers featuring just one hydrogenated tallow (HT) alkyl chain per molecule (as is the case for all o-MMTs apart from C20A and C15A) may still show a templating effect on co-intercalation with an EO. However, due to the wider spacing between the HT chains it is not so easy for them to pack closely enough to result in significantly reduced $\nu_{(CH-H)as}$.

Table 3.16: Values of $\nu_{(CH-H)as}$ and $\Delta\nu_{(CH-H)as}$ for the RO-MMT combinations (a negative value of $\Delta\nu_{(CH-H)as}$ indicates an increase in the level of ordering of surface modifier alkyl tails)

Combination	$\nu_{(CH-H)as}$ (cm^{-1})	$\Delta\nu_{(CH-H)as}$ (cm^{-1})	HT templating	Increased stacking order
RO-C15A	2920.4	-2.8	Yes	Yes
RO-C20A	2922.3	-0.7	Yes	Slight
RO-CAPA	2924.3	-0.2	Yes	Yes
RO-TVZ	2923.8	-0.1	V. Slight	No
RO-C30B	2925.1	-0.5	Slight	Slight

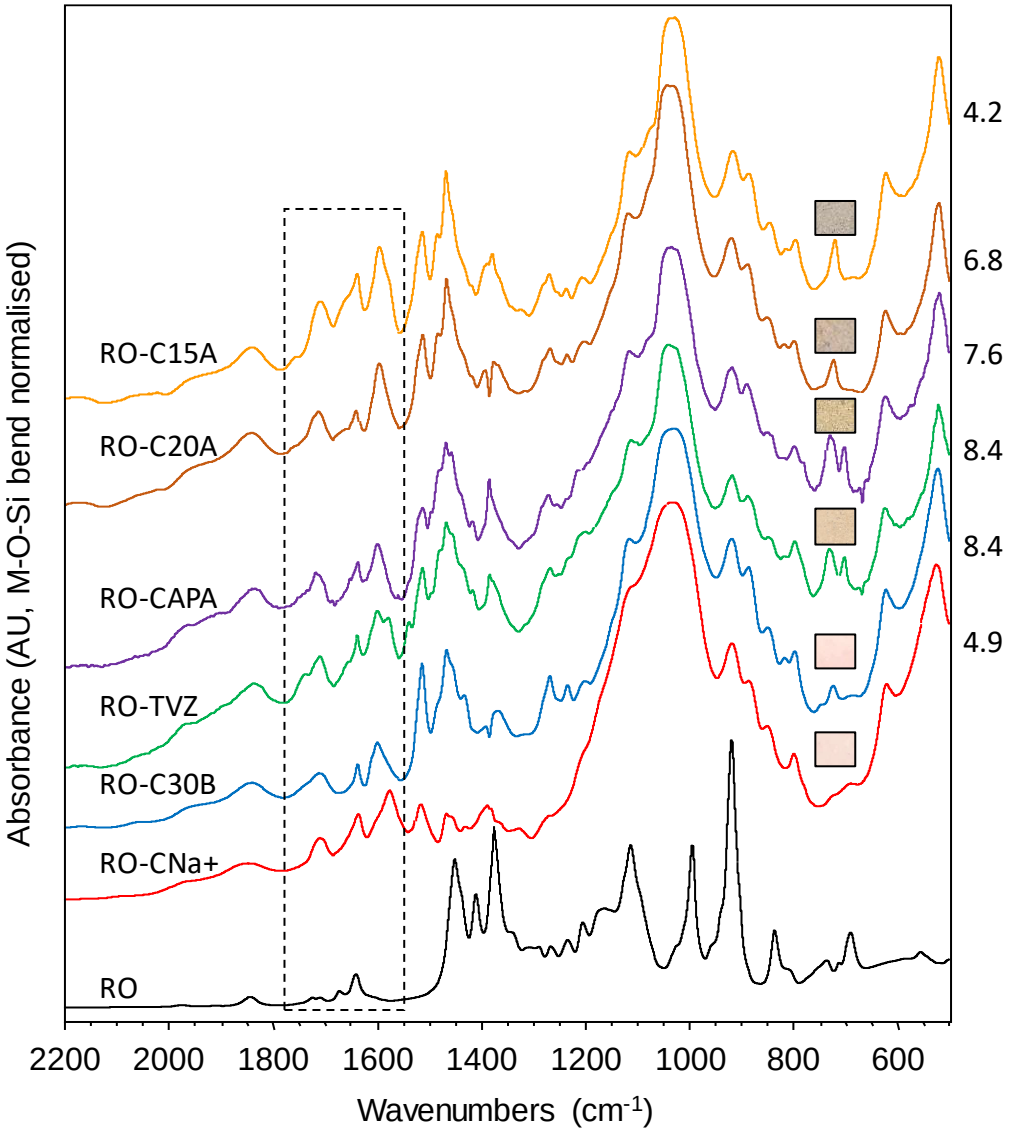

Figure 3.13. DRIFTS spectra (2200 – 500 cm^{-1}) of RO-MMT combinations. The colour of the combination is indicated by the square in the right hand half of the spectrum. The amount of RO adsorbed is in g RO/100 g MMT (or o-MMT) is shown adjacent to each spectrum.

Clove leaf Oil (CLO) – MMT spectra: CLO adsorbed much more strongly than RO, this may have contributed to the generally increased colour intensity. Higher organic modifier levels generally led to increased colour intensity (Figure 3.14) whilst the level of adsorption stayed at a broadly similar level. The $\nu_{(CH\text{-}H)as}$ and $\Delta\nu_{(CH\text{-}H)as}$ values for the CLO-MMT combinations is given in Table 3.17. The positive value of $\Delta\nu_{(CH\text{-}H)as}$ obtained for the combinations based on C15A and C20A were due to these samples being in the form of greasy mass, CLO

components surrounding the majority of the HT alkyl tails led to a more liquid-like state of disorder than in C15A itself. Negative values of $\Delta\nu_{(CH\text{-}H)as}$ could be correlated with increased ordering of HT alkyl tails as supported by increased templating and stacking order.

Table 3.17: Values of $\nu_{(CH\text{-}H)as}$ and $\Delta\nu_{(CH\text{-}H)as}$ for the CLO-MMT combinations (a negative value of $\Delta\nu_{(CH\text{-}H)as}$ indicates an increase in the level of ordering of surface modifier alkyl tails)

Combination	$\nu_{(CH\text{-}H)as}$ (cm^{-1})	$\Delta\nu_{(CH\text{-}H)as}$ (cm^{-1})	HT templating	Increased stacking order
CLO-C15A*	2923.4	+0.2	V.V. slight	No
CLO-C20A*	2923.4	+0.3	V.V. slight	No
CLO-CAPA	2924.0	-0.5	V. slight	No
CLO-TVZ	2923.6	-0.3	Yes	Slight
CLO-C30B	2924.8	-0.8	Yes	Slight

The carbonyl and aromatic and alkenic C-H bending regions for the CLO-MMT combinations show an interesting evolution with increasing organic modifier level. For CLO-CNa there is just a single carbonyl at 1707 cm^{-1}, indicating oxidation of some of the CLO components. The terminal alkenic and aromatic C=C stretching vibrations of eugenol at 1636 and 1612 cm^{-1}, respectively have broadened and the absorption at 1612 cm^{-1} has shifted to 1576 cm^{-1}. These shifts are consistent with the phenyl ring and terminal alkene of eugenol being in contact with the MMT surface, thereby indicating flat adsorption. Addition of increasing levels of organic modifier to the MMT causes the aromatic and alkenic C=C stretching vibration frequencies to generally revert back to what they were in the CLO itself. This trend may be explained by a change in mode of adsorption from flat to vertical due to the gallery space becoming more crowded as the organic modifier level increased.

The number of carbonyl stretching absorptions also increased as the level of organic modifier increased; for C30B a second carbonyl group at 1739 cm^{-1} is emerging alongside that at 1707 cm^{-1} seen in CNa. From TVZ to C15A the carbonyl at 1739 cm^{-1} shifts to 1760 cm^{-1} and a new carbonyl at 1670 cm^{-1} developed. Due to there being components other than eugenol in CLO it is difficult to precisely assign these absorptions. However, it appears that the majority of the eugenol component remains intact as the principal absorptions (including the doublet centred at 800 cm^{-1} aromatic C-H bending vibrations and the collection of C-O absorptions between 1350 and 1200 cm^{-1}) remain dominant in the spectra of the o-MMT based combinations. Increased organic modifier levels appear to lead to greater production of chromophoric species. Due to the complexity of the CLO and the mixture of potential impurities (for example unsaturation and peroxides) in the HT component of the organic modifier, it is not possible to identify the chromophoric species. The brown – black colouration was accompanied by the carbonyl absorption at 1660 – 1670 cm^{-1}, the latter may be assigned to $\alpha\beta$-unsaturated compounds that may be the chromophoric. Quinone methides can form from phenolic species and are highly chromophoric, the carbonyl at 1660 – 1670 cm^{-1} may also be assignable to such species; even a relatively insignificant amount could lead to noticeable darkening in colour.

Manuka Oil (MNO) – MMT spectra (Figure 3.15) MNO also adsorbed to relatively high levels peaking at 24.7 g MNO / 100 g CAPA. The colour of the MNO loaded MMTs was also not quite as intense as the CLO loaded equivalents. This may be indicative of the reduced aromatic content in MNO. The $\nu_{(CH\text{-}H)as}$ and $\Delta\nu_{(CH\text{-}H)as}$ values for the CLO-MMT combinations is given in Table 3.18.

Table 3.18: Values of $\nu_{(CH-H)as}$ and $\Delta\nu_{(CH-H)as}$ for the MNO-MMT combinations (a negative value of $\Delta\nu_{(CH-H)as}$ indicates an increase in the level of ordering of surface modifier alkyl tails)

* Denotes sample in form of greasy mass.

Combination	$\nu_{(CH-H)as}$ (cm^{-1})	$\Delta\nu_{(CH-H)as}$ (cm^{-1})	HT templating	Increased stacking order
MNO-C15A	2922.3	-0.9	Slight	No
MNO-C20A	2924.0	+1.1	Yes	Slight
MNO-CAPA	2924.0	-0.1	Yes	Yes
MNO-TVZ	2920.2	-3.7	Yes	Slight
MNO-C30B*	2925.2	-0.6	No	No

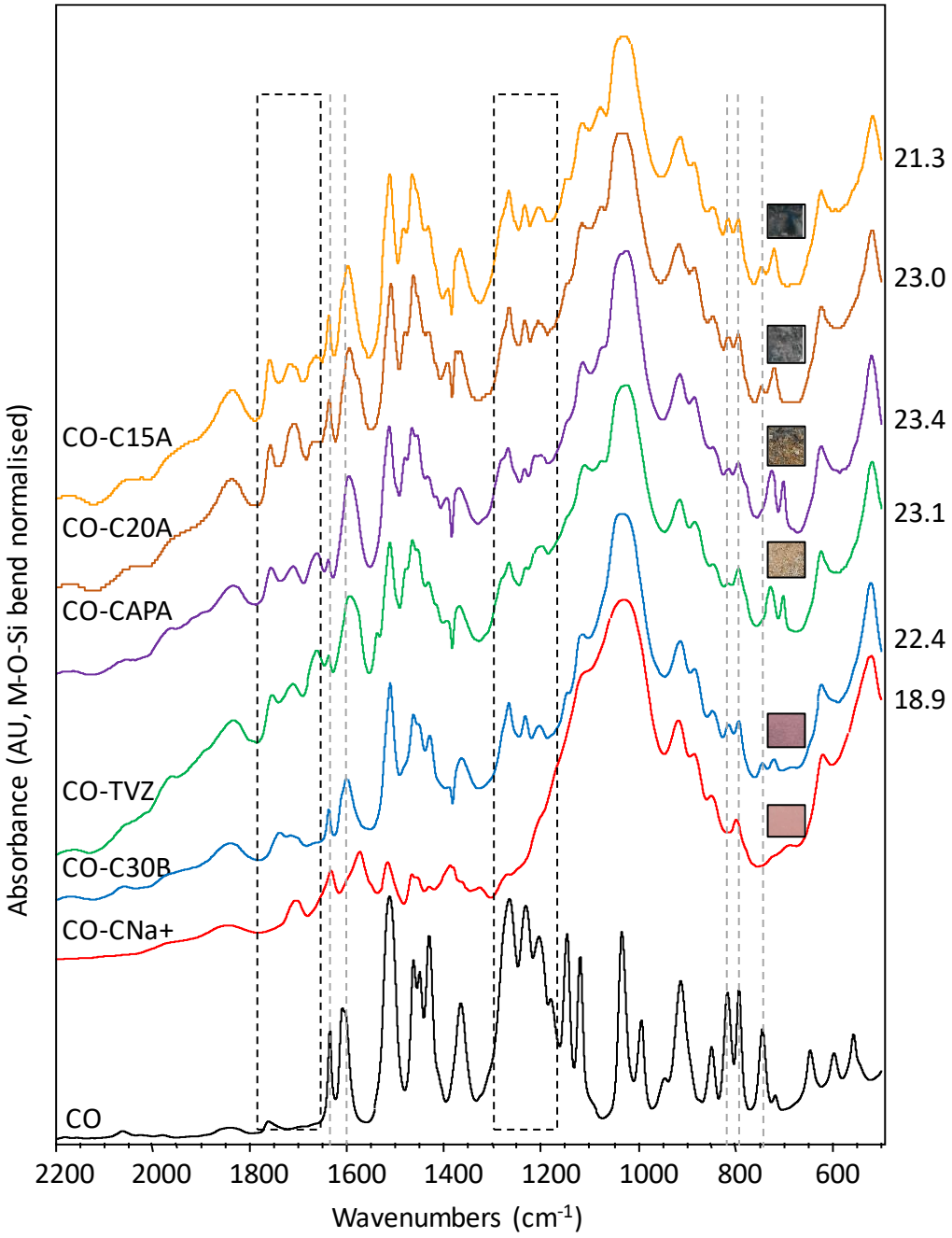

Figure 3.14. DRIFTS spectra (2200 – 500 cm^{-1}) of CLO-MMT combinations. The colour of the combination is indicated by the square in the right hand half of the spectrum. The amount of CLO adsorbed is in g CLO/100 g MMT (or o-MMT) is shown adjacent to each spectrum.

As MNO has six dominant components (rather than just one in the case of CLO and RO) with diverse molecular shapes and varying levels of polarity, it was expected that the level HT templating of the organic modifier in the MNO-o-MMT combinations would not be as significant and possibly variable, relative to the observations made with the simpler EOs. The $\nu_{(CH\text{-}H)as}$ and $\Delta\nu_{(CH\text{-}H)as}$ values obtained for the MNO-o-MMT combinations largely support this idea, though only the data for MNO-C20A and MNO-C30B were not as expected. C20A gave a positive $\Delta\nu_{(CH\text{-}H)as}$ value, despite templating and increased stacking order being evident. However, the MNO-C30B combination was in the form of a greasy mass with a reduction in stacking order (relative to the C30B itself) and no HT templating and but nevertheless gave a negative value of $\Delta\nu_{(CH\text{-}H)as}$.

The ketonic carbonyl groups (1724 cm^{-1}) from the leptospermine component and the C=C stretching vibrations from all the unsaturated species (1674 cm^{-1}) dominate the MNO spectrum. Interaction of MNO with CNa resulted in redshifts of these absorption bands to lower energy (1709 and 1636 cm^{-1}, respectively); a lack of significant colour change in MNO-CNa supported frequency shifting, rather than production of new carbonyl compounds as a result of oxidation.

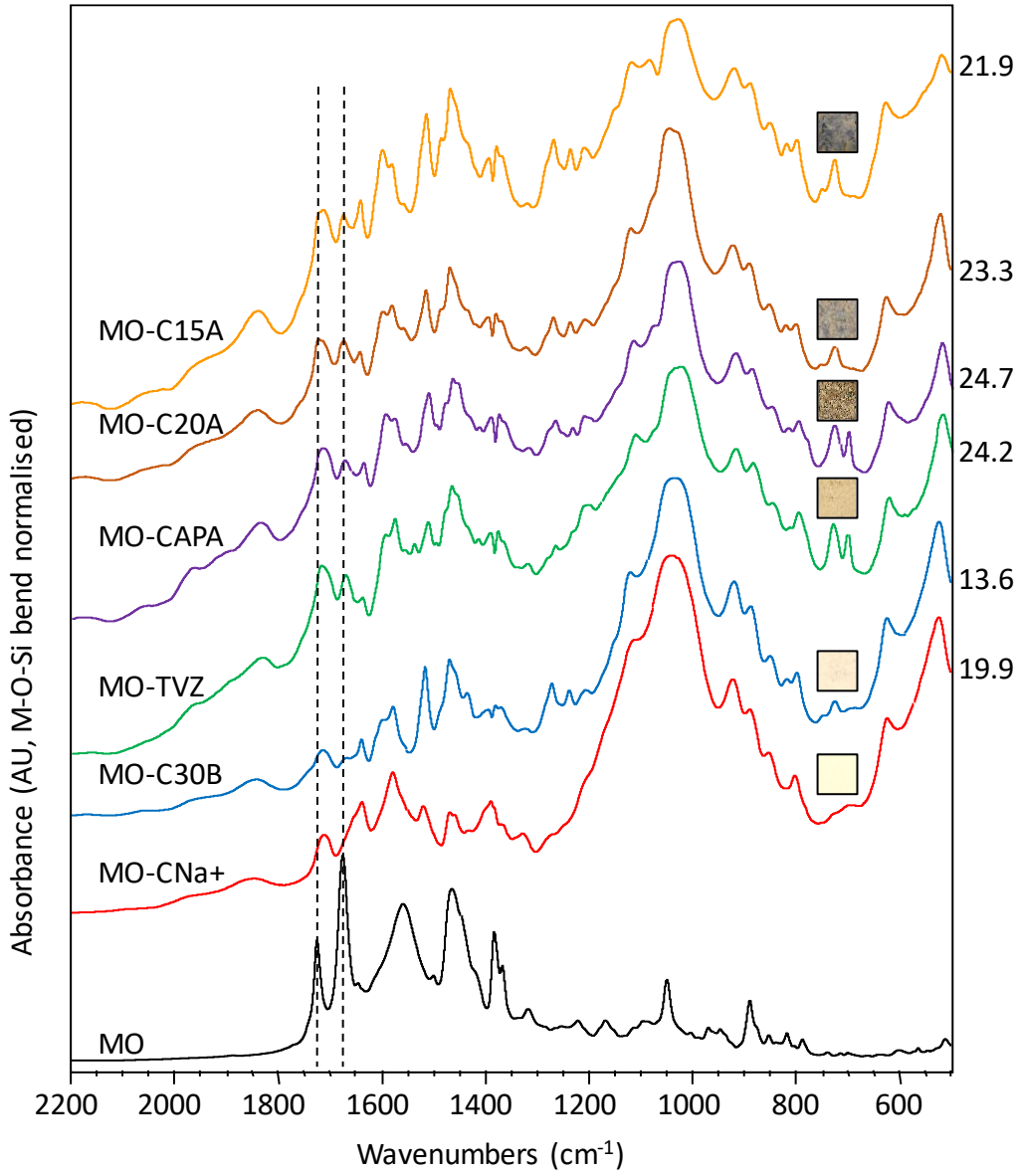

Figure 3.15. DRIFTS spectra (2200 – 500 cm^{-1}) of MNO-MMT combinations. The colour of the combination is indicated by the square in the right hand half of the spectrum. The amount of MNO adsorbed is in g MNO/100 g MMT (or o-MMT) is shown adjacent to each spectrum.

The carbonyl band in the MNO-C30B combination has a somewhat reduced red shift (1713 cm^{-1}) and is broadened further, the original C=C stretching band of MNO at 1674 cm^{-1} may have appeared as a shoulder on the red shifted residual of this band, that peaks at 1638cm^{-1}. As the organic modifier level (and level of MNO adsorption) is further increased, the C=C

stretching band at 1673 cm^{-1} becomes stronger whilst the carbonyl remains in the same position (1713 cm^{-1}). The latter indicates a change from flat (and in contact with the unmodified MMT surface) to vertical adsorption of the leptospermine and unsaturated components. Contact with organic modifier molecules resulted in retention of the band broadening. The noticeable increased darkening of the sample colour from MNO-C30B (lightest) to MNO-C15A (darkest) cannot be explained by the DRIFTS spectra alone.

3.3.2.4 Antimicrobial activity of EOs encapsulated in unmodified and unmodified MMTs

A preliminary qualitative antimicrobial assessment of the antimicrobial activity of the EOs encapsulated into unmodified and modified MMTs was undertaken. The assessment was performed following the procedures previously described in Chapter 1.

An example of these antimicrobial assessments for both *S. aureus* and *P. aeruginosa* is given in Figure 3.16 for CNa unmodified MMT and TVZ as an example of modified MMT (Figure 3.17). Table 3.19 summarises the results of this qualitative assessment. An area of no growth underneath the sample of MMT indicates slight antimicrobial activity and a defined area of no microbial growth around the sample of MMT indicates somewhat stronger antimicrobial activity. In the case of CNa – *S. aureus*, only the MNO gave readily defined antimicrobial activity, followed by CLO and RO. The CNa alone predictably gave no antimicrobial activity. No antimicrobial activity was evident for any of the CNa combinations challenged with *P. aeruginosa.* The TVZ, however, shows strong antimicrobial activity towards S. Aureus when loaded with the EOs investigated, particularly strong activity was noted with CLO. Even TVZ alone shows a small amount of antimicrobial activity, this is not surprising given the fact that the benzyl dimethyl hydrogenated tallow ammonium chloride

has proven antimicrobial activity in the form of benzalkonium chloride (Richards et al., 1978).

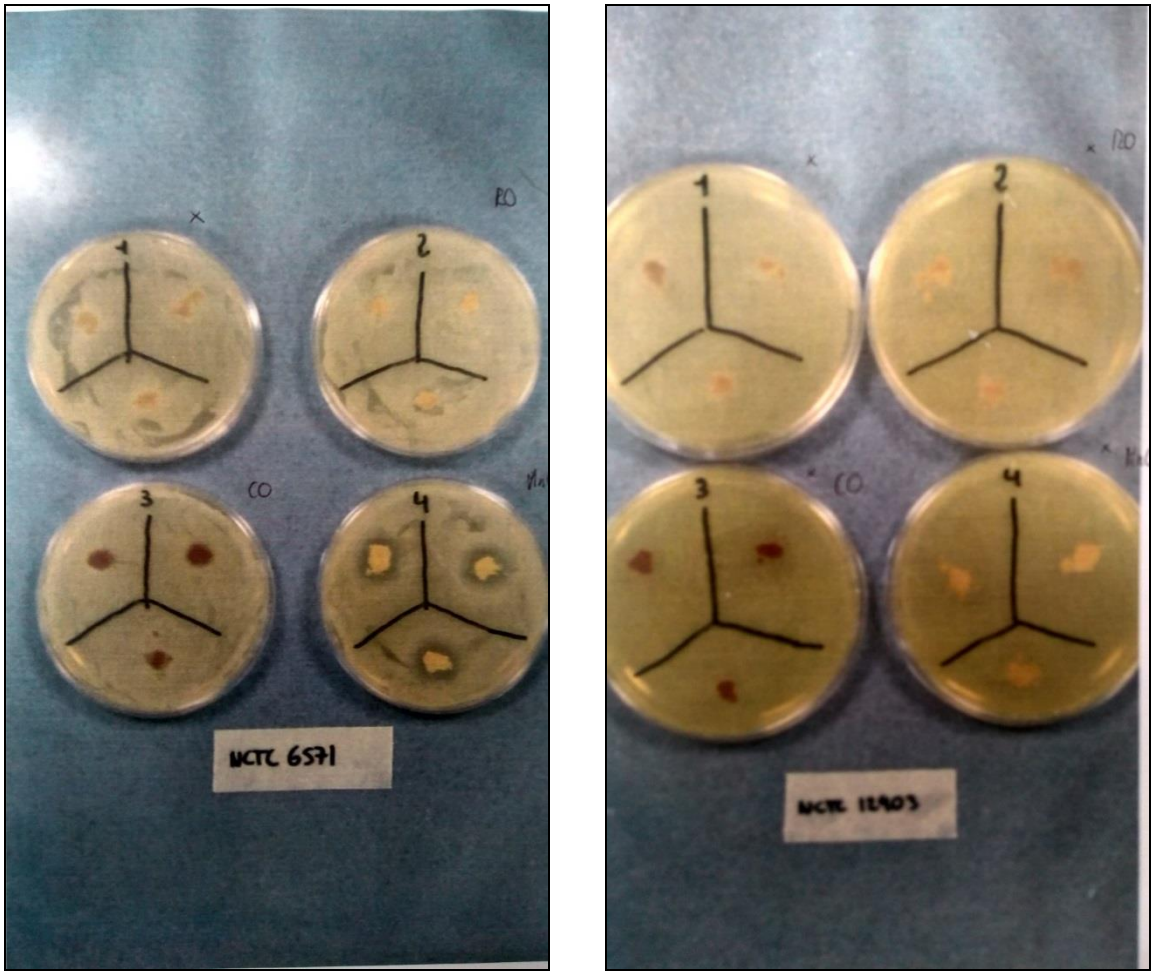

(a) (b)

Figure 3.16. Antimicrobial testing regime for EOs encapsulated in CLNa. (a) *S. aureus* and (b) *P aeruginosa*. Numbers refer to the EOs as follows: 1. CLNa, 2. CLNa-RO, 3. CLNa-CLO, 4. CLNa-MNO.

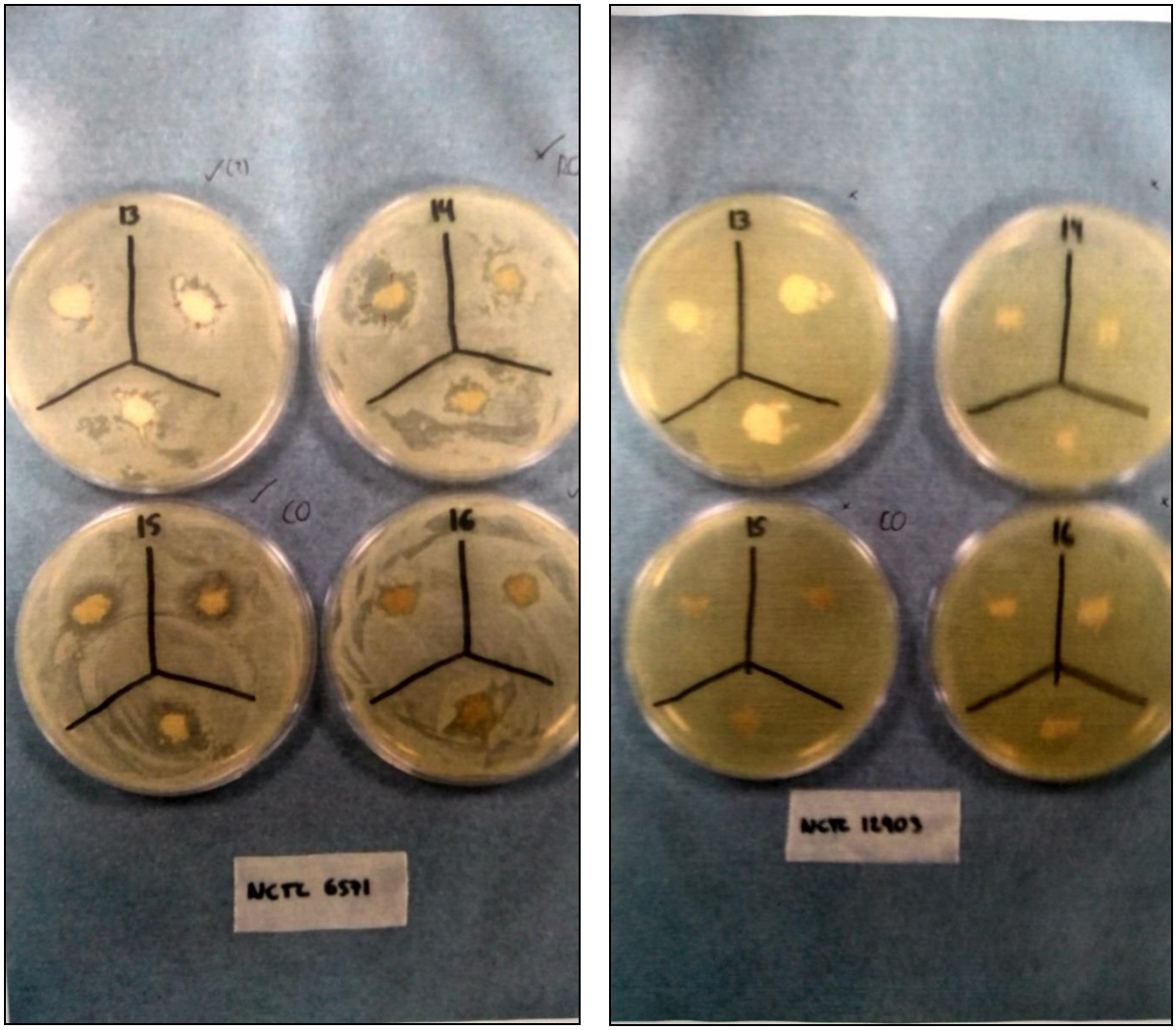

(a) (b)

Figure 3.17. Antimicrobial testing regime for EOs encapsulated in TVZ. (a) *S. aureus* and (b) *P. aeruginosa*. Numbers refer to the EOs as follows: 13. TVZ, 14. TVZ -RO, 15. TVZ -CLO, 16. TVZ -MNO.

Results clearly showed the effectiveness of most of the EOs encapsulated against *S. aureus* (Gram-positive bacteria), whilst this antimicrobial activity barely existed against the Gram-Negative bacteria (*P. aeruginosa*).

The test was designed only for qualitative rapid screening of efficacy – no zone of inhibition was measured.

Table 3.19. Antimicrobial Qualitative assessment on unmodified and modified loaded MMTs

MMTs	Antimicrobial activity with:	
	S. aureus	*P. aeruginosa*
CNa	No	No
CNa-RO	Slightly	No
CNa-CLO	Slightly	No
CNa-MNO	Yes	No
C15A	No	No
C15A-RO	Slightly	No
C15A-CLO	Slightly	No
C15A-MNO	Slightly	No
C20A	No	No
C20A-RO	No	No
C20A-CLO	- (Greasy)	- (Greasy)
C20A-MNO	- (Greasy)	- (Greasy)
C30B	Not Performed	Not Performed
C30B-RO	Not Performed	Not Performed
C30B-CLO	Not Performed	Not Performed
C30B-MNO	Not Performed	Not Performed
CAPA	Yes	No
CAPA-RO	Yes	No
CAPA-CLO	- (Greasy)	- (Greasy)
CAPA-MNO	Yes	No
TVZ	Yes	No
TVZ-RO	Yes	No
TVZ-CLO	Yes	No
TVZ-MNO	Yes	No

3.3.3. Silver Ion incorporation into Na-MMT

Silver was the metal chosen as an antimicrobial agent to be taken forward for this encapsulation study after ZoI, MIC and MBC tests. Silver was only incorporated into the unmodified substrate (incorporation via ion exchange Na^+ / Ag^+).

Silver was incorporated into CNa using a pre-adsorption method (see section 3.2). The nature and level of silver incorporation into the galleries of the layered unmodified substrate used was assessed by the following characterization techniques:

a) Atomic Absorption Spectroscopy (AAS), in which the amount of silver ions present in the supernatant liquid after the encapsulation of silver nitrate into CNa was calculated. The difference between this value and the initial value then gave the intercalated/external surface adsorbed silver level.
b) Energy Dispersive X ray analysis (EDX), in which the total amount of silver present either as accumulated on the surface or adsorbed into the galleries of the layered structures was determined. Removal of surface adsorbed silver by washing was attempted.
c) X-ray diffraction (XRD), which provided insight into the interlayer spacing and platelet stacking uniformity.

3.3.3.1 Determination of silver uptake by analysis of supernatant liquors using AAS

Silver uptake was determined using the method described in section 3.2.4.4.

Results showed for AAS were not conclusive. This method aimed to calculate the Ag^+ present on the unmodified substrate after treatment using the pre-adsorption method using

silver nitrate as silver source. This amount of silver was calculated from the amount of silver left in the supernatant liquid after isolating the substrate by centrifugation.

Higher levels of silver incorporation were expected at higher silver nitrate concentrations. In reality, although evidence of silver incorporation was found the results were variable as shown in Figure 3.18.

Results were expressed as g Ag^{+}/100 g substrate and are shown in Figure 3.19. No results were recorded for Ag at a 0.1 mol L^{-1}, as the amount of silver calculated yielded more silver than was initially loaded. It is shown that the highest level of silver incorporation into the CNa was observed at a silver nitrate concentration of 0.05 mol L^{-1}, whilst the lowest amount of silver incorporated into the CNa was observed at a silver nitrate concentration of 0.02 mol L^{-1}. Given the results obtained, it is not possible to reach a conclusion as to whether or not a limiting level of silver incorporation should be reached as might have been expected. Possible refinements to the experimental procedure are needed, although it can be concluded that silver ions have been incorporated.

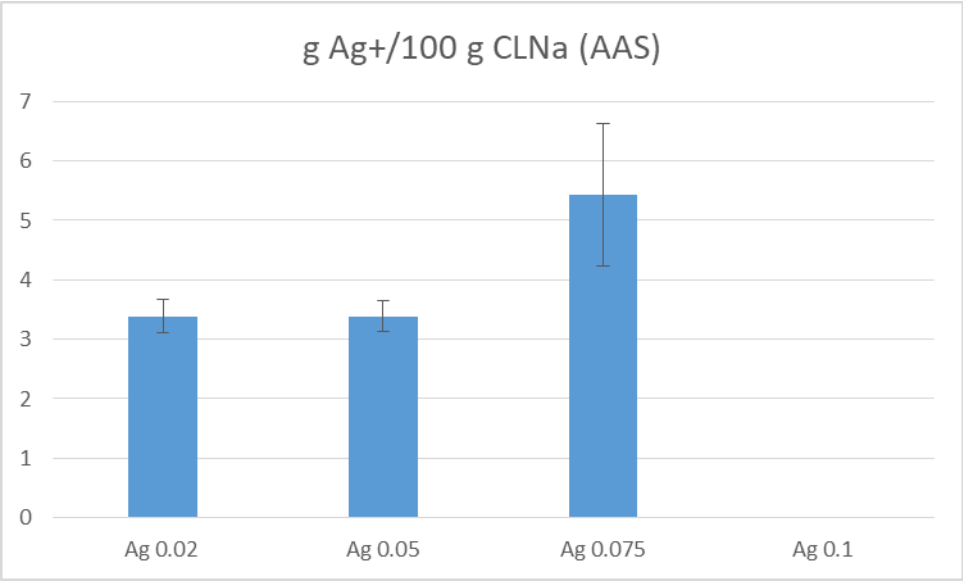

Figure 3.18. Amount of silver effectively incorporated into the unmodified substrate (CLNa).

3.3.3.2 Determination of silver content of Ag-MMT by EDX

Unlike the AAS analysis, Ag^+ present in the substrate (adsorbed and accumulated on the surface) is directly measured by EDX (see section 3.2.4.5 for details).

Two procedures were used. In the first, measurements were made on the sample directly obtained from the treatment. In the second these samples were washed and dried before EDX was performed. The rationale behind this was to see if washing removed silver from the external surfaces of the substrates but left silver effectively incorporated into the galleries.

Results were expressed as wt% Ag^+ and shown as a function of the initial silver nitrate concentration (Figure 3.19). It was observed that both in the un-washed and washed samples, that the amount of silver taken up increases with increasing silver nitrate concentrations. At treatment concentrations above 0.2 mol L^{-1}, washing removed an increasing amount of silver from the Ag-MMT, though a limiting level of retained silver in the MMT was not reached over the silver concentration range examined. These results confirm, as with AAS, that silver ions are being incorporated into the CLNa substrate. Over the concentration range investigated, the trend is as expected in that the level of silver ions incorporated increased as the concentration of silver nitrate solution increased.

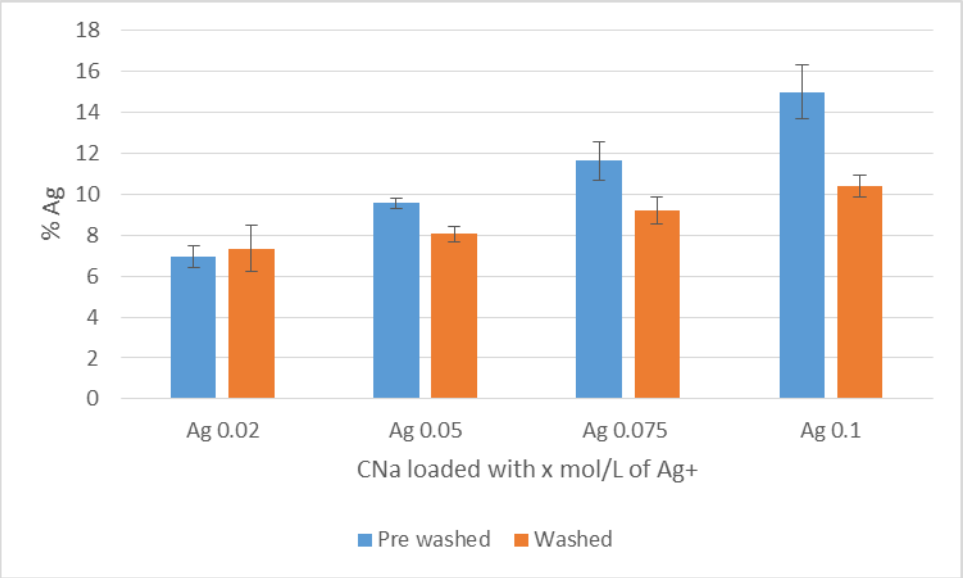

Figure 3.19. Amount of silver (%wt) effectively incorporated into the unmodified substrate (CLNa) before washing and after washing the samples.

3.3.3.3 XRD analysis of Ag-MMT

As was the case with the EO loaded MMTs, XRD was carried out (Section 3.2.4.2) in order to examine the effect of silver incorporation on the interlayer spacing and the platelet stacking uniformity. The family of XRD patterns obtained are shown in figure 3.20. In all samples, apart from that treated with 0.1 mol L^{-1} Ag^{+}, there was a significant loss of order, particularly in the cases of the 0.050 and 0.075 mol L^{-1} treatments, where no reflection peaks can be observed. The loss of order may be explained by the drying of the aqueous mixture from which the treatment was carried out. A very small peak is discernable at the 0.02 mol L^{-1} treatment level. The interlayer spacing observed for the 0.1 and 0.02 mol L^{-1} treatments are 0.42 nm and 0.29 nm, respectively. The ionic radius of silver (Ag^{+}) is 129 pm (0.129 nm), the ion will therefore fit very easily into the gallery space as the water is by far the largest component.

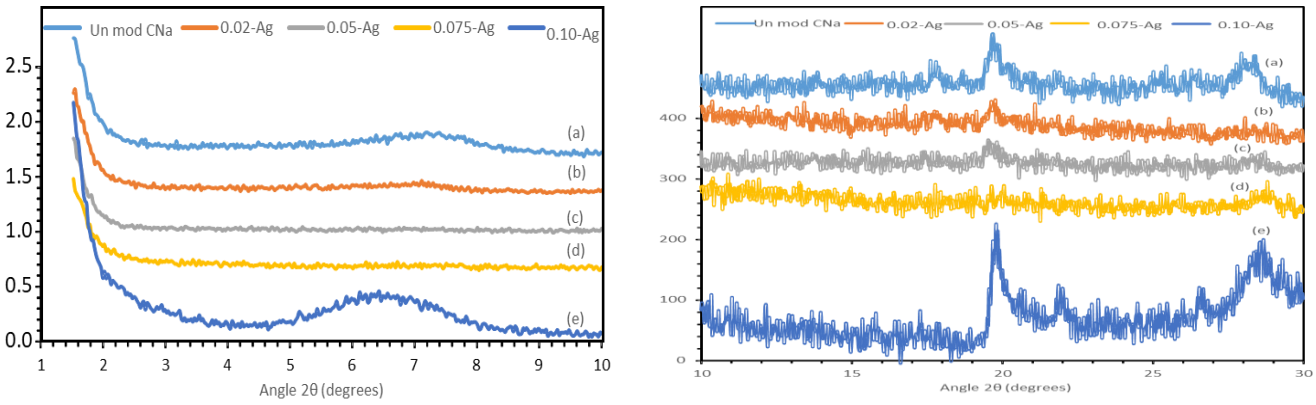

Figure 3.20. XRD for Ag^+ loaded CNa (a) Unmodified CNa, (b) 0.02 Ag, (c) 0.05 Ag, (d) 0.075 Ag, (d) 0.10 Ag

3.3.3.4 Antimicrobial activity of Ag^+ encapsulated in unmodified MMTs

A preliminary qualitative antimicrobial assessment of the antimicrobial activity of the Ag^+ encapsulated into unmodified MMTs (CLNa) was undertaken. The assessment was performed following the procedures previously described in Chapter 1. Observations for *S. aureus* and *P. aeruginosa* are shown in Figures 3.21 and 3.22, respectively; and are summarised in Table 3.20.

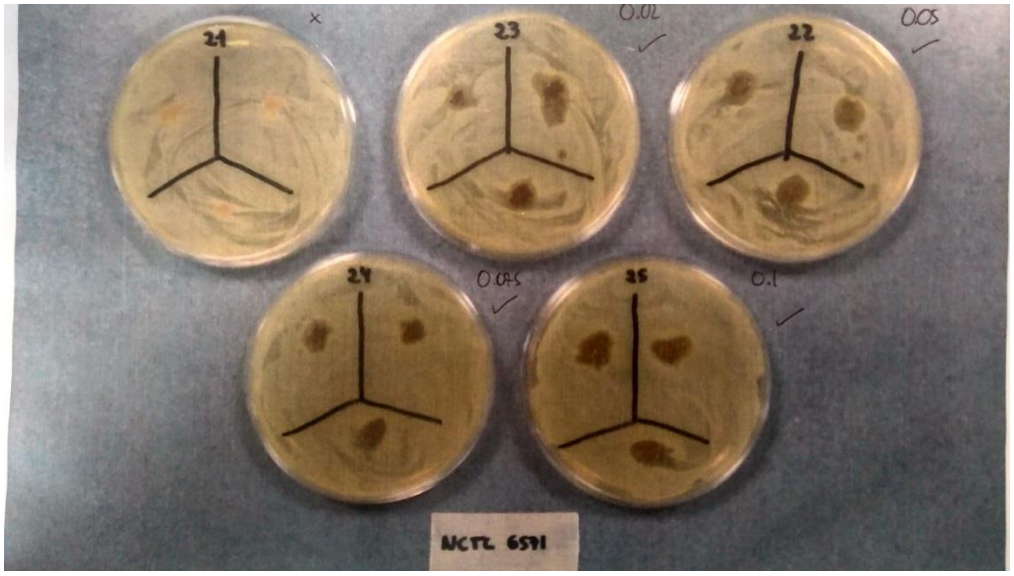

Figure 3.21. Antimicrobial activity assessment of Ag+ unmodified loaded MMTs against *S. aureus*. 21) CLNa, 22) CLNa + 0.025 M Ag+, 23) CLNa + 0.05 M Ag+, 24) CLNa + 0.075 M Ag+, 22) CLNa + 0.1 M Ag+

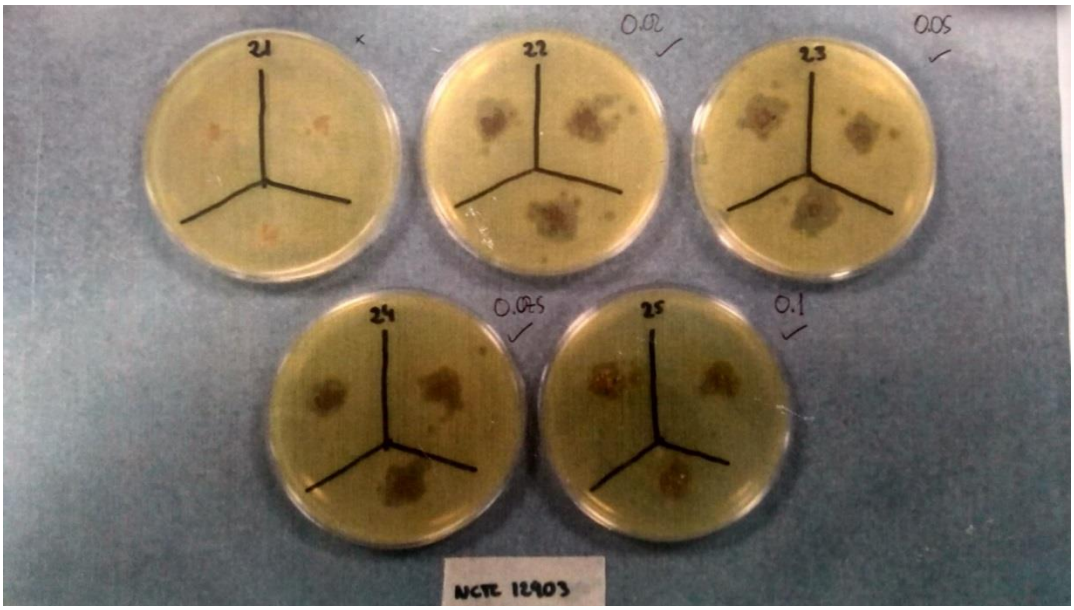

Figure 3.22. Antimicrobial activity assessment of Ag+ unmodified loaded MMTs against *P. aeruginosa* 21) CLNa, 22) CLNa + 0.025 M Ag+, 23) CLNa + 0.05 M Ag+, 24) CLNa + 0.075 M Ag+, 22) CLNa + 0.1 M Ag+

Table 3.20. Antimicrobial Qualitative assessment on unmodified loaded MMTs

MMTs	Microorganism	
	S. aureus	*P. aeruginosa*
CNa	No	No
CNa-0.025 M Ag^+	Yes	Yes
CNa-0.05 M Ag^+	Yes	Yes
CNa-0.075 M Ag^+	Yes	Yes
CNa-0.1 M Ag^+	Yes	Yes

The antimicrobial testing regime previously developed was used to determine the potential antimicrobial activity of the Ag+ encapsulated into the unmodified and MMTs.

Results showed antimicrobial activity of Ag+ loaded unmodified CLNa against both Gram-positive (*S. aureus*) and Gram-negative (*P. aeruginosa*) bacteria as CLNa alone did not show antimicrobial activity.

3.4. Summarising Discussions

3.4.1. General comments

The substrates used as reservoirs to adsorb the EOs can be classified by their increasing order of polarity a follows:

Cloisite 15A < Cloisite 20A < Claytone APA < Tixogel VZ < Cloisite 30B < Cloisite Na

CL15A and CL20A are modified with di-methyl di-hydrogenated tallow ammonium chloride, Tixogel VZ and Claytone APA are modified with benzyl di-methyl hydrogenated tallow ammonium chloride, CL30B is modified with di-ethanol methyl hydrogenated tallow ammonium chloride salt and CLNa is unmodified montmorillonite.

The o-MMTs intercalated with an organic modifier featuring a benzyl group, i.e, Claytone APA and Tixogel VZ, tended show the best incorporation capacity (Figure 3.6) for all three essential oils. This is consistent with the need to match the overall gallery polarity to the polarity of the molecules being encapsulated. The benzyl group is polarizable and hence compatible with molecules of varying polarity. The level of organic modification is, in these o-MMTs, also relatively low, giving space for the EO molecules to reside in the galleries whilst forcing the alkyl tails of the modifier into a vertical orientation to the MMT platelet surfaces (Table 3.13 and 3.14). The latter effect led to an increase in stacking uniformity of the platelets, as manifested in the appearance of higher order reflections in the XRD patterns (Figure 3.11 and 3.12).

The less polar o-MMTs (C20A and C15A) with relatively high levels of fully aliphatic organic modifiers were less effective at adsorbing rosewood oil and formed a greasy mass on addition of clove leaf oil. The major components in rosewood oil and clove leaf oil are linalool (3,7-dimethylocta-1,6-dien-3-ol) and eugenol (4-Allyl-2-methoxyphenol), respectively. The latter was arguably too compatible due to the aromatic ring and the allyl group, and resulted in delamination of the montmorillonite. The former may not have been able to pack easily into the spaces between the pre-adsorbed organic modifier molecules. There was sufficient interaction, however to force the alkyl tails of the organic modifier into a vertical orientation. Manuka oil contains a large proportion of purely hydrocarbon components that have good compatibility with the organic modifier in C20A and C15A. This results in the high level of adsorption and the uniform platelet stacking.

The organic modifier in the most polar o-MMT assessed (C30B) features two hydroxyl groups and is added at a relatively low level. Relatively good compatibility with EO

containing a significant portion of aromatic molecules and hydroxyl functional molecules, particularly clove leaf oil and to a lesser extent rosewood oil, was observed. Manuka oil formed a greasy mass on addition to C30B. This mass showed no significant peaks when analysed by XRD, but the level of adsorption was low, as shown in the TGA analysis, in comparison with the other modified montmorillonites. In this case it is likely that the hydroxyl functional organic modifier in C30B, combined with the low level of modification led to the gallery environment being too polar to allow intercalation.

The CNa (unmodified MMT) adsorbed an unexpectedly high level of EO. The interlayer spacing suggests that the molecules were adsorbed horizontally within the layers as the thickness of an alkyl chain is about 0.4 nm and thickness of a methyl branched alkyl chain is about 0.6 nm. The interlayer spacing observed for the EO treated CNa is consistent with the latter. It should be noted that the sample of CNa used has a somewhat larger basal (001) spacing than the manufacturers and literature values. This may be due to a high water content. The larger than normal basal spacing of the CNa used may have facilitated intercalation by polar EO components and thus explain the relatively high levels of EO adsorption observed.

3.4.2 Analysis of incorporation of essential oils and silver ions

In terms of EOs encapsulation assessment, the effectiveness of the pre-adsorption method of EOs incorporating into the galleries of the layered substrates used and the arrangement of the EOs within the galleries, was assessed by three characterization techniques.

1) Thermo Gravimetric Analysis (TGA), in which the amount of EOs and organic modifiers present on the corresponding organic modified substrates were calculated and further compared with those available literature reported results

2) X-ray diffraction (XRD), in which the internal rearrangement of the substrates inner layered structure was assessed on the EOs incorporation into the substrates.
3) Fourier Transform Infrared Spectroscopy (FTIR) - diffusive reflectance infrared Fourier transform spectroscopy (DRIFTS), in which the incorporation of EOs was assessed and possible interactions EOs major components-substrates organic modifiers were studied.

3.4.2.1. TGA

Results obtained enabled the amount of the corresponding EOs tested that effectively adsorbed into either the unmodified substrates or modified substrates to be determined, as well as to allowing calculation of the percentage of organic modifiers present on the organic modified substrates to be determined.

Only organic modifier percentages for C15A, C20A and C30B have been reported in the literature. No organic modifiers percentage for either Tixogel VZ or Claytone was found in the literature. Results obtained were similar to those reported in literature, C15A (40% (study) vs 43% (literature)), C20A (38%(s) vs 35.1% (l)) and C30B (28% (s) vs 30%(l)) (Nazir et al., 2016).

Results showed that best adsorption was achieved for essential oils adsorption were in all three cases (RO, CLO and MnO) using those natural o-MMT modified with a quaternary benzyl di-methyl hydrogenated tallow ammonium chloride salt (Tixogel VZ and Claytone APA). For RO, best result recorded was using TVZ as reservoir (11.6 gr/100 gr TVZ). For both CLO and MnO, best result recorded was using CAPA as reservoir (23.42 gr/100 gr CAPA) for CLO and (24.71 gr/100 gr CAPA).

3.4.2.2. XRD

The data obtained confirms the suitability of the pre-adsorption method in treating the layered silicate structures with an organic solvent in order to separate the layers so to accommodate the adsorbed structures (EOs). It is expected that the mechanism of interaction will have a major influence on controlled release behaviour of the EOs.

On treating the substrates with toluene, the o-MMT platelets were expected to separate to varying degrees. The increase in this interlayer distance facilitates the incorporation of the EO molecules. The increase of the interlayer distance then correlates with the shifting of the associated peak to lower diffraction angles as showed by the XRD data. This was observed for all samples investigated, including the CNa, if the normally expected (001) 2θ value for this unmodified montmorillonite is considered.

The phenomena was observed on all the samples run. All those unloaded substrates (unmodified and modified) presented a smaller interlayer distance and higher diffraction angles if compared to their loaded counterparts.

In the same fashion, the same trend was observed between the unmodified (CNa) or organically modified substrates. The unmodified substrates presented a smaller interlayer distance and higher diffraction angles compared to those modified substrates.

Overall, the pre-adsorption method has proven to be successful for encapsulating EOs in either unmodified substrates (CLNa) or organic modified (with organic substituents of a diverse polarity) substrates (C15A, C20A, C30B, Tixogel VZ and Claytone APA) at relatively high efficiency.

3.4.2.3. FTIR/DRIFTS

Results confirmed the incorporation of EOs into the unmodified and modified silicate layered structures. Unlike TGA, FTIR is a qualitative method used to confirm the encapsulation of the EOs into the substrates by observing the presence of peaks characteristics of the molecules being incorporated into the clay layers.

The combination of XRD and DRIFTS data supported the proposed templating effect that led to increase stacking uniformity of the MMT platelets.

3.4.2.4. Rudimentary antimicrobial assessment of EO loaded MMTs

Tixogel VZ and Claytone APA provided the highest adsorption capacity for all three EOs. On testing for antimicrobial characteristics, combinations of these o-MMTs with the EOs provided the strongest antimicrobial activity. This is likely to be due to the high adsorption levels combined with the ability for the EOs to be released under the test conditions used. The further qualitative antimicrobial testing regime run on unloaded and Ag+ loaded CLNa clearly showed the latter to show antimicrobial activity.

4. Overall Conclusions

The primary objective of this study was to initially investigate the individual antimicrobial efficacies of a range of essential oils (RO, CLO, OO, MNO and MYO) and metal ions (Ag, Pd and Pt), next possible synergies between combinations of the best individually performing essential oils and metals were investigated. The second objective was to investigate incorporation of the best performing EOs and metal ions into unmodified and organically modified layered silicates.

As for the antimicrobial testing regime, the following conclusions can be made:

- Metals tested on Nutrient Agar (NA) at higher concentrations (>50 mg/L) and Mueller-Hinton (MH) at lower concentrations (<50 mg/L), proved to be to be the appropriate media on which to perform the subsequent antimicrobial testing regime defined and eventually developed against the selected microbial challenges (*S. aureus* and *P. aeruginosa*) during this study.
- The best EO tested was finally MNO (MIC = 2.5 %(v/v)) and the best metallic ion was Ag^+ (MIC = MBC = 25 mg/L).
- FIC eventually showed indifferent activities for those combinations between metals and essential oils claiming the best antimicrobial performance individually, neither synergistic nor antagonistic.

Encapsulation of the EOs and Ag^+ into modified and unmodified MMTs, led to the following conclusions:

- The encapsulation studies yielded clear results as to EOs encapsulation, thus showing natural o-MMT modified with a quaternary benzyl di-methyl hydrogenated

tallow chloride salt (Tixogel VZ and Claytone APA) performed best and adsorbed the EOs to high levels. Although data obtained from AAS, EDX and XRD hinted some evidence of silver incorporation into the unmodified layered silicate CNa, a clear variability on the data collected is also shown and a pattern was therefore not inferred.

- Qualitative antimicrobial testing was performed on the Ag^{+} and EO loaded MMTs using NA. Results showed that most of the loaded layered silicates presented a certain noticeable degree of antimicrobial activity if compared to their unloaded counterparts in the case of EOs as the antimicrobial agents loaded into the structures. The antimicrobial qualitative testing for unloaded and loaded Ag CNa showed greater antimicrobial activity for those layered silicates treated with higher concentrations of $AgNO_3$. This could indicate a more effective controlled release at higher Ag concentrations, as some of the Ag adsorbed might not come out the layered silicates. But this is to be further assessed.

EOs and metals were screened for antimicrobial efficacy against the proposed microbial challenges. Those ones showing the best antimicrobial performance activity (Ag+ for metals and RO,CLO and MNO for EOs) were further incorporated successfully into MMTs.

5. FUTURE WORK

In terms of future work, it is clear that an optimisation of the antimicrobial activity assessment of the EO and Ag^+ loaded unmodified and modified layered silicates is needed (quantitative assessment).

Following rigorous characterization of the antimicrobial activity of the loaded layered silicates and monitoring of the EO and Ag^+ release characteristics, further work could be aimed in variety of directions along which the study could be taken forward:

- Search of potential synergistic combinations using the same metallic ions and essential oils tested performing the best antimicrobial activity.
- Incorporate the loaded layered silicate structures into a given polymeric matrix (the nature of the matrix would obviously be dependent on the targeted application)
- Perform application-specific tests on the resulting composite materials, including leaching studies in which application relevant conditions are replicated. The later could be followed/supplemented by further microbiological assessment to ensure retention of antimicrobial and synergy
- Optimisation of metal ion and EO interactions with the MMT / o-MMT, by tailoring of gallery chemistry.

References

Adams C.P., Walker K.A., Obare S.O., Docherty K.M. (2014) *Size-Dependent Antimicrobial Effects of Novel Palladium Nanoparticles* Plosone.org, 9 (1)

Ahmad A and Viljoen A. (2015) *The in vitro antimicrobial activity of Cymbopogon essential oil (lemon grass) and its interaction with silver ions* Phytomedicine, 22(6) pp. 657-65.

Aristilde L., Lanson B., Miéhé-Brendlé J., Marichal C., Charlet L. (2016) *Enhanced interlayer trapping of a tetracycline antibiotic within montmorillonite layers in the presence of Ca and* Mg Journal of Colloid and Interface Science, 464 pp. 153–159

Ash M. and Ash I., (2004), *Handbook of Preservatives,* New York Endicott

Ashton, D.P., Briggs, D., Liauw, C.M., (2003) *Analytical techniques for characterising filler surfaces*. In: Rothon, R.N. (Ed.), Particulate-Filled Polymer Composites, second edition RAPRA Technology Ltd Shrewsbury (chapter 3)

Baser C. and Buchbauer G., (2010) *Handbook of Essential Oils,* New York CRC Press

Balouiri M. Sadiki M., Ibnsouda S K *Methods for in vitro evaluating antimicrobial activity: A review (2016)* Journal of Pharmaceutical Analysis, 6 pp. 71–79

Belkhair S., Kinninmonth M., Fisher L., Gasharova B., Liauw C.M., Verran J., Mihailovac B. and Tosheva L. (2015) *Silver zeolite-loaded silicone elastomers: a multidisciplinary approach to synthesis and antimicrobial assessment* RSC Advances, 5 (51) pp. 40932-40939

Call D.R., Matthews L., Subbiah M., Liu J., (2013) Do antibiotic residues in soils play a role in amplification and transmission of antibiotic resistant bacteria in cattle populations? Frontiers in Microbiology 4 pp 1-8

Cottarel G., Wierzbowski J. (2007) *Combination drugs, an emerging option for antibacterial therapy* Trends in Biotechnology, 25 (12) pp. 547-55

Coulthwaite L., Bayley K., Liauw C., Craig G., Verran J.(2005) *The effect of free and encapsulated OIT on the biodeterioration of plasticised PVC during burial in soil for 20 months*, International Biodeterioration & Biodegradation, 56(2) pp. 86-93

Cowan, C. T. and White, D. (1958) *The mechanism of exchan-697ge reactions occurring between sodium montmorillonite and various n-primary aliphatic amine salts* Transactions of the Faraday Society, 54 pp. 691-697

Damm C., Neumann M., Munstedt H., (2006) *Properties of Nanosilver Coatings on Polymethyl* Methacrylate Soft Materials, 3 (2-3) pp. 71-88

Das K., Tiwari R. K. S. and Shrivastava D. K. (2010) *Techniques for evaluation of medicinal plant products as antimicrobial agent: Current methods and future trends* Journal of Medicinal Plants Research, 4(2) pp. 104-111

Davis P. (1988) *Aromatherapy an A-Z,* C W Daniel Co Ltd

Dowling D.P., Donnelly K., McConnell M.L. , Eloy R., Arnaud M.N. (2001) *Deposition of anti-bacterial silver coatings on polymeric substrates* Thin Solid Films, 398 pp. 602-606

Dong B., Belkhair S., Zarrour, M., Fisher L., Verran J., Tosheva L., Retoux R., Gilsona J.-P., and Mintova S., (2014) *Silver confined within zeolite EMT nanoparticles: preparation and antibacterial properties*, Nanoscale, 6 pp. 10859-10864

El-Mougy, N.S., Abdel-Kader M.M. and Aly D.E.H. (2009) *Application of plant Resistance Inducers for Controlling Early and Late Blights of Tomato under plastic houses conditions* Journal of Plant protection research, 49 (1) pp. 57-62

FoE Australia and FoE United States (2009) Nano and biocidal report: Extreme germ present a growing threat to public health.

Garavaglia J., M. Markoski M.M., Oliveira A. and Marcadenti A. (2016) *Grape Seed Oil Compounds: Biological and Chemical Actions for Health* Nutrition and Metabolic Insights 9 pp. 59–64

Gilchrist T., Healy D. M., Drake C. (1991), *Controlled silver-releasing polymers and their potential for urinary tract infection control* Biomaterials 12 pp. 76–78

Gómez López A., Aberkane A., Petrikkou E., Mellado E., Rodríguez Tudela J.L. and Cuenca-Estrella M. (2005) *Analysis of the Influence of Tween Concentration, Inoculum Size, Assay Medium, and Reading Time on Susceptibility Testing of Aspergillus spp.* Journal Clinical Microbiology 43 (3) pp. 1251-1255

Goñi P., López P., Sánchez C., Gómez-Lusa R., Becerrila R., Nerín C. (2009) *Antimicrobial activity in the vapour phase of a combination of cinnamon and clove essential oils* Food Chemistry, 116 (4) pp. 982–989

Hammer K.A., Carson C.F. and Riley T.V. (1999) *Antimicrobial activity of essential oils and other plant extracts* Journal of Applied Microbiology, 86 pp. 985–990

Hartwell J.M. (1965) *The Diverse uses of Montmorillonite* Clay Minerals 6 pp. 111-118

Heatley N.G. (1944) *A method for the assay of penicillin*, Biochem J., 38(1) pp. 61–65.

Hendricks, S. B. and Alexander, L. T., (1940), *Semiquantitative estimation of montmorillonite in clays*: Soil Sci. Soc. America Proc, 5 pp. 95-99.

Holla G., Yeluri R. and Munshi A.K. (2012*) Evaluation of minimum inhibitory and minimum bactericidal concentration of nano-silver base inorganic anti-microbial agent (Novaron®) against streptococcus mutans* Contemporary Clinical Dentistry, 3(3) pp. 288–293.

Hobman J.L. and Crossman L., (2014) *Bacterial antimicrobial metal ion resistance.* Journal of Medical. Microbiology, 64 pp. 471-497

Jones F. (1996) *Herbs – useful plants. Their role in history and today* European Journal of Gastroenterology & Hepatology, 8 pp. 1227-1231.

Jung, W. K., Koo, H. C., Kim, K. W., Shin, S., Kim, S. H., and Park, Y. H. (2008) *Antibacterial activity and mechanism of action of the silver ion in Staphylococcus aureus and Escherichia coli*. Applied and Environmental Microbiology, 74 pp. 2171– 2178

Kalan L., Wright G. (2011) *Antibiotic adjuvants: multicomponent anti-infective strategies* Expert reviews in molecular medicine 13, e5

Kato R. (2008) Interfacial Interactions in Polymer Layered Silicates Nanocomposites PhD Thesis Manchester Metropolitan University

Kelleners, T.J., M.S. Seyfried, J.M. Blonquist, Jr., J. Bilskie, and D.G. Chandler. (2005). *Improved interpretation of water reflectometer measurements in soils* Soil Science Society of America, 69 pp. 1684–1690

Kinninmonth M., Liauw C.M., Verran J., Taylor R., Edwards-Jones V., Shaw D., Webb M. (2013) *Investigation into the suitability of layered silicates as adsorption media for essential oils using FTIR and GC–MS* Applied Clay Science 83–84 pp. 415–425

Kinninmonth M., Liauw C.M., Verran J., Taylor R.L., Edwards-Jones V., Shaw D. (2014) *Nano-Layered Inorganic-Organic Hybrid Materials for the Controlled Delivery of Antimicrobials*, Macromolecular Symposia, 338 pp. 36-44

Kramer, U. (2005) *Phytoremediation: novel approaches to cleaning up polluted soils*. Current Opinion in Biotechnology, 16 pp. 133-141.

KMPG-LLP (2014). The Global Impact of AMR. December 2014. United Kingdom, KMPG-LLP

Lang G., Buchbauer G., (2011) *A review on recent research results (2008–2010) on essential oils as antimicrobials and antifungals*. A review Flavour Fragrance Journal, 27 pp. 57-62

Lansdown A.B., (2006) *Silver in health care: antimicrobial effects and safety in use* Curr Probl Dermatol., 33 pp. 17-34.

Lemire J.A., Harrison J.J., Turner R.J., (2013) *Antimicrobial activity of metals: mechanisms, molecular targets and applications* Nature Reviews Microbiology, 11 pp. 371–384

Li Z., Chang P.H., Jean J.S. , Jiang W.T., Wang C.J. (2010) *Interaction between tetracycline and smectite in aqueous solution* Journal of Colloid and Interface Science, 341 pp. 311–319

Liauw, C. M., Wilkinson, A. N., Man, Z., Stanford, J. L., Matikainen, P., Clemens, M. L., Lees, G. C., (2007). *Tensile properties of melt intercalated polyamide 6 - Montmorillonite nanocomposites*. Composites Science and Technology, 67(15-16) pp. 3360-3368

Liauw C.M., Taylor R.L., Maryan C., Kato R., Wilkinson A.N., Cheerarot O. (2011) *Organo-Montmorillonite as a Controlled Release Reservoir for Triclosan in Silicone Elastomer: A Flow Micro-Calorimetry and Leaching Study*, Macromolecular Symposia, 301 pp. 96-103.

Liauw C.M., Taylor R.L., Munro L.J., Wilkinson A.N., (2014) *Effect of Triclosan on Self-Assembly of Alkyl Ammonium Surfactants Adsorbed within Montmorillonite Galleries in Silicone Elastomer Composites,* Macromolecular Symposia, 338 pp. 45–53

Maddocks-Jennings, W., Wilkinson, J. M., Shillington, D. & Cavanagh, H. (2005). *A fresh look at manuka and kanuka essential oils from New Zealand*. International Journal of Clinical Aromatherapy, 15 pp. 141-146.

Magaña S M, Quintana P, Aguilar D H, Toledo J A, Ángeles-Chávez C, Cortés M A, León L, Freile-Pelegrín Y, López T, Torres Sánchez RM. (2008) *Antibacterial activity of montmorillonites modified with silver.* Journal of Molecular Catalysis, 281 pp. 192-199.

Malachová K., Praus P., Pavlíčková Z.,Turicová M., (2009) *Activity of antibacterial compounds immobilised on montmorillonite* Applied Clay Science, 43 pp. 364–368

MarketsandMarkets (2013) Antimicrobial coatings by type (Silver, Copper & Others) BY APPLICATION (Indoor air/HVAC, Medical, Mold remediation, Building & Construction, Food & Beverages, Textiles, & Others) Dallas. MarketsandMarkets

Nguemtchouin M.G.M., Ngassoum M.B., Chalier P., Kamga R., Ngamo L.S.T., Cretin M., (2013) *Ocimum gratissimum essential oil and modified montmorillonite clay, a means of controlling insect pests in stored products* Journal of stored products research, 52 pp. 57-62

Odom, I. E. (1984) *Smectite clay minerals: Properties and uses*: Philos. Trans. Royal Soc. London Set. A 311 pp. 391- 409.

PAN Germany (2013) Biocide-treated Consumer Products Markets – Policies – Risks 2013 Hamburg PAN Germany e.V.

Pavlidou S., Papaspyrides C.D. (2008) *A review on polymer–layered silicate nanocomposites*, Progress in Polymer Science, 33 pp. 1119–1198

Pegoretti A., Dorigato A., Brugnara M., Penati A. (2008) *Contact angle measurements as a tool to investigate the filler–matrix interactions in polyurethane–clay nanocomposites from blocked prepolymer* European Polymer Journal, 44 pp. 1662–1672

Pirbalouti A.G., Mirbagheri H., Behzad Hamedi B., Rahimi E. (2014) *Antibacterial activity of the essential oils of myrtle leaves against Erysipelothrix rhusiopathiae* Asian Pac J Trop Biomed. May; 4(Suppl 1) pp. S505–S509.

Porter N.G., Wilkins AL. (1999) *Chemical, physical and antimicrobial properties of essential oils of Leptospermum scoparium and Kunzea ericoides* Phytochemistry. 50(3) pp. 407-15.

Porubcan LS, Serna CJ, White JL, Hem SL. (1978) *Mechanism of adsorption of clindamycin and tetracycline by montmorillonite*. J Pharm Sci. 67(8) pp. 1081-7.

Praus P, Turicová M., Valásková M. (2008), *Study of silver adsorption on montmorillonite* Journal of the Brazilian Chemical Society 19(8) pp. 549-556

Public Health of England (2014) [Online] [Accessed on 24th January 2016] https://www.gov.uk/government/collections/staphylococcus-aureus-guidance-data-and-analysis

Public Health of England (2014) [Online] [Accessed on 24th January 2016] https://www.gov.uk/government/collections/pseudomonas-aeruginosa-guidance-data-and-analysis

Pukánszky B., Bagdi K., Müller P., *Thermoplastic starch/layered silicate composites: structure, interaction, properties* Composite Interfaces 13 pp. 1-17

RAND Europe (2013) Estimating the cost of AMR 2014 Cambridge RAND Europe

Review on Antimicrobial Resistance: Tackling a crisis for the health and wealth of nations (2014) HM Government

Razafimamonjison G., Jahiel M., Duclos T., Ramanoelina P., Fawbush F., Danthu P. (2014). *Bud, leaf and stem essential oil composition of clove (Syzygium aromaticum L.) from Indonesia, Madagascar and Zanzibar.* International Journal of Basic and Applied Sciences 2 pp. 312-318

Richards RM, Mizrahi LM. (1978) *Differences in antibacterial activity of benzalkonium chloride* Journal of Pharmaceutical Sciences 67(3), pp. 380-3

Samota M.K., Seth G., (2010) *Synthesis, characterization, and antimicrobial activity of palladium(II) and platinum(II) complexes with 2-substituted benzoxazole ligands* Heteroatom Chemistry 21(1) pp. 44-50

Scaffaro R., Botta L., Frache A., Bellucci F. (2013) *Thermo-oxidative ageing of an organo-modified clay and effects on the properties of PA6 based nanocomposites* Thermochimica Acta 552, pp. 37-45

Schierholz J.M., Wachol-Drewekl Z, Lucas L., Pulverer G., (1998) *Activity of Silver Ions in Different Media* Zentralblatt für Bakteriologie 287, pp. 411-420

Sherman L., (2011) *Antimicrobial Additives Targeted to Healthcare* SpecialChem, Dec 21

Singleton P., (2007) *Bacteria in Biology, Biotechnology and Medicine* Chichester John Wiley and Sons

Sondi, Salopek-Sondi B., *Silver nanoparticles as antimicrobial agent: a case study on E. coli as a model for Gram-negative bacteria* Journal of Colloid and Interface Science 275 (1) pp. 177-82.

Staszek M., Siegel J., Kolářová K., Rimpelová S., Švorčík V., (2014) *Formation and antibacterial action of Pt and Pd nanoparticles sputtered into liquid* Micro and Nano Letters 9 (11) pp. 778-189

Tortosa G.J., Funke B.R. and Case, C.L., (2004) *Microbiology an Introduction* San Francisco Pearson Benjamn Cummings

Tyagi M., Chandra S., (2012) *Synthesis, characterization and biocidal properties of platinum metal complexes derived from 2,6-diacetylpyridine (bis thiosemicarbazone)* Open Journal of Inorganic Chemistry, 2, pp. 41-48

Uddin F. (2014) *Environmental Concerns in Antimicrobial Finishing of Textiles* International Journal of Textile Science 3(1A) pp. 15-20

Vaidya M.Y., McBain A.J., Butler J.A., Banks C.E. and Whitehead K.A. (2017) *Antimicrobial efficacy and Synergy of metal ions against Enterococcus faecium, Klebsiella pneumoniae and acinobacter baumanii in plnnktonic and biofilm phenptypes* Scientific Reports 7

Windler L., Height M., Nowack B., *Comparative Evaluation of Antimicrobials for Textile Applications* Environmental international, 53 pp. 62-73

World Bank Group (2016) DRUG-RESISTANT INFECTIONS A Threat to Our Economic Future September 2016 Washington World Bank Group

CHAPTER 1

Appendix 1 – Preparation of metal ions, controls solutions and compositions used for testing antimicrobial efficacy using Zone of Inhibitions (ZoI, wells).

Sample name	Composition	Preparation
M (Ag, Pd, Pt)1000	1000 mg/L (M)	Commercial Product (1000 mg/L of metal in corresponding solution)
M (Ag, Pd, Pt)500	500 mg/L	5 mL Commercial Product + 5 mL d water
M (Ag, Pd, Pt) 100	100 mg/L	1 mL Commercial Product + 9 mL d water
M (Ag, Pd, Pt) 50	50 mg/L	1 mL M 500 + 9 mL d water
M (Ag, Pd, Pt) 10	10 mg/L	1 mL M 100 + 9 mL d water
Acid (2% HNO_3, 5%HCl) 1000	100% (content of original solution)	Solutions of 2% HNO_3 and 5%HCl
Acid (2% HNO_3, 5%HCl) 500	50%	5 mL Solutions + 5 mL d water

Acid (2% HNO_3, 5%HCl) 100	10%	1 mL Solutions + 9 mL d water
Acid (2% HNO_3, 5%HCl) 50	5%	1 mL Acid 500 + 9 mL d water
Acid (2% HNO_3, 5%HCl) 10	1%	1 mL Acid 100 + 9 mL d water

Appendix 2 – Preparation of EOs in grapeseed oil used for testing antimicrobial efficacy (ZoI, wells)

Sample name	Composition (v/v)%	Preparation
EO5 (RO, CO, OO, MyO, MnO)	5.0	250 µL EO + 4,750 mL GO
EO2.5 (RO, CO, OO, MyO, MnO)	2.5	125 µL EO + 4,875 mL GO
EO1 (RO, CO, OO, MyO, MnO)	1.0	50 µL EO + 4,950 mL GO
EO0.5 (RO, CO, OO, MyO, MnO)	0.5	25 µL EO + 4,975 mL GO

Appendix 3 – Preparation of EOs in grapeseed oil used for testing antimicrobial efficacy (ZoI, solid diffusion and vapour diffusion)

Sample name	Composition (v/v)%	Preparation
EO2.5 (RO, CO, OO, MyO, MnO)	2.5	125 µL EO + 4.875 mL GO
EO1 (RO, CO, OO, MyO, MnO)	1.0	50 µL EO + 4.950 mL GO
EO0.5 (RO, CO, OO, MyO, MnO)	0.5	250 µL EO + 4.975 mL GO

Appendix 4 – Composition of samples for the MIC/MBC determination of Essential Oils

Sample name	EOs (v/v)% in GO	Composition	Total volume (µL)	Final EOs (v/v)%
EO20 (RO, CO, OO, MyO, MnO)	20%	75 µL microorganism in TSB (tbc + Tween 20) + 75 µL EO 20% in GO	150 µL	10%
EO10 (RO, CO, OO, MyO, MnO)	10%	75 µL microorganism in TSB (tbc + Tween 20) + 75 µL EO 10% in GO	150 µL	5%
EO5 (RO, CO, OO, MyO, MnO)	5%	75 µL microorganism in TSB (tbc + Tween 20) + 75 µL EO 5% in GO	150 µL	2.5%
EO1 (RO, CO, OO, MyO, MnO)	1%	75 µL microorganism in TSB (tbc + Tween 20) + 75 µL EO 1% in GO	150 µL	0.5%

Appendix 5 – Composition of the samples for determination of MIC/MBC of Metal Ions

Sample name	Metal Ions in solution (mg/L)	Composition	Total volume (µL)	Final Metal Ions (mg/L)
M (Ag, Pd, Pt)1000	1000	75 µL microorganism in TSB (tbc + Tween 20) + 75 µL EO 20% in GO	150 µL	500
M (Ag, Pd, Pt)500	500	75 µL microorganism in TSB (tbc + Tween 20) + 75 µL EO 10% in GO	150 µL	250
M (Ag, Pd, Pt)100	100	75 µL microorganism in TSB (tbc + Tween 20) + 75 µL EO 5% in GO	150 µL	50
M (Ag, Pd, Pt)50	50	75 µL microorganism in TSB (tbc + Tween 20) + 75 µL EO 1% in GO	150 µL	25
M (Ag, Pd, Pt)10	10	75 µL microorganism in TSB (tbc + Tween 20) + 75 µL EO 1% in GO	150 µL	5

Appendix 6 – Metal ion and Essential Oil concentrations present once mixed in the micro titre plate wells with the 150 µL of the cell suspension adjusted to $1x10^6$ CFU/mL in a double strength solution of TSB containing 0.15% (m/v) TBC and 1.5% (m/v) tween 20. As a reminder, 100 µL of the first compound (Ag at the specified concentration) and 50 µL of the second compound (RO or MnO at the specified concentration) were pipetted into the well A3 (Column 1) to give a 2:1 dilution. Seventy five microlitres of both compounds were then pipetted into the well A4 (Column 2) to give a 1:1 dilution and 50 µL of the first compound (Ag) and 100 µL of the second compound (RO or MnO) were pipetted into A5 (Column 3) to give a 1:2 dilution.

Ag (100 mg/L) + RO (20%(v/v))

	Column 1 (2:1)		Column 2 (1:1)		Column 3 (1:2)	
Row A	33 mg/L	3.33% (v/v)	25 mg/L	5% (v/v)	16.7 mg/L	6.7% (v/v)
Row B	17.5 mg/L	1.67% (v/v)	12.5 mg/L	2.5% (v/v)	8.33 mg/L	3.33% (v/v)
Row C	8.25 mg/L	0.83% (v/v)	6.25 mg/L	1.25% (v/v)	4.17 mg/L	1.67% (v/v)
Row D	4.12 mg/L	0.42% (v/v)	3.12 mg/L	0.67% (v/v)	2.08 mg/L	0.83% (v/v)

Ag (100 mg/L) + MnO (5%(v/v))

	Column 1 (2:1)		Column 2 (1:1)		Column 3 (1:2)	
Row A	16.7 m/L	3.33% (v/v)	12.5 mg/L	5% (v/v)	8.33 mg/L	6.7% (v/v)
Row B	8.33 mg/L	1.67% (v/v)	6.25 mg/L	2.5% (v/v)	4.17 mg/L	3.33% (v/v)
Row C	4.17 mg/L	0.83% (v/v)	3.12 mg/L	1.25% (v/v)	2.08 mg/L	1.67% (v/v)
Row D	2.08 mg/L	0.42% (v/v)	1.56 mg/L	0.67% (v/v)	1.04 mg/L	0.83% (v/v)

Ag (50 mg/L) + RO (20%(v/v))

	Column 1 (2:1)		Column 2 (1:1)		Column 3 (1:2)	
Row A	16.7 m/L	0.83% (v/v)	12.5 mg/L	1.25% (v/v)	8.33 mg/L	1.67% (v/v)
Row B	8.33 mg/L	0.41% (v/v)	6.25 mg/L	0.62% (v/v)	4.17 mg/L	0.83% (v/v)
Row C	4.17 mg/L	0.21% (v/v)	3.12 mg/L	0.31% (v/v)	2.08 mg/L	0.41% (v/v)
Row D	2.08 mg/L	0.11% (v/v)	1.56 mg/L	0.15% (v/v)	1.04 mg/L	0.21% (v/v)

Ag (50 mg/L) + RO (5%(v/v))

	Column 1 (2:1)		Column 2 (1:1)		Column 3 (1:2)	
Row A	33 mg/L	0.83% (v/v)	25 mg/L	1.25% (v/v)	16.7 mg/L	1.67% (v/v)
Row B	17.5 mg/L	0.41% (v/v)	12.5 mg/L	0.62% (v/v)	8.33 mg/L	0.83% (v/v)
Row C	8.25 mg/L	0.21% (v/v)	6.25 mg/L	0.31% (v/v)	4.17 mg/L	0.41% (v/v)
Row D	4.12 mg/L	0.11% (v/v)	3.12 mg/L	0.15% (v/v)	2.08 mg/L	0.21% (v/v)

RO (20%(v/v)) + MnO (5%(v/v))

	Column 1 (2:1)		Column 2 (1:1)		Column 3 (1:2)	
Row A	6.7% (v/v)	1.67% (v/v)	5% (v/v)	1.25% (v/v)	3.33% (v/v)	0.83% (v/v)
Row B	3.33% (v/v)	0.83% (v/v)	2.5% (v/v)	0.62% (v/v)	1.67% (v/v)	0.41% (v/v)
Row C	1.67% (v/v)	0.41% (v/v)	1.25% (v/v)	0.31% (v/v)	0.83% (v/v)	0.21% (v/v)
Row D	0.83% (v/v)	0.21% (v/v)	0.67% (v/v)	0.15% (v/v)	0.42% (v/v)	0.11% (v/v)

Note the concentrations given above are the final values estimated from the contents of each well.

Appendix 7 – MIC data from MTP assays, showing the antimicrobial efficacy of the tested silver (Ag) at different concentrations (mg/L). Values are an average taken from three replicates (standard deviations given in brackets).

	Ag100 + RO20	Ag50 + RO20	Ag100 + MnO5	Ag50 + MnO5
2 to 1	22.83 (9)	16.67 (0)	33.3 (0)	16.67 (0)
1 to 1	20.83 (7.2)	12.5 (0)	25 (0)	12.5 (0)
1 to 2	11.11 (4.8)	8.33 (0)	16.67 (0)	8.33 (0)

Appendix 8 – MIC data from MTP assays, showing the antimicrobial efficacy of the tested essential oils (RO, MnO) at different concentrations (%(v/v)). Values are an average taken from three replicates (standard deviations given in brackets).

	Ag100 + RO20	Ag50 + RO20	Ag100 + MnO5	Ag50 + MnO5	R20 + MnO5
1 to 2	2.77(0.9)	3.33(0)	0.83(0)	0.83(0)	0.83(0)
1 to 1	4.17(1.4)	5(0)	1.25(0)	1.25(0)	1.25(0)
2 to 1	4.44(4.8)	6.67(0)	1.67(0)	1.67(0)	1.67(0)

Appendix 9 –MBC data from MTP assays, showing the antimicrobial efficacy of the tested silver (Ag) at different concentrations (mg/L). Values area an average taken from three replicates (standard deviations given in brackets).

	Ag100 + RO20	Ag50 + RO20	Ag100 + MnO5	Ag50 + MnO5
2 to 1	22.83(9.1)	16.67(0)	33.3(0)	16.67(0)
1 to 1	25.00(0)	12.5(0)	25(0)	12.5(0)
1 to 2	16.67(0)	8.33(0)	16.67(0)	8.33(0)

Appendix 10 – MBC data from MTP assays, showing the antimicrobial efficacy of the tested essential oils (RO, MnO) at different concentrations (%(v/v)). Values area an average taken from three replicates (standard deviations given in brackets).

	Ag100 + RO20	Ag50 + RO20	Ag100 + MnO5	Ag50 + MnO5	R20 + MnO5
1 to 2	2.22(0.9)	3.33(0)	0.83(0)	0.83(0)	0.83(0)
1 to 1	5(0)	5(0)	1.25(0)	1.25(0)	1.25(0)
2 to 1	6.67(0)	6.67(0)	1.67(0)	1.67(0)	1.67(0)

Appendix 11 - MIC data from MTP assays, showing the antimicrobial efficacy of the tested silver (Ag) at different concentrations (mg/L). Values are an average taken from three replicates (standard deviations given in brackets).

	Ag100 + RO20	Ag50 + RO20	Ag100 + MnO5	Ag50 + MnO5
2 to 1	33.30(0)	16.67(0)	33.3(0)	16.67(0)
1 to 1	25.00(0)	12.5(0)	25(0)	12.5(0)
1 to 2	16.67(0)	8.33(0)	16.67(0)	8.33(0)

Appendix 12 – MIC data from MTP assays, showing the antimicrobial efficacy of the tested essential oils (RO, MnO) at different concentrations (%(v/v)). Values area an average taken from three replicates (standard deviations given in brackets).

	Ag100 + RO20	Ag50 + RO20	Ag100 + MnO5	Ag50 + MnO5	R20 + MnO5
1 to 2	3.33(0)	3.33(0)	0.83(0)	0.83(0)	0.83(0)
1 to 1	5.00(0)	5(0)	1.25(0)	1.25(0)	1.25(0)
2 to 1	6.67(0)	6.67(0)	1.67(0)	1.67(0)	1.67(0)

Appendix 13 –MBC data from MTP assays, showing the antimicrobial efficacy of the tested silver (Ag) at different concentrations (mg/L). Values are an average taken from three replicates (standard deviations given in brackets).

	Ag100 + RO20	Ag50 + RO20	Ag100 + MnO5	Ag50 + MnO5
2 to 1	22.83(9.1)	16.67(0)	33.3(0)	16.67(0)
1 to 1	25.00(0)	12.5(0)	25(0)	12.5(0)
1 to 2	16.67(0)	8.33(0)	16.67(0)	8.33(0)

Appendix 13 – MIC data from MTP assays, showing the antimicrobial efficacy of the tested essential oils (RO, MnO) at different concentrations (%(v/v)). Values area an average taken from three replicates (standard deviations given in brackets).

	Ag100 + RO20	Ag50 + RO20	Ag100 + MnO5	Ag50 + MnO5	R20 + MnO5
1 to 2	2.22	3.33	0.83	0.83	0.83
1 to 1	5.00	5	1.25	1.25	1.25
2 to 1	6.67	6.67	1.67	1.67	1.67

CHAPTER 2

Appendix 1 – Preparation of EOs (rosewood oil, clove leaf oil and Manuka oil) to be incorporated into unmodified substrates (CLNa) and organic modified substrates (CL15A, CL20A, CL30B, Tix, Cly).

Sample	Foil Tray (gr)				Sample Bag (gr)			
	FT	FT+E	E(7.5)	%	SB	SB+E	E(7.5)	%
CLNa_RO1	5.86	11.92	6.06	80.80	0.65	6.33	5.68	75.73
CLNa_CO1	5.86	13.16	7.30	97.33	0.61	7.50	6.89	91.87
CLNa_MO1	5.86	13.14	7.28	97.07	0.63	7.43	6.80	90.67
CL15A_RO1	5.87	11.63	5.76	76.80	0.65	5.03	4.38	58.40
CL15A_CO1	5.87	12.67	6.80	90.67	0.65	7.50	6.85	91.33
CL15A_MO1	5.87	12.50	6.63	88.40	0.65	7.43	6.78	90.40
CL20A_RO1	5.87	11.26	5.39	71.87	0.65	5.36	4.71	62.80
CL20A_CO1	5.87	11.96	6.09	81.20	0.65	6.08	5.43	72.40
CL20A_MO1	5.87	12.65	6.78	90.40	0.65	6.48	5.83	77.73
CL30B_RO1	5.87	12.18	6.31	84.13	0.65	6.50	5.85	78.00
CL30B_CO1	5.87	13.08	7.21	96.13	0.65	7.08	6.43	85.73
CL30B_MO1	5.87	7.12	1.25	83.33	0.65	1.50	0.85	56.67
TIX_RO1	5.96	12.45	6.49	86.50	1.54	7.48	5.94	79.20
TIX_CO1	5.96	12.23	6.27	83.62	1.54	7.04	5.50	73.33
TIX_MO1	5.96	13.47	7.51	100.16	1.54	8.20	6.66	88.80
CLY_RO1	5.96	11.40	5.44	72.57	1.54	6.13	4.59	61.20
CLY_CO1	5.96	12.22	6.26	83.41	1.54	5.70	4.16	55.47
CLY_MO1	5.96	12.17	6.21	82.74	1.54	5.81	4.27	56.93

Appendix 2 – Results of incorporation of EOs (rosewood oil, clove leaf oil and Manuka oil) into unmodified substrates (CLNa) and organic modified substrates (CL15A, CL20A, CL30B, Tix, Cly) as for gr EOs/ 100 gr substrates. Values are an average taken from three replicates (standard deviations given in brackets).

EOs	Substrates					
	CLNa	CL15A	CL20B	CL30B	Tix	Cly
RO	4.93 (0.81)	4.22 (0.72)	6.76 (0.55)	8.40 (2.91)	11.66 (1.28)	7.58 (0.64)
CO	18.88 (4.94)	21.30 (0.82)	23.04 (1.12)	22.25 (2.83)	23.12 (0.31)	23.42 (2.37)
MnO	19.92 (1.25)	21.89 (0.82)	23.25 (1.04)	13.55 (1.61)	24.23 (0.04)	24.71 (1.92)

Appendix 3 – Results of incorporation of EOs (rosewood oil, clove leaf oil and Manuka oil) into unmodified substrates (CLNa) and organic modified substrates (CL15A, CL20A, CL30B, Tix, Cly) in terms of basal space (d(A)) and diffraction angles (2θ).

CLNa	CLNa_RO	CLNa_CO	CLNa_MnO	
7.13	5.81	5.56	5.84	2θ
12.83	15.81	15.86	15.13	d(A)
CL15A	CL15A_RO	CL15A_CO	CL15A_MnO	
2.95	2.92		2.09	2θ
29.88	38.43		42.14	d(A)
CL20A	CL20A_RO	CL20A_CO	CL20A_MnO	
3.43	2.39		2.16	2θ
26.4	37.03		40.78	d(A)
CL30B	CL30B_RO	CL30B_CO	CL30B_MnO	
4.68	2.51	2.31		2θ
18.86	35.24	38.09		d(A)
Tix	Tix_RO	Tix_CO	Tix_MnO	
4.81	2.49	2.57	2.31	2θ
19	35.4	34.43	38.11	d(A)
Cly	Cly_RO	Cly_CO	Cly_MnO	
4.57	2.45	2.33	2.27	2θ
19.6	36.12	37.89	38.9	d(A)

Appendix 4 – Samples' colours (EO encapsulated into unmodified and modified MMTs)

CLNa	
CLNa-RO	
CLNa-CLO	
CLNa-MNO	
CL15A	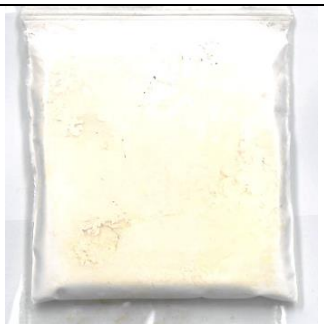

CL15A-RO	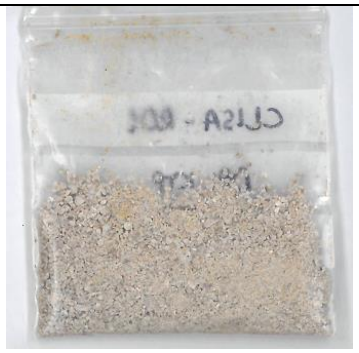
CL15A-CLO	
CL15A-MNO	
CL20A	

CL20A-RO	
CL20A-CLO	
CL20A-MNO	
CL30B	

CL30B-RO	
CL30B-CLO	
CL30B-MNO	
TVZ	

TVZ-RO	
TVZ-CLO	
TVZ-MNO	
CAPA	

CAPA-RO	
CAPA-CLO	
CAPA-MNO	

Appendix 5 – Preparation of silver to be incorporated into unmodified substrate (CLNa).

Sample	Sample Bag (gr)			
	SB	SB+E	E	%
CLNa_Ag 0.02 mol/L	1.36	2.18	0.82	61.59
CLNa_Ag 0.05 mol/L	0.65	1.47	0.82	43.70
CLNa_Ag 0.075 mol/L	1.38	2.30	0.92	40.04
CLNa_Ag 0.1 mol/L	1.38	2.33	0.94	34.68

Appendix 6 – Results of incorporation of silver into the unmodified substrate (CLNa) as for gr EOs/ 100 gr substrates. Values are an average taken from three replicates (standard deviations given in brackets).

	Samples			
	Ag 0.02	Ag 0.05	Ag 0.075	Ag 0.1
g Ag+/100 g CLNa	3.38 (0.48)	7.84 (0.45)	5.43 (2.09)	

Appendix 7 – Results of incorporation of silver into the unmodified substrate (CLNa) as for wt%. Values are an average taken from three replicates (standard deviations given in brackets).

	Ag 0.02 (wt%)	Ag 0.05 (wt%)	Ag 0.075 (wt%)	Ag 0.1 (wt%)
Pre washed	6.95 (0.90)	9.57 (0.43)	11.64 (1.66)	15.01 (2.25)
Washed	7.35 (1.93)	8.06 (0.69)	9.21 (1.14)	10.40 (0.94)